University of Exeter
Department of Mathematics

Stability index for riddled basins of attraction with applications to skew product systems

Ummu Atiqah Mohd Roslan

January 2015

Submitted by Ummu Atiqah Mohd Roslan, to the University of Exeter as a thesis for the degree of Doctor of Philosophy in Mathematics , January 2015.

I certify that all material in this thesis which is not my own work has been identified and that no material has previously been submitted and approved for the award of a degree by this or any other University.

(signature) .....

Abstract

This thesis examines how novel invariants called the "stability index" as proposed by Podvigina and Ashwin can be used to characterize the local geometry of riddled basins of attraction for both skew and non-skew product systems. In particular, it would be interesting to understand how the stability index behaves on the basin boundary between multiple basins of attraction. Then we can ask this question: How can we identify when a basin is riddled? To answer this, we present three models with the presence of riddled basins.

In the first model, we present a skew product system of a simple example of a piecewise linear map. We prove that the riddled basin occurs within a certain range of parameter and calculate the stability index analytically for this map. Our results for the stability index at a point show that for Lebesgue almost all points in the map, the index is positive and for some points the index may be negative. We verify these results with our numerical computation for this index. We also make a corollary claiming that the formula for the stability index at a point can be expressed in terms of the stability index for an attractor and Lyapunov exponents for this map. This suggests that this index could be useful as a diagnostic tool to study bifurcation of the riddled basins of attraction.

In the second model, we refer to a skew product map studied by Keller. Previously, Keller computed the stability index for an attractor in his map whereas in this thesis, we use an alternative way to compute the index; that is on the basins of attraction for Keller's map, found by inverting his map. Using the same map, we also verify maximum and minimum measures as obtained in his paper by studying Birkhoff averages on periodic points of Markov map in his system. We also conjecture result by Keller and Otani on the dimension of zero sets of invariant graph (i.e. basin boundary) that appears in Keller's map to a complete range of a parameter in the map.

The last model is a non-skew product map which is also has a riddled basin. For this map, we compute the stability index for an attractor on the baseline of the map. The result indicates that the index is positive for Lebesgue almost all points whenever the riddled basin occurs.

Acknowledgements

In the name of Allah The Most Gracious and The Most Merciful.

First of all, I would like to express my deepest thanks to my supervisor Prof. Peter Ashwin who accepted me to be his student, for his aspiring guidance all the way throughout my PhD's journey. To me, he is a very inspiring teacher. A lot of thanks to my second supervisor Ana Rodrigues for her willingness to read and comment my thesis and Mark Holland for the discussion of the ergodic theory. Thanks also go to my previous second supervisor Sebastian Wieczorek for his pleasure to hear my talk about my research, who is now in Cork, Ireland.

I am using this opportunity to thank the Center for Systems, Dynamics and Control at Exeter for giving me opportunity to organize the weekly seminars for our dynamics reading group, this became a platform for me to enhance my leadership and communication skills. I express my warm thanks to Liz Roberts, Karen Pope, Robert O'Neale and other staff members, without them I would not be able to go for all the conferences and workshops, helping me with the software and stuff.

I am truly thankful to Dr. Olga Podvigina from International Institute of Earthquake Prediction Theory and Mathematical Geophysics (MITPAN), Moscow, Russia for her visiting at Exeter in 2012 which gave me chance to discuss about the concepts in stability index. Also my sincere thanks to Alexander Lohse from University of Hamburg for his willingness to explain to me his approach to the stability index while his visiting to Exeter in 2012. Alex then come again to Exeter recently in February 2015, just couple of days before my viva.

A special mention for Dr. Tobias Jäger from University of Vienna for his suggestion about the connection between stability index with local dimensions of measures which we include in Chapter 3. Special thanks to Prof. Dr. Gerhard Keller from University of Erlangen-Nuremberg for answering all my questions through emails, where we finally met each other during his visit to Exeter in September 2014. It was such a nice chatting during dinner at The Rusty Bike Exeter.

Also not to forget my colleagues and friends, Clare, Congping, Yiwei, Vadim, Norziha, Sabrina Camargo (from Dynamics Days Europe in Madrid), Jack Campbell,

Sam Durston, Xavier, Tomas, Sara, Qiong and Paul. I learn a lot from you; MATLAB, Xfig and LaTeX. A great appreciation for my sponsorship; the Ministry of Higher Education Malaysia and to Universiti Malaysia Terengganu for supporting me and my family with full financial.

My special personal thanks and appreciation to my husband, Muhammad Nuzul who always support me 24/7, for his willingness to sacrifice his job in Malaysia in order to accompany me here. May Allah bless you forever. Finally, I would like to thank to my family especially my parents Mohd Roslan A Samat and Norzaini Bahari for their unstoppable prayer for me, wishing me luck as well as for their advice.

Contents

List of Tables

List of Figures

1 Introduction

In dynamical systems, every attractor has a basin of attraction, a set of initial points whose orbits are attracted to the attractor, i.e. basin with positive measure. This thesis will deal with a special and interesting type of basin of attraction; exists because of the symmetries in dynamical systems, the so-called *riddled basin*; a basin that has positive measure but contains no open sets [1]. The non-riddled basin is in some sense trivial (an open set must has positive Lebesgue measure) and not interesting, whereas a riddled basin is a highly non-trivial set and has very complicated structure. Generally speaking, a basin is said to be riddled if for any point that approaches the attractor in the basin, there is a point nearby that escapes to a basin of another attractor [49]. This type of basin was introduced by Alexander *et al.* [1] in 1992 and has been studied afterwards in several papers including Sommerer and Ott [61], Ott *et al.* [58], Ott *et al.* [57], Ashwin *et al.* [6; 7], Buescu [17] and Ashwin and Terry [8]. We discuss the definition more precisely in Section 2.4.

We show a schematic diagram for a riddled basin in Figure 1.1 where we refer to Camargo *et al.* [18]. Ott *et al.* [58; 57] states that to have a riddled basin, there must exists an attractor for which all points in its basin of attraction have pieces of another attractor basin arbitrarily nearby. That is, if p is any point in the basin, then, for every ε, however small, there are displacements δ, where $|\delta| < \varepsilon$, such that the point $p + \delta$ is in the basin of another attractor. In addition, the set of these points has nonzero phase space volume (positive Lebesgue measure).

Riddled basins can be found in many models of systems of physical and biological interest, for example in learning dynamical systems [55], coupled chaotic oscillators [6; 69], mechanical systems [67], electronic systems [54] and especially in coupled maps [32]. In addition, the applications of riddling can also appear in forced double-well Duffing oscillator [57; 58; 61], coupled nonlinear electronic circuits [6; 33], coupled elastic arches [67], ecological population model [21], chemical reactions of the Belouzov-Zhabotinsky type [68] and in models of interdependent open economies [72].

In fact all of the above authors investigate the global structure of the basin, but none of them consider for the local structure. In this work, we will introduce a *stability index* to quantify the local structure of the riddled basins. The stability index was

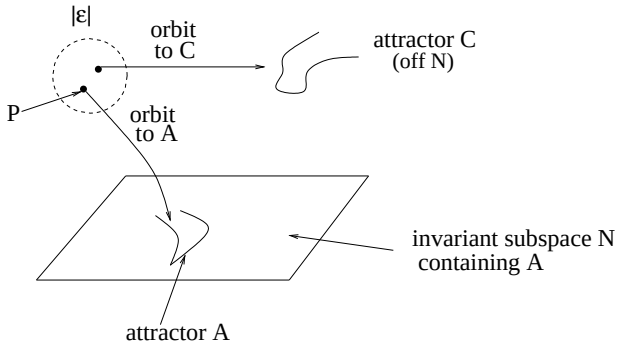

Figure 1.1 Schematic diagram [18] showing a situation with a riddled basin of attraction. This picture shows that there are two attractors A and C with basins $\hat{A}$ and $\hat{C}$. Basin $\hat{A}$ is riddled by basin $\hat{C}$ if for every point p in $\hat{A}$, a small ball of radius ε centred at p, $B_\varepsilon(p)$, has a positive Lebesgue measure of points belonging to basin $\hat{C}$, irrespective of how small ε might be.

introduced recently by Podvigina and Ashwin [59] to characterize the local structure of basins of heteroclinic attractors and we will adapt their definition to characterize the local geometry of riddled basin more precisely.

In this thesis, we concentrate on discrete time systems which can be written as

$$x_{n+1} = f(x_n),$$

where $x \in \mathbb{R}^n$ and $f : \mathbb{R}^n \to \mathbb{R}^n$. Such systems are generated by iteration of a map f.

The riddled basin can be found in *skew product dynamical systems*. In this thesis, we present some examples of skew product systems including a system which we modified from Ott *et al.* [57] and also one from Keller [44]. We consider a skew product on a space $B = X \times Y$ where X is the *base space* and Y is the *fibre space*. For each $x \in X$, the set $\{x\} \times Y$ is the *fibre over* x [2]. The skew product system $T : B \to B$ can be written as

$$T(x, y) = (f(x), g(x, y)), \tag{1.1}$$

where $f(x)$ is the *base map* from a base space to itself. For any $x \in X$ the *fibre map* $g(x, y)$ maps the fibre over x to a fibre over $f(x)$ [2]. In other words, the set $\{x\} \times Y$ is mapped to the set $\{f(x)\} \times Y$ by the fibre map $g(x, y)$. Note that x dynamics evolve independently of y dynamics in the base map [30]. See also [2; 4; 62; 64] for futher discussion about skew product systems. In Alsedá and Misiurewicz [2], they explain basic differences between a skew product system with a "usual" system; for example in terms of the space of convergence of orbits to the attractor in a system. In particular, in the usual system, this convergence is in the whole metric space while in the skew product system, this convergence is *fibrewise*, i.e. on the sets

$\{x\} \times Y$.

In fact, these systems may have attractors of the form of invariant graphs, where these invariant graphs play role as the boundary between the basins of attraction. With the presence of this boundary, one can characterize the convergence of orbits of points in the basins whether they start from below or above the invariant graph. For example, if the point starts from below the invariant graph, then its orbit will converge to an attractor in lower basin. Meanwhile, if the point starts from above the invariant graph, then its orbit will goes to an attractor in upper basin. To detect the riddled basin, the stability index is applied where we take a neighbourhood around a point in the attractor on the baseline and investigate the proportions of points that converge to an attractor as the size of the neighbourhood is varied. We will explain precisely about the invariant graph in the next section and in Chapter 3 for definition of the stability index.

In Figure 1.2 we show the relations between three main topics in this thesis which consist of the riddled basins, the skew product systems and the stability index. Note that the non-skew product systems can also have attractors with riddled basins.

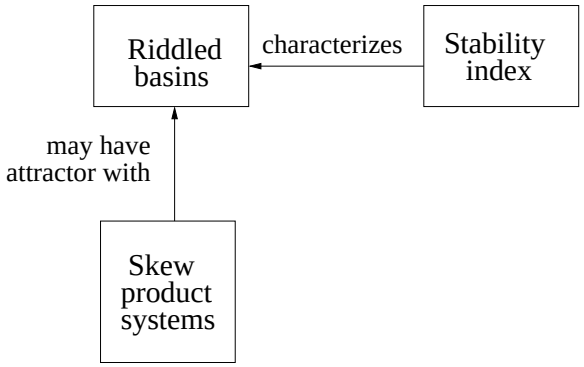

Figure 1.2 The relations between the three main topics that are analyzed in this thesis.

1.1 Invariant graph

From (1.1), we consider a map $f : \mathbb{T} \to \mathbb{T}$ where $\mathbb{T}$ denotes 1-dimensional torus $\mathbb{T} = \mathbb{R}/\mathbb{Z}$ and $g : I \to I$ where $I = [0, \infty)$.

Definition 1.1 *If $T : \mathbb{T} \times I \to \mathbb{T} \times I$ is a skew product and $\varphi : \mathbb{T} \to I$ is a function, we say φ is an* invariant graph *for T if $\{(\theta, \varphi(\theta)) : \theta \in \mathbb{T}\}$ is T-invariant.*

An invariant graph, if it exists, is a very useful tool to connect the base dynamics with the fibre dynamics. Generally speaking, it is an invariant set that is the graph of a function φ from the base space $\mathbb{T}$ to the fibre space I [62]. For example, Stark [62; 63], Kaplan *et. al* [41] and Hirsch *et. al* [34] have investigated existence and

regularity properties of invariant graphs in skew product systems. Another example is from Hadjiloucas *et. al* [31] where they consider the regularity of invariant graphs of skew product systems with uniform hyperbolic in the base map and both uniform and non-uniform contraction in the fibre map.

Invariant graphs also play a similarly important role in skew product systems as fixed points, for the case of unperturbed maps. However, in contrast to fixed points, we can characterize invariant graphs into two types. In the simpler case, the graph is continuous and in the more complicated case, it is non-continuous graph [37]. Invariant graphs have been applied in many branches of nonlinear dynamics and have become a subject of interest by many authors such as Stark [62; 63], Campbell [19], Broomhead [16], Jäger [37; 38], etc.

Here we define three different types of continuity of a function. Let $h : \mathbb{T} \to I$ be a function where I is a real interval.

Definition 1.2 (Upper semi-continuous) *A function h is* upper semi-continuous *if for all $\theta \in \mathbb{T}$ and $\varepsilon > 0$, there is a $\delta > 0$ such that for all $\tilde{\theta}$;*

$$\theta - \delta < \tilde{\theta} < \theta + \delta \quad \Longrightarrow \quad h(\tilde{\theta}) < h(\theta) + \varepsilon. \tag{1.2}$$

Definition 1.3 (Lower semi-continuous) *A function h is* lower semi-continuous *if for all $\theta \in \mathbb{T}$ and $\varepsilon > 0$, there is a $\delta > 0$ such that for all $\tilde{\theta}$;*

$$\theta - \delta < \tilde{\theta} < \theta + \delta \quad \Longrightarrow \quad h(\theta) - \varepsilon < h(\tilde{\theta}). \tag{1.3}$$

Definition 1.4 (Continuous) *A function h is said to be* continuous *if for all $\theta \in \mathbb{T}$ and $\varepsilon > 0$, there is a $\delta > 0$ such that for all $\tilde{\theta}$;*

$$\theta - \delta < \tilde{\theta} < \theta + \delta \quad \Longrightarrow \quad h(\theta) - \varepsilon < h(\tilde{\theta}) < h(\theta) + \varepsilon. \tag{1.4}$$

In other words, h is continuous if and only if it is both upper and lower semi-continuous.

For example, Stark [62] proves the existence of a continuous invariant graph (whenever the contraction in the fibre map is uniform) in the following theorem [62, Theorem 2.1] for one-dimensional fibres

Theorem 1.1 *Let $f : \mathbb{T} \to \mathbb{T}$ and $g : \mathbb{T} \times I \to I$. Suppose that $(f, g) : \mathbb{T} \times I \to \mathbb{T} \times I$ is a skew product with f invertible satisfying the uniform contraction*

$$\left| \frac{dg^{(n)}}{dx}(\theta) \right| \leq c\delta^n,$$

for all $\theta \in \mathbb{T}$ *and* $x \in I$ *and some* $0 < \delta < 1$, $c > 0$ *where* $g^{(n)}\theta$ *is the second component of* $(f, g)^n$. *Then there exists a continuous function* $\varphi : \mathbb{T} \to I$ *such that the graph of* φ *is* (f, g)*-invariant and attracting for all* $(\theta, x) \in \mathbb{T} \times I$.

However, in many cases, invariant graphs maybe discontinuous even if they are attracting. For instance, Jäger [37] considers a continuous skew product map

$$T : \mathbb{T} \times I \to \mathbb{T} \times I,$$

defined by

$$T(\theta, x) = (f(\theta), g(\theta, x)), \tag{1.5}$$

where all of the fibre maps g are monotonically increasing on I. We refer to Wheeden and Zygmund [66] for the definition of a function to be monotonic increasing and below we show in the case of fibre maps:

Definition 1.5 (Monotonic increasing in fibre) *A function* g *is monotonic increasing in fibre map if for all* $x_1, x_2 \in I$ *such that* $x_1 \leq x_2$ *and* $\theta \in \mathbb{T}$, *then*

$$g(\theta, x_1) \leq g(\theta, x_2),$$

where this means that if we start with higher value, then its image cannot be lower than the lower value.

If $\varphi : \mathbb{T} \to I$ is an invariant graph for T

$$T(\theta, \varphi(\theta)) = (f(\theta), \varphi(f(\theta))) \tag{1.6}$$

or equivalently,

$$g(\theta, \varphi(\theta)) = \varphi(f(\theta)) \tag{1.7}$$

for all $\theta \in \mathbb{T}$. We show action of the skew product T in (1.6) as in Figure 1.3.

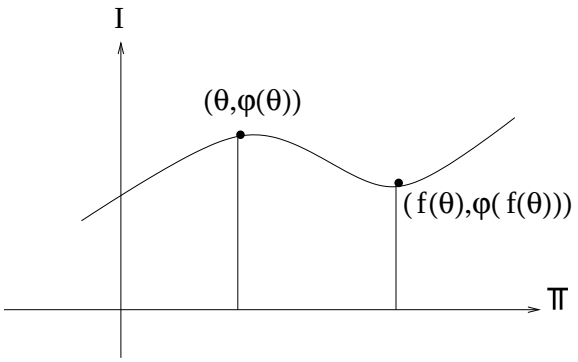

Figure 1.3 The schematic diagram showing the action of skew product T on the invariant graph φ.

Now, suppose that $K \subseteq \mathbb{T} \times I$ is a compact invariant set. We can define *upper bounding graph of* K as

$$\varphi^+(\theta) = \max\{x \in I : (\theta, x) \in K\}. \tag{1.8}$$

Thus by compactness of K, $\varphi^+(\theta)$ will be upper semi-continuous. In the same way, one can define the *lower bounding graph* of K:

$$\varphi^-(\theta) = \min\{x \in I : (\theta, x) \in K\},$$

which is also invariant. The following lemma proves that the upper bounding graph $\varphi^+(\theta)$ is invariant. Note that this has been stated in Jäger's paper [37] but we give a proof here for completeness of this research project.

Lemma 1.1 *Let $\varphi^+(\theta)$ be as in (1.8) and g is monotonic increasing in the fibre. Then $\varphi^+(\theta)$ is invariant.*

Proof. From (1.7) and (1.8), we have that for all $\theta \in \mathbb{T}$,

$$\begin{aligned} g(\theta, \varphi^+(\theta)) &= g(\theta, \max\{x \in I : (\theta, x) \in K\}), \\ &= \max\{g(\theta, x) : (\theta, x) \in K\}, \end{aligned}$$

but $(\theta, x) \in K$ if and only if

$$T(\theta, x) = (f(\theta), g(\theta, x)) \in K,$$

i.e. the images are also in K since K is invariant. Thus,

$$\begin{aligned} g(\theta, \varphi^+(\theta)) &= \max\{g(\theta, x) : (f(\theta), g(\theta, x)) \in K\}, \\ &= \max\{z : (f(\theta), z) \in K\}, \\ &= \varphi^+(f(\theta)). \blacksquare \end{aligned}$$

Note that the proof that $\varphi^-(\theta)$ is invariant is similar replacing max by min.

Now we want to prove that $\varphi^+(\theta)$ is upper semi-continuous. This also has been stated in Jäger's paper [37] but we give the proof here.

Theorem 1.2 *Let $T : \mathbb{T} \times I \to \mathbb{T} \times I$ be a continuous skew product where the fibre map is monotonic increasing and K is a compact invariant set. Then the upper bounding graph $\varphi^+(\theta)$ is upper semi-continuous.*

Proof. Suppose $\varphi^+(\theta)$ is not upper semi-continuous at some $\theta \in \mathbb{T}$. Then there is an $\varepsilon > 0$ such that for all $\delta > 0$ there exists $\tilde{\theta}$ such that

$$\theta - \delta < \tilde{\theta} < \theta + \delta.$$

We pick $\delta = 1/n$ and let $\tilde{\theta}_n$ be such that

$$|\theta - \tilde{\theta}_n| < \frac{1}{n} \quad \text{and} \quad \varphi^+(\tilde{\theta}_n) > \varphi^+(\theta) + \varepsilon.$$

By compactness, there is a subsequence $\tilde{\theta}_{n_k}$ such that $\varphi^+(\tilde{\theta}_{n_k}) \to H \geq \varphi^+(\theta) + \varepsilon$ and $\tilde{\theta}_{n_k} \to \theta$ as $k \to \infty$. However, since $\varphi^+(\theta)$ is already a maximum as in (1.8), there is no such H. Thus, we have proved that $\varphi^+(\theta)$ is upper semi-continuous. ■

We can also show that the lower bounding graph $\varphi^-(\theta)$ is lower semi-continuous by using the contradiction of Definition 1.3.

Jäger [37] called the set K 'filled-in' where

$$K = [\varphi^-, \varphi^+] = \{(\theta, x) : \varphi^-(\theta) \leq x \leq \varphi^+(\theta).\}$$

Interestingly, under certain circumstances K represents the *global attractor* [30] of system F, which is defined as

$$K = \bigcap_{n \in \mathbb{N}} T^n(\mathbb{T}^1 \times I).$$

Although we have explained that invariant graphs appear in the skew product systems, not all skew product systems have invariant graphs. In this work, we will consider some skew product systems which have non-continuous invariant graphs.

1.2 Thesis outline

This thesis is mainly about the characterization of stability index on the local structure of riddled basins of attraction for both skew product and non-skew product maps.

The rest of this thesis is organized as follows. In Chapter 2, we review the theory of dynamical systems in the contexts of topological and measurable dynamics. We consider systems defined on metric spaces (X, d) by a continuous map $f : X \to X$. We introduce the concepts of metric spaces and ω-limit set of the orbits f^n in the first and second sections respectively. In Section 2.3 we discuss some background on measure theory as we use the Lebesgue measure ℓ to measure the basins of the

attractor. In this section, we also discuss one of techniques in dimension theory, namely, Hausdorff measure and its dimension where we will use them to estimate the dimension of zero and non-zero sets of the invariant graph for Keller's map. To define an attractor A, some basic notions including basins of attraction $\mathcal{B}(A)$ and Milnor attractor are discussed in Section 2.4. Follow from these, a formal definition for riddled basin is given where it has positive Lebesgue measure, i.e. $\ell(\mathcal{B}(A)) > 0$ but does not contain any open set. In Section 2.5, we review ergodic theory which involves the study of invariant measures for measurable transformations f. We will use one of the main results of ergodic theory, namely Birkhoff's Ergodic Theorem to calculate the stability index for a simple example of piecewise linear map in Chapter 4. Moreover, in Section 2.6 two examples of Markov maps are explored namely the doubling map and the more generalized skewed doubling map, where both of them satisfy the piecewise expanding and Markov properties.

In the first section of Chapter 3, we discuss the stability index defined for a point as initially proposed by Podvigina and Ashwin [59]. As we said earlier, the stability index has been applied firstly in the case of heteroclinic cycles. In Section 3.2, we relate the results obtained by Podvigina and Ashwin [59] and Lohse [52] with our stability index. Next, in Section 3.3, we give a stronger result on the basic properties of the stability index for the point by showing that the proportion of the points that are attracted to A inside the ε-neighbourhood is *exponentially asymptotically tightly bounded* (denoted as $\tilde{\Theta}$) by ε^c for some constants c. Section 3.4 is our first result where we establish a relation between the stability index at a point and the local dimension of measures. This result was suggested by Tobias Jäger (private communication). Finally, we introduce the stability index modified from [59] for a set of in particular for the attractor A.

In Chapter 4, we use an analytical approach in order to compute the stability index for riddled basin for a simple example of a skew product system. We consider a piecewise expanding linear map which has two coexisting Milnor attractors where the first basin is riddled with the second basin. Hence, our first aim of this chapter is to prove the existence of this riddled basin. Before we do the proof, we define the boundary between the two basins in Section 4.2. To show the presence of riddled basin, we prove in our main theorem, Theorem 4.4 in Section 4.3. First we show that the measure for both basins is full since for almost all points that start below the boundary will tend to the first basin and for almost all points that start above the boundary will tend to the second basin. Secondly, we prove that the first basin can has either positive or zero measure depending on the range of the parameters. Finally we show that the second basin is everywhere dense and has positive measure in any neighbourhood in the whole space X. After that, we calculate the stability index both at a point as well as for the attractor in sections 4.4 and 4.5 respectively.

Interestingly, we obtain that the formula of the stability index at a point contains the formula of stability index for the attractor and the local Lyapunov exponents where we produce this result as in Corollary 4.8. This is obtained only when the limit of the stability index converges or exists. We also show that it is possible to obtain a case where the limit is not converge in Section 4.6. Instead, the index oscillates between the liminf and limsup. Our main results for the stability indices are of theorems 4.5, 4.6, 4.7 and 4.9. All materials in this chapter are original.

We use Keller's skew product map [44] in both Chapter 5 and 6. Chapter 5 is about the numerical computation of the stability index for the points on the attractor. In [44], Keller computed the stability index for the points under the invariant graph. In our study, we take another approach to understand his map, i.e. by inverting the map to obtain attractors whose basins of attraction have a basin boundary. By doing so, the invariant graph which is an attractor in Keller's map becomes a basin boundary in the inverse map. In Chapter 6 we present the computation of Birkhoff averages for periodic points in Markov maps where we verify the maximum and minimum measures as obtained in Keller [44, Example 1]. Furthermore, we also investigate the dimension for both zero and non-zero sets for the invariant graph using the Hausdorff dimension. To do this, we conjecture Theorem 2 in Keller and Otani [46] to a complete range of parameter r of Keller's map.

In Chapter 7, we consider a non-skew product map with a riddled basin from Ashwin *et al.* [6; 7] and we compute the stability index numerically for the attractor of the system.

We complete our work by summarizing our contributions in this thesis mainly for the stability index for the local geometry of riddled basins in Chapter 8. We also discuss some limitations of our results which we think it is possible to obtain more general results on the stability index. Some appendices regarding the basic asymptotic notations and MATLAB and Maple codes for the three models are also included.

2 Topological and Measurable Dynamics

In this chapter we discuss some topological and measure properties of dynamical systems. Generally speaking, topological dynamics investigates the asymptotic properties of the orbits in dynamical systems. In particular, it is a study of a topological space X with continuous transformations f. We begin by reviewing metric spaces and mappings together with the ω-limit set of the orbits of points x in the system.

In order to discuss measurable dynamics, we give some background of measure theory and we relate this with the section of attractors in dynamical systems in the sense that every basin has its own measure where we equip this basin with Lebesgue measure. In this thesis, we use this measure to approximate the measure for the riddled basins. Besides Lebegue measure, we also consider the Dirac delta measure; a measure which we compute for the periodic points. Moreover, we briefly discuss Hausdorff measure and Hausdorff dimension.

Moreover, we explore some basic ideas of ergodic theory including the well-known result; Birkhoff's Ergodic Theorem which was established by George Birkhoff in 1931. This result can be used to compute the averages of periodic points which approach to certain limits. We also present the well-known example of Markov maps where one can investigate the behaviour of orbits using *symbolic dynamics*.

Finally, we discuss the Lyapunov exponents which measures the complexity (or chaos) of a system. In this thesis, we will use the Lyapunov exponents to identify the riddled basin in the skew product system and properties of these are very useful to characterize attractors in a system.

2.1 Metric spaces

Let X be a nonempty set. A function $d : X \times X \to \mathbb{R}$ is a metric on X, also called a *distance function*, assigning to each ordered pair (x, y) a nonnegative real number $d(x, y)$, satisfying the following properties:

(i) (*Positivity*): If $x \neq y$, then $d(x, y) > 0$.

(ii) $d(x, x) = 0$ for all $x \in X$.

(iii) (*Symmetry*): $d(x, y) = d(y, x)$ for all $x, y \in X$.

(iv) (*Triangle inequality*): $d(x, y) + d(y, z) \geq d(x, z)$ for all $x, y, z \in X$.

The set X together with a metric d, (X, d) is called a *metric space*. Also, one calls $d(x, y)$ the distance from x to y [13].

Let X be a metric space. For any $x \in X$, and any $\varepsilon > 0$, an *open ball of radius ε around x* is the set

$$B_\varepsilon(x) = \{y \in X : d(y, x) < \varepsilon\},$$

and a *closed ball of radius ε around x* is defined by

$$U_\varepsilon(x) = \{y \in X : d(y, x) \leq \varepsilon\}.$$

We can think of $B_\varepsilon(x)$ and $U_\varepsilon(x)$ as small neighbourhoods around the point x. The notation of $B_\varepsilon(x)$ will be used throughout this thesis as it appears in the definition of stability index. Other important definitions for this thesis are as follows:

Definition 2.1 (Open set [66]) *A set U is said to be* open *in X if for each point x in U, there exists a real number $\varepsilon > 0$ such that any open ball of radius ε around x is contained in U, i.e.,*

$$\forall x \in U \quad \exists \varepsilon > 0 \text{ such that } B_\varepsilon(x) \subset U. \tag{2.1}$$

Definition 2.2 (Closed set [66]) *A set U is called* closed *if the complement of U is open.*

Definition 2.3 (Closure of a set [66]) *The* closure of U, *written as $\overline{U}$, is the union of a set U and all its limit points, i.e.*

$$\overline{U} = U \cup \{x : |x_k \to x| \to 0 \text{ as } k \to \infty \text{ for a sequence } \{x_k\} \text{ of } U\}.$$

In fact, we can write $\overline{B_\varepsilon(x)} = U_\varepsilon(x)$.

Definition 2.4 (Dense set [66]) *A set $U \subset X$ is said to be* dense *in X if for every $x \in X$ and $\varepsilon > 0$, there is a point $\tilde{x} \in U$ such that $0 < |x - \tilde{x}| < \varepsilon$. Thus U is dense in X if every point of X is a limit point of U.*

Definition 2.5 (Compact set [26]) *A set $U \subset X$ is* compact *if any collection of open sets which covers U (i.e. with union containing U) has a finite subcollection*

which also covers U.

Note that if $U \in \mathbb{R}^n$, then U is compact if and only if it is closed and bounded [66].

2.2 Mappings: Fixed, periodic and pre-periodic points

From now on, we will denote X as a metric space. We may often suppose that $f : X \to X$ is a continuous map; where the definition is as below:

Definition 2.6 (Continuous map [51]) *Let X be a metric space. A map $f : X \to X$ is said to be* continuous *if for every open set $U \subset X$, $f^{-1}(U)$ is open in X. In other words, f is continuous if the preimage of any open set is an open set.*

The *orbit* of a point $x_0 \in X$ is

$$\{f^n(x_0)\}_{n=0}^{\infty} = \{x_0, f(x_0), f(f(x_0)), \ldots, f^n(x_0), \ldots\},$$

where f^n denotes the nth iterate of f, i.e.,

$$f^n(x_0) = f(f(f(\ldots f(f(x_0))\ldots))), \quad n \geq 0.$$

The point $x_0 \in X$ is a *fixed point* for $f : X \to X$ if:

$$f(x_0) = x_0.$$

The point $x_0 \in X$ is a *periodic point* of period n for $f : X \to X$ if:

$$f^n(x_0) = x_0,$$

for some $n > 0$. Therefore we say n is the *period* of x_0 and $\{x_0, f(x_0), f^2(x_0), \ldots, f^{n-1}(x_0)\}$ is a *period-n* orbit of f. We can define the ω-limit set, from the orbit of x as follows:

Definition 2.7 (ω-limit set [4]) *Let $x \in X$. The ω-limit set $\omega(x)$ is defined as*

$$\omega(x_0) = \{\textit{limits of } f^n(x_0) \textit{ as } n \to \infty\} = \bigcap_{m \geq 0} \overline{\bigcup_{n \geq m} f^n(x_0)}. \tag{2.2}$$

2.3 Measure theory

A measure is a way of assigning a 'size' on a set such that if a set is decomposed into a finite or infinite (but still countable) number of pieces, then the size of the whole is the sum of the sizes of the pieces. A particularly important example is the Lebesgue measure on a Euclidean space $\mathbb{R}^n$. For definitions in measure theory, we mainly refer to the books by Walters [65] and Falconer [26].

Definition 2.8 (**σ-algebra [65]**) *Let X be a set. A collection $\mathfrak{B}$ of subsets of X is called* σ-algebra *if:*

(i) $X \in \mathfrak{B}$.

(ii) *if* $B \in \mathfrak{B}$ *then* $X \setminus B \in \mathfrak{B}$.

(iii) *if* $B_n \in \mathfrak{B}$ *for* $n \geq 1$ *then* $\bigcup_{n=1}^{\infty} B_n \in \mathfrak{B}$.

We then call the pair $(X, \mathfrak{B})$ a *measurable space*. Note that from the condition (iii) above, $\mathfrak{B}$ is closed under countable unions. However, when $\mathfrak{B}$ is closed under finite unions, we have that if $B_1, \ldots, B_n \in \mathfrak{B}$, then $\bigcup_{i=1}^{n} B_i \in \mathfrak{B}$. In this case we call $\mathfrak{B}$ an *algebra* of subsets of X. Thus, it is clear that every σ-algebra is an algebra [65].

Now we introduce *Borel sets* $\mathfrak{B}$ which are defined to be the smallest collection of subsets of X which have the following properties [26]:

(a) every open set and every closed set is a Borel set, i.e. if U is open or closed then $U \in \mathfrak{B}$.

(b) the union of every finite or countable collection of Borel sets is a Borel set, i.e. if $\{U_i\} \in \mathfrak{B}$ is countable, then $\cup_i U_i \in \mathfrak{B}$.

(c) the intersection of every finite or countable collection of Borel sets is a Borel set, i.e. if $\{U_i\} \in \mathfrak{B}$ is countable, then $\cap_i U_i \in \mathfrak{B}$.

In other words, the Borel sets $\mathfrak{B}$ are generated from the open sets (or closed sets) through the operations of countable union and countable intersection. Moreover, for a metric space X, the collection of all the Borel sets on X forms a σ-algebra, known as the *Borel σ-algebra*. This Borel σ-algebra is the σ-algebra generated by the open sets (or by the closed sets) [65]. We will still use the notation $\mathfrak{B}$ to denote a Borel σ-algebra for later use.

Now we want to define a measure on the Borel sets. Any measure defined on the Borel sets is called a *Borel measure*. Let $X \subset \mathbb{R}^n$. One can define a Borel measure for each subset of X as follows:

Definition 2.9 (Borel measure [26]) *μ is said to be a* measure *on $\mathbb{R}^n$ if μ assigns a non-negative number, possibly ∞, to each subset of $\mathbb{R}^n$ such that*

(a) $\mu(\emptyset) = 0$, (null empty set)

(b) $\mu(A) \leq \mu(B)$ if $A \subset B$ where $A, B \in \mathfrak{B}$, (monotonicity)

(c) If $A_1, A_2, \ldots$ is a countable (or finite) sequence of sets then

$$\mu\left(\bigcup_{i=1}^{\infty} A_i\right) \leq \sum_{i=1}^{\infty} \mu(A_i), \text{ (countable subadditivity)}$$

and if A_i are disjoint Borel sets, the following equality holds:

$$\mu\left(\bigcup_{i=1}^{\infty} A_i\right) = \sum_{i=1}^{\infty} \mu(A_i),$$

where $A_i \in \mathfrak{B}$.

We call $\mu(A)$ the measure of the set A. Note that condition (a) says that the empty set has zero measure, condition (b) says that a larger set has larger measure and condition (c) says that if a set is a union of a countable number of pieces (which may overlap) then the sum of the measure of all pieces is at least equal to the measure of the whole set. If a set is decomposed into a countable number of disjoint Borel sets then the total measure of the pieces equals the measure of the whole [26].

According to Walters [65], we call a triple $(X, \mathfrak{B}, \mu)$ a *measure space*. If $\mu(X) < \infty$, then we say μ is a *finite measure*. Moreover, if $\mu(X) = 1$, then we call μ is a *probability measure* and $(X, \mathfrak{B}, \mu)$ is said to be a *probability space*. From the above definition, any measure μ defined on the Borel σ-algebra is also called a *Borel probability measure*. Therefore, throughout this thesis, we will denote $\mathcal{M}(X)$ the set of all Borel probability measures on X.

2.3.1 Examples of measures

In this section, we consider two examples of measures, namely the Lebesgue measure and the Dirac delta measure.

Lebesgue measure

The Lebesgue measure is a standard way to measure a set of the n-dimensional Euclidean space. It is in fact a generalization of 'length' or 'area' or 'volume'

to a large collection of subsets of $\mathbb{R}^n$ which includes the Borel sets [25]. For instances, 1-dimensional Lebesgue measure ℓ^1 coincides with the measure of length, 2-dimensional Lebesgue measure ℓ^2 with the measure of area and 3-dimensional Lebesgue measure ℓ^3 with the measure of volume.

For ℓ^1, the length of open and closed intervals is $\ell^1(a,b) = \ell^1[a,b] = b - a$. If $A_i = \cup_i [a_i, b_i]$ is a finite or countable union of disjoint intervals, then the sum of the length of the intervals is $\ell^1(A) = \sum(b_i - a_i)$.

Definition 2.10 (1-dimensional Lebesgue measure [25]) *Let A be an arbitrary subset of $\mathbb{R}^n$. Then the 1-dimensional Lebesgue measure of A, $\ell^1(A)$ is defined as*

$$\ell^1(A) = \inf\left\{\sum_{i=1}^{\infty}(b_i - a_i) : A \subset \bigcup_{i=1}^{\infty}[a_i, b_i]\right\},$$

which can be generalized to the n-dimensional case:

Definition 2.11 (n-dimensional Lebesgue measure [25]) *If $A = \{(x_1, \ldots, x_n) \in \mathbb{R}^n : a_i \leq x_i \leq b_i\}$, then the n-dimensional Lebesgue measure ℓ^n is given by*

$$\ell^n(A) = \inf\left\{\sum_{i=1}^{\infty} vol^n(A_i) : A \subset \bigcup_{i=1}^{\infty} A_i\right\},$$

where $vol^n(A) = (b_1 - a_1)(b_2 - a_2)\ldots(b_n - a_n)$.

Throughout this thesis, we will denote the n-dimensional Lebesgue measure on $\mathbb{R}^n$ by $\ell(\cdot)$ if the context is clear.

Dirac delta measure

In general, the delta function can be defined either as a distribution or as a measure. We define the delta function as a function from Borel subsets of X to $\{0,1\}$, i.e.,

$$\delta_x(A) : \mathfrak{B} \to \{0,1\}$$

and for a given $x \in X$ the measure is defined by

$$\delta_x(A) = \begin{cases} 1 & \text{if } x \in A, \\ 0 & \text{if } x \notin A, \end{cases} \tag{2.3}$$

for every measurable set $A \in \mathfrak{B}$. Then δ_x is said to be the *Dirac delta measure supported at x*. We can also think this as a point mass concentrated at x since the

support of δ_x is a singleton $\{x\}$. In this thesis, we will use δ_x on the periodic points in order to compute the Birkhoff averages for the case of skew product system.

2.3.2 The restriction of Lebesgue measure

The restriction of any measure to a Borel set is also a measure.

Definition 2.12 (Restriction of a measure to a Borel set [26]) *Let ℓ be a measure on $\mathbb{R}^n$ and N a Borel subset of $\mathbb{R}^n$. We define a measure μ on $\mathbb{R}^n$ the* restriction of ℓ to N *by*

$$\mu(A) = \ell(A \cap N),$$

for every set A. Then μ is a measure on $\mathbb{R}^n$ with support contained in $\overline{N}$.

The above measure can also be written as $\ell|_N(A)$.

The restriction of a measure is also a measure because one can verify that the following properties hold:

(a) $\ell|_N(A) = \ell(A \cap N) > 0$. (nonnegativity)

(b) Suppose $B \subseteq A$, which implies $B \cap N \subseteq A \cap N$. Then

$$\ell|_N(B) = \ell(B \cap N) \leq \ell(A \cap N) = \ell|_N(A). \text{ (monotonicity)}$$

(c) If $A_1, A_2 \in \mathfrak{B}$ then

$$\begin{aligned} \ell|_N(A_1 \cup A_2) &= \ell(A_1 \cup A_2 \cap N), \\ &= \ell(A_1 \cap N \cup A_2 \cap N) \leq \ell(A_1 \cap N) + \ell(A_2 \cap N), \\ &= \ell|_N(A_1) + \ell|_N(A_2). \text{ (subadditivity)} \end{aligned}$$

We will use $\ell|_N(A)$ to relate the stability index with the local dimension of measures in Chapter 3.

2.3.3 Local dimensions of measures

In this section, we discuss the notion of lower and upper local dimension for a measure. In fact, we are interested in the dimension of sets rather than just the measure of the sets. Some authors use the term of pointwise dimension instead of local dimension. This local dimension is basically related to the measure of small balls in the phase space and the local dimension of a point is always defined with

respect to a measure. This local dimension was introduced by Young [71] and has been studied by many papers for examples Farmer *et al.* [27], Ledrappier and Young [50], Young [70], Barreira *et al.* [11], Barreira and Wolf [12] and Olsen [56].

The following definition of lower and upper local dimension can be used to characterize the local geometrical stucture of measure ℓ and are also important tools in the theory of dimension of dynamical systems [10; 24; 35; 71]. In Falconer [25], the *lower* and *upper local dimension* of a measure μ at $x \in X$ with respect to μ are defined respectively by

$$\underline{\dim}_{loc}\mu(x) = \liminf_{\varepsilon\to 0} \frac{\log \mu(B_\varepsilon(x))}{\log \varepsilon}$$

and

$$\overline{\dim}_{loc}\mu(x) = \limsup_{\varepsilon\to 0} \frac{\log \mu(B_\varepsilon(x))}{\log \varepsilon},$$

where $B_\varepsilon(x)$ is the ε-neighbourhood around x. This local dimension exists at x if $\underline{\dim}_{loc}\mu(x) = \overline{\dim}_{loc}\mu(x)$, and we will use $\dim_{loc}\mu(x)$ to denote the common value, i.e. the local dimension of the measure μ at point x is

$$\dim_{loc}\mu(x) = \lim_{\varepsilon\to 0} \frac{\log \mu(B_\varepsilon(x))}{\log \varepsilon}, \tag{2.4}$$

provided that this limit exists.

2.3.4 Hausdorff measure and its dimension

In this section, we introduce the notions of Hausdorff measure and its dimension. Generally speaking, Hausdorff dimension for a point is zero, Hausdorff dimension for a line or curve is 1, Hausdorff dimension for a plane is 2, etc. Meanwhile with Hausdorff measure, we are counting the number of points in a set, measure the length of a curve in a set, measure the area, volume, etc [26]. We refer their definitions in Falconer's book [26].

Let (X, d) be a metric space. For any subset $U \subset X$, the *diameter* of U is defined as

$$|U| := \sup\{d(x, y) : x, y \in U\},$$

i.e., the greatest distance between any two points in U. If $\{U_i\}$ is a countable (or finite) collection of sets of diameter at most δ that cover S, i.e. $S \subset \bigcup_{i=1}^{\infty} U_i$ with $0 \le |U_i| \le \delta$ for each i, we say $\{U_i\}$ is a δ-*cover* of S.

Suppose that S is a subset of X and α is a non-negative number. For any $\delta > 0$ we

define

$$\mathcal{H}^{\alpha}_{\delta}(S) := \inf\left\{\sum_{i=1}^{\infty}|U_i|^{\alpha} : \{U_i\} \text{ is a } \delta\text{-cover of } S\right\}. \tag{2.5}$$

From the above, we want to minimize the sum of αth powers of the diameters. As δ decreases, the permissible covers of S in (2.5) is reduced. Therefore the infimum $\mathcal{H}^{\alpha}_{\delta}(S)$ approaches to a limit as $\delta \to 0$. Thus, we can define *α-dimensional Hausdorff measure* of S

$$\mathcal{H}^{\alpha}(S) = \lim_{\delta \to 0} \mathcal{H}^{\alpha}_{\delta}(S), \tag{2.6}$$

where this limit exists for all Borel subsets of X.

Definition 2.13 ([26]) *The* Hausdorff dimension *of $S \subset X$ is defined to be*

$$\dim_H(S) = \inf\{\alpha : \mathcal{H}^{\alpha}(S) = 0\} = \sup\{\alpha : \mathcal{H}^{\alpha}(S) = \infty\}.$$

From this definition, we say that $\dim_H(S)$ can be defined as the infimum of the set $\alpha = [0, \infty)$ such that the α-dimensional Hausdorff measure of S (in (2.6)) is zero. Similarly, it can also be defined as the supremum of the set $\alpha = [0, \infty)$ such that the α-dimensional Hausdorff measure of S is infinite. Note also that α can be both integer and non-integer values.

In fact, this Hausdorff measure can be related to the Lebesgue measure where in the space of $\mathbb{R}^n$, the n-dimensional Hausdorff measure, within a constant multiple, is just the n-dimensional Lebesgue measure ℓ^n (Definition 2.11). More precisely, if S is a Borel set of $\mathbb{R}^n$, then

$$\mathcal{H}^n(S) = c_n^{-1}\mathrm{vol}^n(S),$$

where c_n is the volume of an n-dimensional ball of diameter 1 and vol^n is n-dimensional Lebesgue measure. If n is even, then

$$c_n = \frac{\pi^{n/2}}{2^n(n/2)!},$$

and if n is odd, then

$$c_n = \frac{\pi^{(n-1)/2}((n-1)/2)!}{n!}.$$

See examples in [26]. In this thesis, we will use Hausdorff dimension for both zero and non-zero sets of invariant graph for a skew product system which will be discussed in Chapter 6. Recall that from Definition 1.1, we know that the invariant graph $\varphi : \mathbb{T} \to I$. The zero set of φ is the subset of $\mathbb{T}$ on which $\varphi(\theta) = 0$ where $\theta \in \mathbb{T}$.

More precisely, we denote

$$\varphi^{-1}(0) = \{\theta \in \mathbb{T} : \varphi(\theta) = 0\}.$$

Meanwhile the non-zero set of φ is the subset of $\mathbb{T}$ on which φ is nonzero, i.e. it is the complement of the zero set of φ [48].

2.3.5 Absolute continuity of measures

In this study, we will consider the case where a measure μ is absolutely continuous with respect to (w.r.t.) the Lebesgue measure ℓ. Let $(X, \mathfrak{B})$ be a measurable space and let ℓ and μ be two measures on $(X, \mathfrak{B})$.

Definition 2.14 (Absolute continuity [66]) *The measure μ on Borel subsets A of $\mathfrak{B}$ is* absolutely continuous *w.r.t. ℓ if $\mu(A) = 0$ for every $A \subset \mathfrak{B}$ such that $\ell(A) = 0$ [1]. If ℓ is finite, i.e. $\ell(X) < \infty$, then for any $\varepsilon > 0$, there is $\delta > 0$ such that $\mu(A) < \varepsilon$ for every $A \subset \mathfrak{B}$ if $\ell(A) < \delta$.*

From the above definition, we can also say that μ is absolutely continuous w.r.t. ℓ if

$$\forall A \subset \mathfrak{B},\ \ell(A) = 0 \implies \mu(A) = 0.$$

The theorem below is a consequence from the above definition.

Theorem 2.1 (Radon-Nikodym [66]) *If μ is absolutely continuous w.r.t. ℓ, there exists a unique Lebesgue integrable function $f \in L^1(\mathfrak{B})$ such that*

$$\mu(A) = \int_A f \ d\ell \tag{2.7}$$

for every measurable Borel subsets $A \subset \mathfrak{B}$.

Moreover, we call $f = \frac{d\mu}{d\ell}$ the *Radon-Nikodym derivative* that is depends on two measures, μ and ℓ [43].

2.4 Attractors in dynamical systems

Recall that we consider X to be a metric space and $f : X \to X$ to be a continuous map. Before we proceed with definition of riddled basins, let us review some basic concepts that are vital in the study of topological dynamics.

[1] Mathematically, μ is absolutely continuous w.r.t. ℓ if $\mu(A) = 0\ \forall A \in \{A \subset \mathfrak{B} : \ell(A) = 0\}$.

2.4.1 Basic definitions

We begin this subsection with the definition of invariant set. Some examples of invariant sets are the fixed points, periodic orbits, limit cycles and attractors. More precisely,

Definition 2.15 (**Invariant set [29]**) *A compact set $A \subset X$ is a* forward invariant set *(or* backward invariant set*) if $x \in A$ implies that $f(x) \in A$ (or $f^{-1}(x)$). A is* invariant *if it is both forward invariant and backward invariant.*

Note that the ω-limit set as defined in Definition 2.7 is an invariant set, in particular invariant under f. Following from the definition of ω-limit set, Milnor [54] defines *basin of attraction* as

Definition 2.16 (**Basin of attraction**) *The basin of attraction $\mathcal{B}(A)$ is the set of points $x \in X$ whose ω-limit set is contained in A, i.e.,*

$$\mathcal{B}(A) = \{x \in X : \omega(x) \subset A\}, \tag{2.8}$$

where the $\omega(x)$-limit set of x is as defined in (2.2).

Alexander *et al.* [1] describes that the word 'contained in' in the above definition means the set of points whose orbits are asymptotic to A. The basin of attraction in (2.8) can also be written as

$$\mathcal{B}(A) = \{x \in X : \omega(x) \subset A\} = \{x : \lim_{n\to\infty} d(f^n(x), A) \to 0\}, \tag{2.9}$$

where $d(x, A) = \inf_{y\in A} |x - y|$ is the Hausdorff distance.

We use the definition of basin of attraction to define the notions of attractor. In 1985, Milnor [54] introduced the definition of an attracting set or *attractor* as follows:

Definition 2.17 (**Milnor attractor**) *A compact invariant subset $A \subset X$ is called an* attractor *if it satisfies the following conditions:*

(i) the basin of attraction $\mathcal{B}(A)$, consisting of all points $x \in X$ for which $\omega(x) \subset A$, must have strictly positive Lebesgue measure.

(ii) there is no strictly smaller closed set $A' \subset A$ so that $\mathcal{B}(A') = \mathcal{B}(A)$ up to a set of Lebesgue measure zero.

In the skew product case, the attractor is defined only by considering attraction in the fibres. In particular, the distance of a point c from the attractor A is measured as the distance of c from the intersection of the attractor A and the fibre containing c. As a consequence, the attraction means that this distance goes to zero [2].

Ashwin *et al.* [7] characterize other commonly considered notions of attraction as follows.

Definition 2.18 (**Lyapunov stable**) *A is Lyapunov stable if for any neighbourhood U of A there exists a neighbourhood V of A s.t. $f^n(V) \subset U$ for all $n \in \mathbb{N}$.*

Definition 2.19 (**Asymptotically stable attractor**) *A is an asymptotically stable attractor if it is Lyapunov stable and $\mathcal{B}(A)$ contains a neighbourhood of A.*

2.4.2 Attractors with riddled basins

In this subsection, we first discuss the notion of the riddled basin as defined by Alexander *et al.* [1].

Definition 2.20 (**Riddled basin [1]**) *The basin of attraction of an attractor is riddled if its complement intersects every disk in a set of positive measure.*

Note that the term 'disk' in the above definition refers to the open ball with radius $\varepsilon > 0$ or the ε-neighbourhood in our case.

To be more specific, let X be a metric space and let $f : X \to X$ be a continuous map. Suppose A is an attractor for f and A is a compact invariant set $A \subset X$. We recall that $B_\varepsilon(x)$ the open ball with radius ε at point x in X. Previously, Ashwin *et al.* [7] has defined the following:

Definition 2.21 (**Riddled and intermingled basins [7]**) *A Milnor attractor A has a* riddled basin *if for all $x \in \mathcal{B}(A)$ and $\varepsilon > 0$, then*

$$\ell(B_\varepsilon(x) \cap \mathcal{B}(A))\ell(B_\varepsilon(x) \cap \mathcal{B}(A)^c) > 0. \tag{2.10}$$

If there is another Milnor attractor C such that $\mathcal{B}(A)^c$ in (2.10) can be replaced with $\mathcal{B}(C)$, then the basin of A is riddled with the basin of C. If $\mathcal{B}(A)$ and $\mathcal{B}(C)$ are riddled with each other (i.e. $\mathcal{B}(A)$ is riddled with $\mathcal{B}(C)$ and $\mathcal{B}(C)$ is riddled with $\mathcal{B}(A)$), then the basins are intermingled.

In this thesis, we will consider for more specific case where there are only two attractors such that the basin of one of the attractor is riddled with the basin of the other attractor:

Definition 2.22 *The basin of a Milnor attractor A is riddled with the basin of a second Milnor attractor C, if for all $\varepsilon > 0$ and $x \in \mathcal{B}(A)$,*

$$\ell(B_\varepsilon(x) \cap \mathcal{B}(A)) > 0 \text{ and } \ell(B_\varepsilon(x) \cap \mathcal{B}(C)) > 0. \tag{2.11}$$

The above definition says that basin of A is riddled with basin of C, where if we take any point x in the first basin $\mathcal{B}(A)$, then there is a positive probability that the nearby point y within $B_\varepsilon(x)$ will be inside the second basin $\mathcal{B}(C)$. Note that if $\mathcal{B}(C)$ is open and dense in X and A is a Milnor attractor then $\ell(B_\varepsilon(x) \cap \mathcal{B}(C)) > 0$ for any $x \in \mathcal{B}(A)$ and $\varepsilon > 0$ and this implies that basin of A is riddled with basin of C. Thus, the condition (2.11) must be satisfied.

2.5 Ergodic theory

In this section, we discuss some essential concepts from ergodic theory. Generally speaking, ergodic theory is the study of invariant measures for a measurable transformation $f : X \to X$. Let $(X, \mathfrak{B}, \mu)$ be a probability space. If $A \in \mathfrak{B}$, we can define

$$f^{-1}(A) = \{x \in X | f(x) \in A\},$$

where $f^{-1}(A)$ is the *pre-image* of A under f.

Definition 2.23 [65] *A transformation $f : X \to X$ is* measurable *if for all $A \in \mathfrak{B}$ we have $f^{-1}(A) \in \mathfrak{B}$.*

2.5.1 Invariant measures

An invariant measure is a measure that is preserved by maps. There is a paper by Hunt *et al.* [36] which discusses some examples of maps that have invariant measures.

Definition 2.24 ([9]) *Let $f : X \to X$ be a measurable transformation. A measure μ in X is said to be* f-invariant *if*

$$\mu(A) = \mu(f^{-1}A), \tag{2.12}$$

for all $A \in \mathfrak{B}$.

From Section 2.3, we recall that $\mathcal{M}(X)$ is the set of all Borel probability measures on X. Now let X be a metric space and $f : X \to X$ a continuous transformation. Then we say f induces a map on $\mathcal{M}(X)$ where $f : \mathcal{M}(X) \to \mathcal{M}(X)$ which implies that $(f\mu)(A) = \mu(f^{-1}A)$. Here we are interested with the members of $\mathcal{M}(X)$ that are invariant for f. Therefore we define the following

Definition 2.25 ([65]) *Let $\mathcal{P}(f)$ be the set of all f-invariant probability measures, i.e.*

$$\mathcal{P}(f) = \{\mu \in \mathcal{M}(X) \mid f\mu = \mu\}.$$

From this definition, $\mathcal{P}(f) \subset \mathcal{M}(X)$. The above set consists of all $\mu \in \mathcal{M}(X)$ which makes f as a measure-preserving transformation (m.p.t.) of $(X, \mathfrak{B}, \mu)$.

Definition 2.26 ([65]) *$f : X \to X$ is an* m.p.t. *for $\mu \in \mathcal{M}(X)$ if f is measurable and $\mu(f^{-1}(A)) = \mu(A)$ for all $A \in \mathfrak{B}$.*

2.5.2 Ergodic measures

Definition 2.27 ([9]) *A measure $\mu \in \mathcal{P}(f)$ is said to be* ergodic *for f if for any f-invariant measurable set $A \subset X$ (means that $f^{-1}A = A$) either $\mu(A) = 0$ or $\mu(X \setminus A) = 0$.*

We denote the set of ergodic measures by $\mathcal{E}(f)$ and therefore $\mathcal{E}(f) \subsetneq \mathcal{P}(f)$.

The following theorem shows a fundamental result from ergodic theory which was proved by G.D. Birkhoff in 1931. We denote $L^1(X)$ the set of Lebesgue integrable functions from X to $\mathbb{R}$. Note that this theorem holds if and only if μ is ergodic.

Theorem 2.2 (Birkhoff's Ergodic Theorem [14]) *Let $f : X \to X$ be a measurable transformation and let $\varphi : X \to \mathbb{R}$ be a measurable function. For each $\mu \in \mathcal{P}(f)$ and $\varphi \in L^1(X)$, if μ is an invariant ergodic probability measure, then for μ-almost all $x \in X$ the following holds*

$$\lim_{n\to\infty} \frac{1}{n} \sum_{i=0}^{n-1} \varphi(f^i(x)) = \int \varphi \, d\mu. \tag{2.13}$$

In particular, the limit exists for μ-almost all $x \in X$.

The left hand side of (2.13) shows how often the orbit of x (namely $x, f(x), f^2(x), \ldots$) lies in A while the right hand side is the measure of A. The function φ can be defined as a *characteristic function* for some subset $A \subset X$ such that

$$\varphi(x) = \begin{cases} 1 & \text{if } x \in A, \\ 0 & \text{if } x \notin A. \end{cases}$$

2.5.3 Invariant probability measures on periodic points

We illustrate the particular case of a measure μ on a periodic point x. Suppose that $x = f^n(x)$ is a periodic point with period n. Then the probability measure

$$\mu = \frac{1}{n}\sum_{i=0}^{n-1} \delta_{f^i(x)}, \tag{2.14}$$

satisfies (2.12) and $\mu(X) = 1$, and so is an invariant probability measure. So from (2.13);

$$\begin{aligned}\int \varphi \, d\mu &= \int \varphi(x) \frac{1}{n}\sum_{i=0}^{n-1} \delta_{f^i(x)}(x) \, dx \\ &= \frac{1}{n}\sum_{i=0}^{n-1} \int \varphi(x) \, \delta_{f^i(x)}(x) \, dx \\ &= \frac{1}{n}\sum_{i=0}^{n-1} \varphi(f^i(x)).\end{aligned}$$

We use Theorem 2.2 above to compute the Birkhoff averages (on the left hand side of (2.13)) for periodic points for the case of a Markov map in Chapter 5.

2.6 Examples: Markov maps

Markov map is a very useful tool in the theory of dynamical systems, where it allows one to use the methods of symbolic dynamics. We follow the notations from Pollicott and Yuri [60] and Jenkinson and Pollicott [39]. In here we discuss the its properties for both doubling and skewed doubling maps folllowed by discussion of the invariant measures for both maps.

2.6.1 Dynamical setting

Let $I = [0, 1]$ be an interval. Let also $\mathcal{I} = \{I_i\}_{i=1}^k$ be a *partition* of the interval I into a finite number of closed sub-intervals $I_i = [x_{i-1}, x_i]$ for $i = 1, \ldots, k$, with endpoints $0 = x_0 < x_1 < \cdots < x_k = 1$.

Definition 2.28 (Markov map [60]) *We consider a map $T : I \to I$ which C^1 and monotone for each open intervals int$(I_i) = (x_{i-1}, x_i)$ and in order for T to be a Markov map, therefore it must satisfy the following properties:*

(i) Piecewise expanding*: There exists* $\lambda > 1$ *such that for all* $x \in \cup_i int(I_i)$ *we have* $|T'(x)| \geq \lambda$.

(ii) Markov property*: If* $T(int(I_i)) \cap int(I_j) \neq \emptyset$*, then* $T(int(I_i)) \supset int(I_j)$ *for* $i, j = 1, \ldots, k$.

For this piecewise expanding Markov interval map, we can define a $k \times k$ matrix A with entries either 0 or 1 as in the following definition.

Definition 2.29 (Transition matrix [60]) *A transition matrix* A *is defined by*

$$A(i,j) = \begin{cases} 1 & \text{if } T(int(I_i)) \cap int(I_j) \neq \emptyset, \\ 0 & \text{if } T(int(I_i)) \cap int(I_j) = \emptyset. \end{cases} \tag{2.15}$$

The first condition in (2.15) can also be written as $T(\text{int}(I_i)) = \bigcup_{j:A(i,j)=1} I_j$. In this case, we call $\mathcal{I}$ a *Markov partition* for T, and this Markov partition is not unique since any *refinement* $\bigvee_{i=0}^{n-1} T^{-i}\mathcal{I}$ is also a Markov partition [39]. Note that if $\mathcal{I}, \mathcal{J}$ are partitions, then $\mathcal{I} \bigvee \mathcal{J} = \{I_i \cap J_j : I_i \in \mathcal{I}, J_j \in \mathcal{J}\}$.

2.6.2 Example 1: The doubling map

We consider the one-dimensional doubling map $T : [0,1) \to [0,1]$ defined by

$$T(x) = 2x \pmod 1, \tag{2.16}$$

with the associated partitions $\{I_1, I_2\}$ where $I_1 = [0, 1/2)$ and $I_2 = [1/2, 1]$. Note that we can also write (2.16) as follows:

$$T(x) = \begin{cases} 2x & \text{if } 0 \leq x < 1/2, \\ 2x - 1 & \text{if } 1/2 \leq x \leq 1. \end{cases} \tag{2.17}$$

Note that this map satisfies property (i) in Definition 2.28 where it is piecewise expanding since the slope for every partition is 2, i.e. $T'(x) = 2 > 1$. This map also satisfies the Markov property since the images of I_1 and I_2 are equal to the union of the two partitions, i.e. $T(0, 1/2) = T(1/2, 1) = (0, 1) \supset (0, 1/2) \cup (1/2, 1)$. For this map, the symbolic dynamics is captured by the *transition graph* given schematically in Figure 2.1. Hence, the transition matrix for this map is

$$A = \begin{pmatrix} 1 & 1 \\ 1 & 1 \end{pmatrix}. \tag{2.18}$$

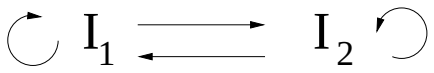

(a)

Figure 2.1 The transition graph for doubling map T and skewed doubling map T_s.

2.6.3 Example 2: The skewed doubling map

In this section, we introduce a generalization of the doubling map (2.17) to a *skewed doubling map*. It is so-called because the division of the interval into $[0, s)$ and $[s, 1]$ is not necessarily symmetric; and the usual doubling map is the special case for $s = 1/2$. This skewed doubling map has been studied by some authors including Ashwin [5] and Georgiou *et al.* [28].

We consider the one-dimensional map $T_s : [0, 1] \to [0, 1]$

$$T_s(x) = \begin{cases} \frac{x}{s} & \text{if } 0 \leq x < s, \\ \frac{x-s}{1-s} & \text{if } s \leq x \leq 1, \end{cases} \tag{2.19}$$

where we assume that $s \in [0, 1]$ and the corresponding partition is $\{[0, s), [s, 1]\}$. This map is also a piecewise expanding map since its derivatives are bounded away from 1, i.e. $T_s'(x) = 1/s > 1$ for interval $[0, s)$ and $T_s'(x) = 1/(1 - s) > 1$ for interval $[s, 1]$. It also satisfies the Markov property such that $T(\text{int}I_i) \supset I_1 \cup I_2$ for $i = 1, 2$. In addition, this map shares the same symbolic dynamics as T and therefore has the same transition matrix as in (2.18) and transition graph (Figure 2.1).

However, this map has different behaviour compared to T in terms of proportion of time the orbit of point x visiting in a certain interval. For the map T, the proportion of time the orbit in T that lies in each interval is the same, i.e. $(1/2, 1/2)$, whereas in T_s the proportion of time the orbit lies in $[0, s)$ is s and the proportion of time the orbit lies in $[s, 1]$ is $1 - s$ where $s \neq 1/2$.

2.6.4 Invariant measures for Markov maps

It is a well-known fact that the doubling map preserves the Lebesgue measure for which it is T-invariant. Here we would like to show that the Lebesgue measure is also invariant for the skewed doubling map. Let T_s be as in (2.19). Let ℓ be the Lebesgue measure on the Borel σ-algebra $\mathfrak{B}$ of the interval $[0, 1]$. Then the inverse map $T_s^{-1} : [0, 1] \to [0, 1]$ is given by

$$T_s^{-1}(x) = \begin{cases} sx & \text{if } 0 \leq x < s, \\ (1 - s)x + s & \text{if } s \leq x \leq 1. \end{cases} \tag{2.20}$$

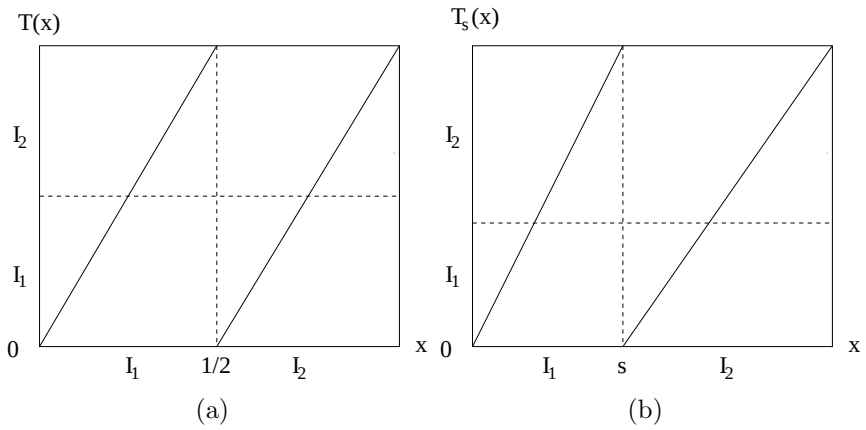

Figure 2.2 The schematic diagrams showing a) the doubling map T and b) the skewed doubling map T_s with associated partition I_i. Both maps are Markov maps since they have derivative bounded away from 1 at each interval I_i and satisfy the Markov property such that $T(\text{int}(I_i)) \supset I_1 \cup I_2$ for $i = 1, 2$.

In order to show that the Lebesgue measure ℓ is invariant for T_s, first we show that for any subinterval $[a, b] \subset [0, 1]$, we have (2.12). By (2.20) we get

$$T_s^{-1}([a, b]) = [sa, sb] \cup [(1 - s)a + s, (1 - s)b + s].$$

To show the invariance, we find the measure for the above set;

$$\begin{aligned} \ell(T_s^{-1}([a, b]) &= \ell([sa, sb] \cup [(1 - s)a + s, (1 - s)b + s]), \\ &= sb - sa + (1 - s)b + s - (1 - s)a - s, \\ &= b - a, \\ &= \ell([a, b]), \end{aligned}$$

where this shows that (2.12) holds for all intervals. Secondly, since if $J = \cup_i J_i$ is a (finite or countable) union of disjoint intervals $J_i = [a_i, b_i]$, we have

$$\ell(J) = \sum_i |b_i - a_i|,$$

we also have that $\ell(f^{-1}(J)) = \ell(J)$ holds for all J such that J is the algebra of finite unions of intervals. Finally, if the σ-algebra $\mathfrak{B}$ is generated by an algebra $\mathfrak{A}$, then ℓ is invariant for T_s if and only if

$$\ell(f^{-1}(A)) = \ell(A),$$

for all $A \in \mathfrak{A}$. Thus, this shows that it is sufficient to check only for the elements of algebra $\mathfrak{A}$ where this implies that it also holds for all Borel measurable sets $A \in \mathfrak{B}$ [53].

Besides Lebesgue measure, there are many other invariant measures for Markov

maps. This is because Markov maps are non-invertible maps and therefore have infinitely many periodic points which implies that there are infinitely many invariant measures in these maps [23]. For example, we can consider the Dirac delta measure on the fixed point. Both maps T and T_s have fixed points at 0 and 1, i.e. δ_0 and δ_1 respectively. Thus the Dirac delta measures at these points of T and T_s are invariant. In this thesis, we use both the Lebesgue and the Dirac delta measures. Moreover, there is a theorem from de Melo and van Strien [23] proving that Markov maps have a measure that is absolutely continuous w.r.t the Lebesgue measure.

Theorem 2.3 ([23]) *Let $f : X \to X$ be a Markov map and let $\cup_i I_i$ be the associated partition. Then there exists a f-invariant probability measure μ on the Borel sets of X which is absolutely continuous w.r.t. the Lebesgue measure.*

Proof. See [23], Theorem 2.2. ■

It has been revealed [23] that the existence of an invariant measure which is absolutely continuous w.r.t. the Lebegue measure ℓ is associated to chaotic dynamics in the maps.

2.7 Lyapunov exponents

Lyapunov exponents are classical tools to measure complexity or chaos in a system. They were introduced around year 1900 when J. Hadamard employ them to prove the hyperbolicity of geodesic flows on manifolds. We first give their definition in $\mathbb{R}^d$ and in terms of the interval maps [15].

Let $f : \mathbb{R}^d \to \mathbb{R}^d$ be a measurable map and let $x \in \mathbb{R}^d$. There are real numbers

$$-\infty \leq \lambda^{(1)}(x) < \lambda^{(2)}(x) < \cdots < \lambda^{(r(x))}(x) < \infty,$$

where $r(x)$ is an integer with $1 \leq r(x) \leq d$ and linear subspaces of $\mathbb{R}^d$

$$\{0\} = V^{(0)}(x) \subset V^{(1)}(x) \subset \cdots \subset V^{(r(x))}(x) = \mathbb{R}^d$$

such that

$$\lim_{n\to\infty} \frac{1}{n} \log \left| \frac{df^n}{dx}(x) \cdot v \right| = \lambda^{(i)}(x)$$

for all $v \in V^{(i)}(x) \setminus V^{(i-1)}(x)$, $i = 1, \ldots, r(x)$. The numbers $\lambda^{(1)}(x), \ldots, \lambda^{(r(x))}(x)$ are called the *Lyapunov exponents* of f at x and $V^{(1)}(x) \subset \cdots \subset V^{(r(x))}(x) = \mathbb{R}^d$ is called the associated filtration. For example, if X is the interval $I = [0, 1]$, then we

have only one Lyapunov exponent given by [15]

$$\Lambda_f(x) = \lim_{n\to\infty} \frac{1}{n} \log \left| \frac{df^n}{dx}(x) \right|.$$

Moreover, to compute the Lyapunov exponents, we can use Birkhoff's ergodic theorem which was discussed in Section 2.5. Therefore the Lyapunov exponent for μ is given by

$$\lambda_\mu = \int \log \left| \frac{df}{dx}(x) \right| d\mu(x). \tag{2.21}$$

If μ is ergodic, then by the Birkhoff's ergodic theorem in (2.13), (2.21) is equal to the time average for $\log |Df(x)|$ as follows:

$$\lambda_\mu = \int \log \left| \frac{df}{dx}(x) \right| d\mu(x) = \lim_{n\to\infty} \frac{1}{n} \sum_{i=0}^{n-1} \log \left| \frac{df}{dx}(f^i(x)) \right|, \tag{2.22}$$

for μ-almost all points x [39].

2.7.1 Lyapunov exponents for attractor in a skew product map

Lyapunov exponents are very useful for identifying riddled basins. From our discussion in Section 2.4, we know that a basin is riddled if and only if the basin has positive measure.

Recall that our skew product system has the form

$$F(x, y) = (f(x), g(x, y)),$$

where f only depends on x and is independent from y. Let $N = \{(x, 0)\}$ be an invariant subspace under F such that $F(N) \subset N$ and we denote the restriction of F to N as $F_N : N \to N$. Let A be an attractor for F with basin $\mathcal{B}(A)$. For each point $(x, 0) \in A$, it has at most two Lyapunov exponents; one is Lyapunov exponent that measures the exponential rate of stretching on A when F is restricted to x-axis and the other Lyapunov exponents measures the exponential rate of expansion on A on y-axis [1]. In this thesis, we denote for both Lyapunov exponents as $\lambda_\parallel$ and $\lambda_\perp$ respectively. If $\lambda_\perp$ is negative, this means that A attracts a set of positive Lebesgue measure, and the nearer the point to A the larger the proportion of points that are in $\mathcal{B}(A)$ [1].

The Lyapunov exponent in x-direction is denoted by

$$\lambda_{\parallel}(x) = \lim_{n\to\infty} \frac{1}{n} \sum_{i=0}^{n-1} \log \left| \frac{df}{dx}(f^i(x)) \right|,$$

for μ-almost all x and the Lyapunov exponent in y-direction is denoted by

$$\lambda_{\perp}(x) = \lim_{n\to\infty} \frac{1}{n} \sum_{i=0}^{n-1} \log \left| \frac{\partial g}{\partial y}(f^i(x), 0) \right|.$$

for μ-almost all x. We shall use these Lyapunov exponents and the formula in (2.22) on our example of piecewise linear map in Chapter 4.

3 Basic properties of stability index and relation to local dimension of measures

The stability index was introduced by Podvigina and Ashwin [59] to characterize the local geometry of basins of attraction for heteroclinic cycles. Recently this index has been employed by Keller [44] for chaotically driven concave maps. More recently, Lohse [52] and Castro and Lohse [20] used it to understand stability of simple heteroclinic networks in $\mathbb{R}^4$. In this thesis, we will apply the stability index to study the local geometry of riddled basins of attraction.

In this chapter we first redefine the stability index for a point from [59]. Next, we give stronger results on the basic properties of the stability index using notation from asymptotic analysis. In addition, we relate the stability index and the local dimension of measures using the restriction of Lebesgue measure on a set. Besides computing the stability index at a point, one can also define it for any set (i.e. for limit cycle, attractor etc.) in the basins of attraction. We therefore introduce a definition of stability index for a set at the end of this chapter.

3.1 The stability index

In the following, we denote by $B_\varepsilon(x)$ an ε-neighbourhood of a point $x \in X$. Let A be any invariant set in X and $\mathcal{B}(A)$ its basin of attraction.

Definition 3.1 (Stability index [59]) *For a point $x \in X$ and $\varepsilon > 0$, define*

$$\Sigma_\varepsilon(x) := \frac{\ell(B_\varepsilon(x) \cap \mathcal{B}(A))}{\ell(B_\varepsilon(x))}, \tag{3.1}$$

i.e.,

$$1 - \Sigma_\varepsilon(x) := \frac{\ell(B_\varepsilon(x) \cap \mathcal{B}(A)^c)}{\ell(B_\varepsilon(x))}, \tag{3.2}$$

where $0 \leq \Sigma_\varepsilon(x) \leq 1$. *Then the* stability index *of* A *at* x *is defined to be*

$$\sigma(x) := \sigma_+(x) - \sigma_-(x), \tag{3.3}$$

where

$$\sigma_-(x) := \lim_{\varepsilon \to 0} \left[\frac{\log(\Sigma_\varepsilon(x))}{\log \varepsilon} \right], \quad \sigma_+(x) := \lim_{\varepsilon \to 0} \left[\frac{\log(1 - \Sigma_\varepsilon(x))}{\log \varepsilon} \right],$$

as long as these limits converge.

We use the convention that $\sigma_-(x) = \infty$ if there is $\varepsilon > 0$ such that $\Sigma_\varepsilon(x) = 0$ and $\sigma_+(x) = \infty$ if there is $\varepsilon > 0$ such that $\Sigma_\varepsilon(x) = 1$, or of the limits are infinite. Then we can assume that $\sigma(x) \in [-\infty, \infty]$.

This stability index $\sigma(x)$ of a point $x \in A$ is related to the local geometry of basins of attraction of A. If $\sigma(x) > 0$, this means that there is an increasingly large proportion of points that are attracted to A as the neighbourhood $B_\varepsilon(x)$ shrinks, i.e. $\Sigma_\varepsilon(x)$ goes to 1 as $\varepsilon \to 0$. On the other hand, if $\sigma(x) < 0$, this means that there is a decreasingly small proportion of points that are attracted to A as $B_\varepsilon(x)$ shrinks, i.e. $\Sigma_\varepsilon(x)$ goes to 0 as $\varepsilon \to 0$ [20]. We show the schematic diagram for the relation between stability index with the local geometry of basins of attraction in Figure 3.1.

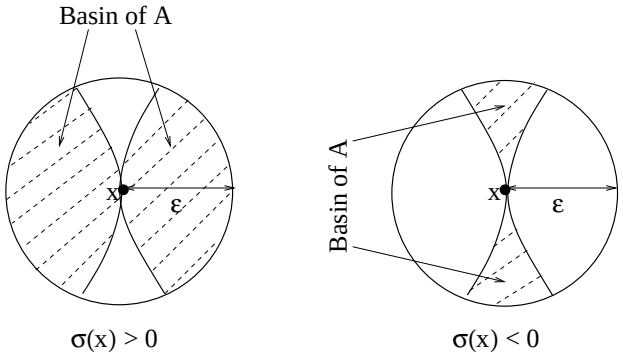

Figure 3.1 The schematic diagram showing the relation of stability index for a point x with the geometry of the basins of attraction. The dashed area represents $\mathcal{B}(A)$ while the blank area represents the basin complement $\mathcal{B}(A)^c$. For $\sigma(x) > 0$, the measure of basin $\mathcal{B}(A)$ that is in the ε-neighbourhood $B_\varepsilon(x)$ goes to 1 as $\varepsilon \to 0$. For $\sigma(x) < 0$, the measure of basin $\mathcal{B}(A)^c$ that is in the ε-neighbourhood $B_\varepsilon(x)$ goes to 1 as $\varepsilon \to 0$.

We also discuss some sufficient conditions for the convergence to fail and so $\sigma(x)$ is not well-defined. We prove this in the last section of next chapter.

3.2 Background study: stability index for heteroclinic cycles

The stability index was introduced to describe the local geometry of the basin of attraction of an invariant set. This quantity was first used on the basin of attraction of invariant set, in particular of heteroclinic cycles by Podvigina and Ashwin [59]. In fact, this index is also useful to study other types of invariant sets. It has been stated in [59] that this index is very useful in describing the structure of invariant sets for riddled and intermingled basins. Therefore, in this thesis, we will apply the stability index on the invariant set which is an attractor with riddled basin of attraction.

In some cases, the index can be expressed in terms of other quantities from the dynamics. For example, Podvigina and Ashwin [59] and Lohse [52] computed the stability index in terms of eigenvalues of the linearization at equilibria of an ordinary differential equation. Keller showed [44] that for a skew product map there may be a formula for the stability index in terms of Lyapunov exponents and Loynes' exponent. In our case, we will compare our stability index with those of Keller [44].

3.3 Basic properties of stability index

In this section, we give more precise results than [59] for basic properties of stability index in terms of asymptotic notation. In [59], they used asymptotic upper bound (denoted as 'big Oh' (O)) whereas in this thesis, we use stronger notion of an *exponentially asymptotically tight bound* (denoted as 'big theta tilde' ($\tilde{\Theta}$)). Therefore, we would like to show that $\Sigma_\varepsilon(x)$ and $1-\Sigma_\varepsilon(x)$ in (3.1) and (3.2) respectively are exponentially asymptotically tight bound by $\varepsilon^{\sigma_-(x)}$ and $\varepsilon^{\sigma_+(x)}$ respectively, i.e., $\Sigma_\varepsilon(x) = \tilde{\Theta}(\varepsilon^{\sigma_-(x)})$ and $1-\Sigma_\varepsilon(x) = \tilde{\Theta}(\varepsilon^{\sigma_+(x)})$ respectively. We give the definition of $\tilde{\Theta}$ and details in Appendix A.

Theorem 3.1 *Suppose x is such that $\sigma_-(x)$ and $\sigma_+(x)$ exist. For a point $x \in X$ and $\varepsilon > 0$, $\Sigma_\varepsilon(x) = \tilde{\Theta}(\varepsilon^{\sigma_-(x)})$ and $1-\Sigma_\varepsilon(x) = \tilde{\Theta}(\varepsilon^{\sigma_+(x)})$.*

Proof. Suppose that $\lim_{\varepsilon\to 0} \frac{\log \Sigma_\varepsilon(x)}{\log \varepsilon} = \sigma_-(x) > 0$. Then for all $\delta > 0$, there exists $0 < \varepsilon_0 < 1$ such that for $0 < \varepsilon \le \varepsilon_0$,

$$\left| \frac{\log \Sigma_\varepsilon(x)}{\log \varepsilon} - \sigma_-(x) \right| < \delta,$$

i.e.,

$$\sigma_-(x) - \delta < \frac{\log \Sigma_\varepsilon(x)}{\log \varepsilon} < \sigma_-(x) + \delta,$$

if and only if

$$(\sigma_-(x) - \delta) \log \varepsilon > \log \Sigma_\varepsilon(x) > (\sigma_-(x) + \delta) \log \varepsilon.$$

Then

$$\log \varepsilon^{(\sigma_-(x)-\delta)} > \log \Sigma_\varepsilon(x) > \log \varepsilon^{(\sigma_-(x)+\delta)},$$

and by dropping the 'log' we get

$$\varepsilon^{(\sigma_-(x)-\delta)} > \Sigma_\varepsilon(x) > \varepsilon^{(\sigma_-(x)+\delta)},$$

i.e.,

$$\varepsilon^{-\delta}\varepsilon^{(\sigma_-(x))} > \Sigma_\varepsilon(x) > \varepsilon^{\delta}\varepsilon^{(\sigma_-(x))}.$$

Therefore, for all $\delta > 0$, there exist constants $c_1 > 0, c_2 > 0$ and for all $0 < \varepsilon \leq \varepsilon_0$ such that

$$c_1\varepsilon^{\delta}\varepsilon^{\sigma_-(x)} < \Sigma_\varepsilon(x) < c_2\varepsilon^{-\delta}\varepsilon^{\sigma_-(x)}.$$

as $\varepsilon \to 0$. This shows that $\Sigma_\varepsilon(x)$ is bounded above and below by $\varepsilon^{\sigma_-(x)}$, i.e., $\Sigma_\varepsilon(x) = \tilde{\Theta}(\varepsilon^{\sigma_-(x)})$. Using the similar way, we obtain for $1 - \Sigma_\varepsilon(x) = \tilde{\Theta}(\varepsilon^{\sigma_+(x)})$. ■

Thus, using this theorem, we summarize some basic properties of this index [59, Lemma 2.2] in the following lemma.

Lemma 3.1 *Suppose that $\sigma(x)$ is defined for some $x \in X \subset \mathbb{R}^n$, then the following hold:*

(a) If one of $\sigma_\pm(x)$ converges to a positive value then the other converges to zero (i.e. only one of $\sigma_+(x)$ and $\sigma_-(x)$ can be non-zero).

(b) If $\sigma(x) = c > 0$, then $1 - \Sigma_\varepsilon(x) = \tilde{\Theta}(\varepsilon^c)$ (in particular $\Sigma_\varepsilon(x) \to 1$ as $\varepsilon \to 0$).

(c) If $\sigma(x) = -c < 0$, then $\Sigma_\varepsilon(x) = \tilde{\Theta}(\varepsilon^c)$ (in particular $\Sigma_\varepsilon(x) \to 0$ as $\varepsilon \to 0$).

Proof.

(a) Note that if $\sigma_-(x) > 0$, then $\lim_{\varepsilon\to 0} \Sigma_\varepsilon(x) = 0$. This implies that $1 - \Sigma_\varepsilon(x)$ converges to 1 as $\varepsilon \to 0$ and so $\sigma_+(x) = 0$. On the other hand, if $\sigma_+(x) > 0$, then $\lim_{\varepsilon\to 0} 1 - \Sigma_\varepsilon(x) = 0$. This implies that $\Sigma_\varepsilon(x)$ converges to 1 as $\varepsilon \to 0$ and so $\sigma_-(x) = 0$.

(b) Follows from noting in (a) that $c = \sigma(x) = \sigma_+(x) > 0$ and $\sigma_-(x) = 0$. Hence we have from the definition of $\sigma_+(x)$ that $1 - \Sigma_\varepsilon(x) = \tilde{\Theta}(\varepsilon^c)$ as $\varepsilon \to 0$.

(c) Follows from noting in (a) that

$$-c = \sigma(x) = \sigma_+(x) - \sigma_-(x) = 0 - c = -c,$$

and so $\sigma_-(x) = c$ and $\sigma_+(x) = 0$. Hence we have from the definition of $\sigma_-(x)$ that $\Sigma_\varepsilon(x) = \tilde{\Theta}(\varepsilon^c)$ as $\varepsilon \to 0$. ■

Moreover, it has been proved in [59] that the stability index is in fact constant along the orbit of x. In other words, the value of stability index for a point is same as the value of the stability index for its orbits, i.e. $\sigma(x) = \sigma(f^n(x))$.

Theorem 3.2 **[59]** *Let X be a compact invariant set for a continuously differentiable map f. Then for any point $x \in X$, the stability index $\sigma(x)$ is constant along orbits (or trajectories for flows) whenever it exists.*

Proof. See [59], Theorem 2.2. ■

3.4 Relation between stability index and local dimension of measures

There is a connection between the stability index and the local dimension of measures. In fact, the stability index consists of the difference of two local dimension of measures, namely of the measures μ and ℓ where μ is the restriction of Lebesgue measure ℓ to a set N. We give the proof in this section.

To show this, we use the definition of restriction of measures in Section 2.3.2 and the local dimension of measures in Section 2.3.3. This connection was pointed out to us by Tobias Oertel-Jäger (personal communication).

Theorem 3.3 *If A is a compact set and N a set with positive Lebesgue measure, $D(x) = \lim_{\varepsilon\to 0} \frac{\log \ell(B_\varepsilon(x)\cap N)}{\log \varepsilon}$ and $\overline{D}(x) = \lim_{\varepsilon\to 0} \frac{\log \ell(B_\varepsilon(x)\cap N^c)}{\log \varepsilon}$, then*

$$\sigma(x) = \overline{D}(x) - D(x).$$

Proof. Suppose the local dimension of the measure $\mu = \ell|_N$ at x is $D(x)$. Recall

that from the definition of $\sigma_-(x)$ in Definition 3.1 we have

$$\begin{aligned}\sigma_-(x) &= \lim_{\varepsilon\to 0}\frac{\log\left(\frac{\ell(B_\varepsilon(x)\cap N)}{\ell(B_\varepsilon(x))}\right)}{\log\varepsilon},\\ &= \lim_{\varepsilon\to 0}\frac{\log\ell(B_\varepsilon(x)\cap N)-\log\ell(B_\varepsilon(x))}{\log\varepsilon}\\ &= \lim_{\varepsilon\to 0}\frac{\log\mu(B_\varepsilon(x))}{\log\varepsilon}-\lim_{\varepsilon\to 0}\frac{\log\ell(B_\varepsilon(x))}{\log\varepsilon}\\ &= \dim_{loc}\mu(x)-\dim_{loc}\ell(x),\\ &= D(x)-d.\end{aligned} \tag{3.4}$$

where d is the dimension of the phase space $\mathbb{R}^d$. Here, $\mu(B_\varepsilon(x))$ denotes the restriction of ℓ to N, i.e., $\mu(B_\varepsilon(x)) = \ell|_N(B_\varepsilon(x)) = \ell(B_\varepsilon(x)\cap N)$ for all x. A similar relation also hold for $\sigma_+(x)$ where:

$$\begin{aligned}\sigma_+(x) &= \lim_{\varepsilon\to 0}\frac{\log\left(\frac{\ell(B_\varepsilon(x)\cap N^c)}{\ell(B_\varepsilon(x))}\right)}{\log\varepsilon},\\ &= \lim_{\varepsilon\to 0}\frac{\log\ell(B_\varepsilon(x)\cap N^c)-\log\ell(B_\varepsilon(x))}{\log\varepsilon}\\ &= \lim_{\varepsilon\to 0}\frac{\log\overline{\mu}(B_\varepsilon(x))}{\log\varepsilon}-\lim_{\varepsilon\to 0}\frac{\log\ell(B_\varepsilon(x))}{\log\varepsilon}\\ &= \dim_{loc}\overline{\mu}(x)-\dim_{loc}\ell(x),\\ &= \overline{D}(x)-d.\end{aligned} \tag{3.5}$$

The $\overline{\mu}(B_\varepsilon(x))$ denotes the restriction of ℓ to N^c, i.e., $\overline{\mu}(B_\varepsilon(x)) = \ell|_{N^c}(B_\varepsilon(x)) = \ell(B_\varepsilon(x)\cap N^c)$ for all x and $\overline{D}(x)$ is the local dimension of $\overline{\mu} = \ell|_{N^c}$. Therefore, from the definition of stability index in (3.3), we have

$$\sigma(x) = \overline{D}(x) - D(x). \blacksquare$$

3.5 Stability index for a set

In [59], the stability index has been computed for an individual point. In this thesis, we also consider the stability index for a set.

Definition 3.2 *Let $A \subset X$ be an invariant set and let $\varepsilon > 0$. We define*

$$\Sigma_\varepsilon(A) := \frac{\ell(B_\varepsilon(A)\cap\mathcal{B}(A))}{\ell(B_\varepsilon(A))}, \tag{3.6}$$

so that

$$1-\Sigma_\varepsilon(A) := \frac{\ell(B_\varepsilon(A)\cap\mathcal{B}(A)^c)}{\ell(B_\varepsilon(A))}, \tag{3.7}$$

where $B_\varepsilon(A)$ is an ε-neighbourhood of the set A, $\mathcal{B}(A)$ is basin of attraction of the set A and $\mathcal{B}(A)^c$ is the complement of $\mathcal{B}(A)$. Note that $0 \leq \Sigma_\varepsilon(A) \leq 1$. Then the stability index for the invariant set A is defined to be

$$\sigma(A, \mathcal{B}(A)) := \sigma_+(A) - \sigma_-(A), \tag{3.8}$$

which exists when the following converge:

$$\sigma_-(A) := \lim_{\varepsilon \to 0} \frac{\log(\Sigma_\varepsilon(A))}{\log \varepsilon}, \quad \sigma_+(A) := \lim_{\varepsilon \to 0} \frac{\log(1 - \Sigma_\varepsilon(A))}{\log \varepsilon}. \tag{3.9}$$

4 Stability index for an attractor in a piecewise linear map

In this chapter, we consider a simple example of a skew product system, namely a piecewise linear map F from $[0,1]^2$ to itself. In this thesis, this map contains points $(\theta, x) \in [0,1]^2$. This map is slightly modified from Ott *et al.* [57] in the sense that we assume there is a second attractor at $x = 1$ while [57] consider $x > 1$ as a second attractor. In this model, there can be two coexisting Milnor attractors such that basin of the first attractor is riddled with basin of the second attractor. We wish to examine the existence of this riddled basin by measuring its Lebesgue measure. The main results for proving riddled basin are theorems 4.1, 4.2, 4.3 and 4.4. Then we compute the stability index for a point as well as for an attractor in the system and we show the results in theorems 4.5, 4.6, 4.9 and 4.7 which includes the non-convergence of the stability index.

4.1 The model: piecewise linear map

We consider the skew product transformation in the unit square $(\theta, x) \in [0,1]^2$

$$F(\theta, x) = (T_s(\theta), h(\theta, x)) \tag{4.1}$$

where the base map

$$T_s(\theta) = \begin{cases} \frac{\theta}{s} & \text{if } 0 \leq \theta < s, \\ \frac{\theta - s}{1-s} & \text{if } s < \theta \leq 1, \end{cases} \tag{4.2}$$

is the skewed doubling map of (2.19) and the fibre map

$$h(\theta, x) = \begin{cases} \min(\gamma x, 1) & \text{if } 0 \leq \theta < s \text{ and } 0 \leq x < 1, \\ \delta x & \text{if } s < \theta \leq 1 \text{ and } 0 \leq x < 1, \\ 1 & \text{if } x = 1, \end{cases} \tag{4.3}$$

where $0 < s < 1$, $\gamma > 1$, $0 < \delta < 1$. Note that γ and δ represent expansion and contraction respectively. For this model, we study the special case $\gamma = 1/\delta$. We

define here that

$$\kappa := 1 - 2s, \tag{4.4}$$

which will be used later in Section 4.3.

To describe system (4.1), we start by choosing θ_0 randomly in $[0, 1]$. Then from (4.2), its orbit, θ_n spends a proportion s in $0 \leq \theta_n < s$ and a proportion $1 - s$ in $s < \theta_n \leq 1$. Next, if we choose $x_0 = 0$, then by the first and second conditions in (4.3), x_n remains zero for all θ. Hence, this clearly shows that $x = 0$ is an invariant set. On the other hand, if $x_0 = 1$, then by the last condition in (4.3) x_n remains 1 for all θ. Thus, this shows that $x = 1$ is also an invariant set. To be more precise, we denote

$$A_0 = [0, 1] \times \{0\},$$
$$A_1 = [0, 1] \times \{1\},$$

and note that A_0 and A_1 are disjoint compact invariant sets. The basins are

$$B_0 := \mathcal{B}(A_0) = \{(\theta, x) : d(F^n(\theta, x), A_0) \to 0 \text{ as } n \to \infty\},$$
$$B_1 := \mathcal{B}(A_1) = \{(\theta, x) : d(F^n(\theta, x), A_1) \to 0 \text{ as } n \to \infty\},$$

where $d(x, A) = \inf_{y \in A} \|x - y\|$ and where $F^n(\theta, x)$ is the nth iterate of (θ, x). Since our base map is Markov we can divide $[0, 1]^2$ using the following partition:

$$[0, 1]^2 = \bigcup_{k=1}^{\infty} X_k,$$

where

$$X_k = X_{k,1} \dot{\bigcup} X_{k,2},$$
$$X_{k,1} = [0, s] \times [\delta^k, \delta^{k-1}],$$
$$X_{k,2} = [s, 1] \times [\delta^k, \delta^{k-1}],$$

where $\dot{\bigcup}$ denotes the disjoint union.[1] Therefore, we now have the partitions $X_{k,1}$ which are on the left of s and $X_{k,2}$ on the right of s, for $k = 1, 2, 3, \ldots$. We show the map (4.1) as a schematic diagram in Figure 4.1. For $X_{k,1}$, the map F on $X_{k,1}$ goes up one level above and occupy the whole of X_{k-1}, for $k \geq 2$. Meanwhile the mapping F on $X_{k,2}$ goes down one level and occupy the whole of X_{k+1} for $k \geq 1$. Moreover, from the last condition in (4.3), the map F on $X_{1,1}$ goes up and occupy

[1] Note that the skew product map F (4.1) is Markov but has an infinite number of pieces in the partition.

the whole of A_1. More precisely, we note

$$F(X_{k,1}) = X_{k-1} \text{ for } k \geq 2, \tag{4.5}$$

$$F(X_{1,1}) = A_1, \tag{4.6}$$

$$F(X_{k,2}) = X_{k+1} \text{ for } k \geq 1. \tag{4.7}$$

For examples, $F(X_{2,1}) = X_{1,1} \dot{\bigcup} X_{1,2}$ and $F(X_{1,2}) = X_{2,1} \dot{\bigcup} X_{2,2}$. We show schematic diagrams for (4.5), (4.6) and (4.7) in Figure 4.2-4.4 respectively.

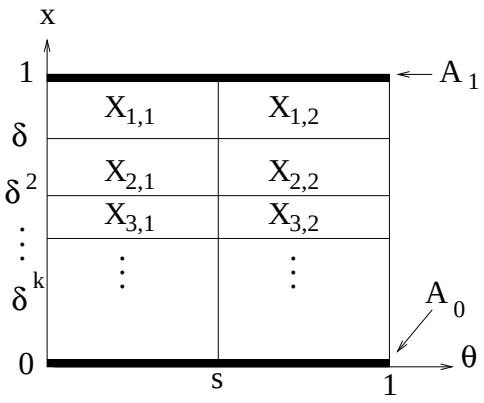

Figure 4.1 The schematic diagram for map F (4.1).

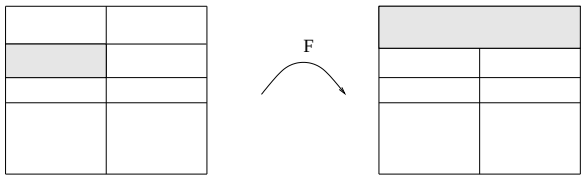

Figure 4.2 The effect of F on $X_{k,1}$ for $k \geq 2$, stretches by $1/s$ in the θ-direction and expands by $\gamma = 1/\delta$ in the x-direction.

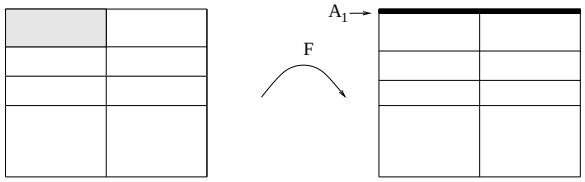

Figure 4.3 The effect of F on $X_{1,1}$: $F(X_{1,1}) = A_1$.

4.2 Basin boundary between B_0 and B_1

Before we proceed proving the existence of a riddled basin, we would like to prove that there is a boundary between basins B_0 and B_1. Thus, in this section, Lemma 4.1 proves the behaviour of orbit of (θ_0, x_0) and following from this, we manage to define the basin boundary $\hat{\varphi}_\infty(\theta)$ in Definition 4.1. We also investigate how the orbit of (θ, x_0) behaves as it starts from below or above $\hat{\varphi}_\infty(\theta)$ (Lemma 4.2). We end this section by characterizing the zero and non-zero sets for $\hat{\varphi}_\infty(\theta)$ in Lemma 4.3.

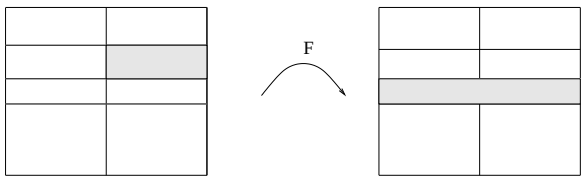

Figure 4.4 The effect of F on $X_{k,2}$ for $k \geq 1$, stretches by $1/(1-s)$ in the θ-direction and shrinks by δ in the x-direction.

First we consider $[s,1] \subset [0,1]$ and we want to investigate how frequently the orbit of a point $\theta \in \mathbb{T}$ under the skewed doubling map $T_s(\theta)$ visit the right interval $[s,1]$. Let us define

$$n_k(\theta) := \begin{cases} 0 & \text{if } T_s^k(\theta) < s, \\ 1 & \text{if } T_s^k(\theta) \geq s, \end{cases} \tag{4.8}$$

for $k = 0, \ldots, N-1$ where $n_k(\theta)$ is the characteristic function

$$n_k(\theta) = \chi_{[s,1]}(T_s^k(\theta)).$$

Then we can define

$$i_N(\theta) := \sum_{k=0}^{N-1} n_k(\theta), \tag{4.9}$$

which denote the number of the first N points in the orbit of θ that lie in $[s,1]$ and

$$\frac{i_N(\theta)}{N} = \frac{1}{N} \sum_{k=0}^{N-1} n_k(\theta)$$

denotes the proportion of the first N points in the orbit of θ that lie in $[s,1]$. Hence

$$\lim_{N\to\infty} \frac{i_N(\theta)}{N} = \lim_{N\to\infty} \frac{1}{N} \sum_{k=0}^{N-1} n_k(\theta) \tag{4.10}$$

denotes the frequency with which the orbit of θ lie in $[s,1]$. Since ℓ is ergodic, we can apply the Birkhoff's Ergodic Theorem which says that for ℓ-almost all $\theta \in [0,1]$

$$\lim_{N\to\infty} \frac{1}{N} \sum_{k=0}^{N-1} n_k(\theta) = \lim_{N\to\infty} \frac{1}{N} \sum_{k=0}^{N-1} \chi_{[s,1]}(T_s^k(\theta)) = \int_0^1 \chi_{[s,1]}(y) d\ell(y) = 1 - s, \tag{4.11}$$

i.e. the proportion of time that the orbit of θ spends in the interval $[s,1]$ is equal to the length of the interval itself, i.e. $1-s$.

Moreover, from the skew product transformation F in (4.1), let us denote the iterations $(\theta_N, x_N) = F^N(\theta_0, x_0)$ for $N \geq 0$. We note that $\theta_N = T_s^N(\theta)$ and define

$$\begin{cases} y_k &= \delta^{n_{k-1}(\theta)} \delta^{-(1-n_{k-1}(\theta))} y_{k-1}, \\ y_0 &= x_0, \end{cases}$$

so that

$$y_N = \delta^{2i_N(\theta)-N} x_0, \tag{4.12}$$

where $i_N(\theta)$ is as defined in (4.9). More precisely,

Lemma 4.1 *Suppose* $(\theta_N, x_N) = F^N(\theta_0, x_0)$ *for* $N \geq 0$. *Let* $y_N = \delta^{2i_N(\theta)-N} x_0$. *Then* $\theta_N = T_s^N(\theta)$ *and*

$$x_N = \begin{cases} y_N & \text{if } \max\{y_\ell : 1 \leq \ell \leq N\} < 1, \\ 1 & \text{otherwise.} \end{cases}$$

Proof. Note that if $x_1 < 1$ then

$$x_1 = y_1 = \delta^{n_0(\theta)} \delta^{-(1-n_0(\theta))} y_0.$$

Similarly, if $x_\ell < 1$ for $1 \leq \ell \leq N$ then

$$x_N = y_N = \delta^{n_{N-1}(\theta)} \delta^{-(1-n_{N-1}(\theta))} y_{N-1}.$$

On the other hand, if $y_\ell \geq 1$ for some ℓ then $x_N = 1$ for all $N \geq \ell$.

This means that as long as $y_N < 1$, $x_N = y_N$ but when $y_N \geq 1$, we will only take the maximum value $x_N = 1$. ■

From the above lemma, we can now define a basin boundary where $x_N = y_N$ if $\max\{y_\ell : 1 \leq \ell \leq N\} < 1$ for all N which means that $x_N = y_N$ if

$$\sup_{N \geq 0}\{y_N\} < 1.$$

Using (4.12),

$$\sup_{N \geq 0}\{\delta^{2i_N(\theta)-N} x_0\} < 1.$$

We have

$$\sup_{N \geq 0}\{\delta^{2i_N(\theta)-N}\} x_0 < 1$$

which implies

$$x_0 < \frac{1}{\sup_{N \geq 0}\{\delta^{2i_N(\theta)-N}\}},$$

this is

$$x_0 < \inf_{N \geq 0}\{\delta^{N-2i_N(\theta)}\}.$$

Thus, the basin boundary is defined from the right hand side in the above equation.

Definition 4.1 *The* basin boundary *is defined as follows:*

$$\hat{\varphi}_\infty(\theta) = \inf_{N\geq 0} \left\{\delta^{N-2i_N(\theta)}\right\}.$$

The following lemma shows that $\hat{\varphi}_\infty(\theta)$ determines the orbit of (θ, x_0) depending on whether it starts from below or above the basin boundary.

Lemma 4.2 *Suppose* $(\theta_N, x_N) = F^N(\theta_0, x_0)$ *for* $N \geq 0$.

(i) If $x_0 < \hat{\varphi}_\infty(\theta)$ *then* $x_N = y_N$ *for all* N.

(ii) If $x_0 > \hat{\varphi}_\infty(\theta)$ *there exists* M *such that* $x_N = 1$ *for all* $N \geq M$.

Proof. (i) If $x_0 < \hat{\varphi}_\infty(\theta)$, then by Definition 4.1; $x_0 < \inf_{N\geq 0}(\delta^{N-2i_N(\theta)})$ which implies that

$$\frac{x_0}{\inf_{N\geq 0}\{\delta^{N-2i_N(\theta)}\}} < 1,$$

this is

$$\sup_{N\geq 0}\{\delta^{2i_N(\theta)-N}x_0\} < 1.$$

Thus, we have

$$\sup_{N\geq 0}\{y_N\} < 1$$

which implies

$$y_N < 1 \quad \text{for all } N \in \mathbb{N}.$$

By Lemma 4.1, we have $x_N = y_N$ for all $N \in \mathbb{N}$.

(ii) If $x_0 > \hat{\varphi}_\infty(\theta)$, then $x_0 > \inf_{N\geq 0}\{\delta^{N-2i_N(\theta)}\}$ which implies that

$$\sup_{N\geq 0}\{\delta^{2i_N(\theta)-N}x_0\} > 1,$$

and so

$$\sup_{N\geq 0}\{y_N\} > 1$$

which implies that

$$y_N > 1 \quad \text{for some } N \in \mathbb{N}.$$

By Lemma 4.1, $x_k = 1$ for all $k \geq N$. ■

Below we characterize the zero and non-zero sets of $\hat{\varphi}_\infty(\theta)$.

Lemma 4.3 *Suppose* θ *is such that* $\lim_{N\to\infty} \frac{i_N(\theta)}{N}$ *converges.*

(i) If $\lim_{N\to\infty} \frac{i_N(\theta)}{N} < \frac{1}{2}$, *then* $\theta \in \hat{\varphi}_\infty^{-1}(0)$.

(ii) If $\lim_{N\to\infty} \frac{i_N(\theta)}{N} > \frac{1}{2}$, *then* $\theta \notin \hat{\varphi}_\infty^{-1}(0)$.

Proof. We denote the zero set of $\hat{\varphi}_\infty(\theta)$ by $\hat{\varphi}_\infty^{-1}(0)$.

(i) Note that $\theta \in \hat{\varphi}_\infty^{-1}(0)$ if and only if

$$\inf_{N\geq 0} \left\{\delta^{N-2i_N(\theta)}\right\} = 0.$$

By taking logs;

$$\inf_{N\geq 0} \log\left\{\delta^{N-2i_N(\theta)}\right\} = -\infty.$$

Then

$$\liminf_{N\to\infty} (N - 2i_N(\theta)) \log\delta = -\infty.$$

Dividing by $\log\delta$;

$$\liminf_{N\to\infty} (N - 2i_N(\theta)) = \infty.$$

Dividing by N and noting that the sequence $i_N(\theta)/N$ converges means that;

$$\lim_{N\to\infty} \left(1 - \frac{2i_N(\theta)}{N}\right) = \alpha > 0.$$

Solving the above, we obtain

$$\lim_{N\to\infty} \frac{i_N(\theta)}{N} = \frac{1}{2} - \frac{\alpha}{2} = \beta < \frac{1}{2}.$$

Thus this proves that $\theta \in \hat{\varphi}_\infty^{-1}(0)$ when $\lim_{N\to\infty} \frac{i_N(\theta)}{N} < \frac{1}{2}$.

(ii) Meanwhile $\theta \notin \hat{\varphi}_\infty^{-1}(0)$ if and only if

$$\inf_{N\geq 0} \left\{\delta^{N-2i_N(\theta)}\right\} > 0.$$

By taking logs;

$$\inf_{N\geq 0} \log\left\{\delta^{N-2i_N(\theta)}\right\} > -\infty.$$

Then

$$\liminf_{N\to\infty} (N - 2i_N(\theta)) \log\delta > -\infty.$$

Dividing by $\log\delta$;

$$\liminf_{N\to\infty} (N - 2i_N(\theta)) > \infty.$$

Dividing by N and noting that the sequence $i_N(\theta)/N$ converges means that;

$$\lim_{N\to\infty} 1 - \frac{2i_N(\theta)}{N} > \alpha > 0.$$

Solving the above then we obtain

$$\lim_{N\to\infty} \frac{i_N(\theta)}{N} > \frac{1}{2} - \frac{\alpha}{2} = \beta > \frac{1}{2}.$$

Thus this proves that $\theta \notin \hat{\varphi}_\infty^{-1}(0)$ when $\lim_{N\to\infty} \frac{i_N(\theta)}{N} > \frac{1}{2}$. ■

4.3 Proving the existence of a riddled basin

First, in Theorem 4.1, we show that B_1 has positive measure. Secondly, in Theorem 4.2, we show that the union of B_0 and B_1 has full measure. Then, in Theorem 4.3, we prove that B_0 has either positive or zero measure which depends on specific range. Finally in Theorem 4.4 we prove that B_0 is riddled with B_1.

Theorem 4.1 *For any $0 < s < 1$ and $0 < \delta < 1$, we have that $\ell(B_1) > 0$.*

Proof. This follows by noting that $X_{1,1} \subset B_1$ since $F(X_{1,1}) = A_1$ where $A_1 \subset B_1$, so $\ell(X_{1,1}) \leq \ell(B_1)$ and using the assumptions that $0 < s < 1$ and $0 < \delta < 1$, the measure of $\ell(X_{1,1}) = s(1-\delta) > 0$ and so $\ell(B_1) > 0$. ■

Note that the above theorem implies that A_1 is an attractor since it attracts a set of positive measure, i.e. $\ell(B_1) > 0$ (this satisfies the first condition for A_1 to be a Milnor attractor).

The theorem below proves that the union of the basins of A_0 and A_1 has full measure.

Theorem 4.2 *For any $0 < \delta < 1$, $0 < s < 1$, $s \neq 1/2$ and almost all θ,*

(i) if $x_0 < \hat{\varphi}_\infty(\theta)$, then $(\theta, x_0) \in B_0$,

(ii) if $x_0 > \hat{\varphi}_\infty(\theta)$, then $(\theta, x_0) \in B_1$.

Hence $\ell(B_0 \cup B_1) = 1$.

Proof.

(i) By taking the logs of (4.12), we get

$$\log y_N - \log x_0 = (2i_N(\theta) - N)\log\delta.$$

Dividing each side by $N \log\delta$ to get

$$\frac{\log y_N - \log x_0}{N\log\delta} = \frac{2i_N(\theta)}{N} - 1.$$

We know from (4.11) that for ℓ-almost all θ, $\lim_{N\to\infty} \frac{i_N(\theta)}{N} = 1 - s$, hence we have

$$\lim_{N\to\infty} \frac{\log y_N - \log x_0}{N \log \delta} = \lim_{N\to\infty} 2(1-s) - 1,$$
$$\lim_{N\to\infty} \frac{\log y_N - \log x_0}{N \log \delta} = \lim_{N\to\infty} 1 - 2s.$$

Recall that $\kappa := 1 - 2s$ in (4.4), so that

$$\lim_{N\to\infty} \frac{\log y_N - \log x_0}{N \log \delta} = \lim_{N\to\infty} 1 - 2s = \kappa. \tag{4.13}$$

Rearranging (4.13) we get

$$\lim_{N\to\infty} \frac{\log y_N - \log x_0}{N} = \kappa \log \delta.$$

This means that if $\kappa < 0$ (or $s > 1/2$), then

$$\lim_{N\to\infty} \frac{\log y_N - \log x_0}{N} = \kappa \log \delta > 0.$$

We recall that $\log \delta < 0$ since $0 < \delta < 1$. For this case, since the right hand side is positive, therefore $\log y_N \to \infty$ as $N \to \infty$. This implies that $y_N > 1$ and from Lemma 4.2(ii), $x_N = 1$ for some N. Thus, for ℓ-almost all θ and almost all x_0 there exists (θ, x_0) in the basin of A_1, i.e. $(\theta, x_0) \in B_1$.

(ii) On the other hand, if $\kappa > 0$ (or $s < 1/2$), then

$$\lim_{N\to\infty} \frac{\log y_N - \log x_0}{N} = \kappa \log \delta < 0,$$

which means that $\log y_N \to -\infty$ as $N \to \infty$. This implies that $y_N \to 0$ as $N \to \infty$. Thus, for ℓ-almost all θ there exists an x_0 such that $y_N < 1$ and from Lemma 4.2(i), $x_N = y_N$ for all N. Thus $(\theta, x_0) \in B_0$ for ℓ-almost all θ and almost all x_0. Therefore, from both cases we have shown above, almost all points (θ, x_0) are either in B_0 or B_1, i.e. $(\theta, x_0) \in B_0 \cup B_1$ and hence $\ell(B_0 \cup B_1) = 1$. ■

Note that we do not consider the case when $s = 1/2$ in the above theorem.

Below we prove B_0 can has positive or zero measure depending on the values of s.

Theorem 4.3 *For any $0 < \delta < 1$,*

(i) $\ell(B_0) > 0$ if $s < 1/2$,

(ii) $\ell(B_0) = 0$ if $s > 1/2$.

Proof. Suppose that A is any invariant set in $[0,1]^2$ for F. Let $A_{i,j} = A \cap X_{i,j}$ and $L_{i,j} := \ell(A_{i,j})$. Before we proceed the proofs for first and second cases above, we need to obtain the general solution for $L_{i,j}$.

From (4.5), when $A \cap X_{k,1}$ we have

$$\begin{aligned} F(A_{k,1}) &= F(A \cap X_{k,1}), \\ &= A \cap X_{k-1}, \\ &= A \cap \left(X_{k-1,1} \dot{\bigcup} X_{k-1,2} \right), \\ &= (A \cap X_{k-1,1}) \dot{\bigcup} (A \cap X_{k-1,2}), \\ &= A_{k-1,1} \dot{\bigcup} A_{k-1,2} \text{ for } k \geq 2. \end{aligned} \tag{4.14}$$

Meanwhile from (4.7), when $A \cap X_{k,2}$ we have

$$\begin{aligned} F(A_{k,2}) &= F(A \cap X_{k,2}), \\ &= A \cap X_{k+1}, \\ &= A \cap \left(X_{k+1,1} \dot{\bigcup} X_{k+1,2} \right), \\ &= (A \cap X_{k+1,1}) \dot{\bigcup} (A \cap X_{k+1,2}), \\ &= A_{k+1,1} \dot{\bigcup} A_{k+1,2} \text{ for } k \geq 1. \end{aligned} \tag{4.15}$$

Since we define $L_{i,j} = \ell(A_{i,j})$, then we can write (4.14) and (4.15) in the form of $L_{i,j}$. Note that $F|_{X_{k,1}}$ stretches by $1/s$ in the θ-direction and expands by $\gamma = 1/\delta$ in the x-direction. Meanwhile, $F|_{X_{k,2}}$ stretches by $1/(1-s)$ in the θ-direction and shrinks by δ in the x-direction. Thus for any invariant set A, if $L_{i,j} = \ell(A \cap X_{i,j})$, we have the following:

$$\frac{1}{s\delta} L_{k,1} = L_{k-1,1} + L_{k-1,2} \text{ for } k \geq 2, \tag{4.16}$$

$$\frac{\delta}{1-s} L_{k,2} = L_{k+1,1} + L_{k+1,2} \text{ for } k \geq 1, \tag{4.17}$$

where $L_{k,1} = \ell(A_{k,1}) = \delta s \ell(F(A_{k,1}))$ from the left hand side of (4.14) and $L_{k,2} = \ell(A_{k,2}) = ((1-s)/\delta)\ell(F(A_{k,2}))$ from the left hand side of (4.15).

We can solve (4.16) to get

$$L_{k,2} = \frac{1}{s\delta} L_{k+1,1} - L_{k,1} \tag{4.18}$$

and substitute into (4.17) and obtain the second-order linear recurrence equation

$$\frac{1}{s\delta}L_{k+2,1} - \frac{1}{s(1-s)}L_{k+1,1} + \frac{\delta}{1-s}L_{k,1} = 0. \tag{4.19}$$

We solve the above equation for $L_{k,1}$ by noting that $L_{k,1} = r^k$ is a solution if and only if

$$\frac{1}{s\delta}r^{k+2} - \frac{1}{s(1-s)}r^{k+1} + \frac{\delta}{1-s}r^k = 0.$$

Dividing each term by r^k, we get

$$\frac{1}{s\delta}r^2 - \frac{1}{s(1-s)}r + \frac{\delta}{1-s} = 0.$$

From (4.4) we have $s = \frac{1-\kappa}{2}$ and $1-s = \frac{1+\kappa}{2}$ for $-1 < \kappa < 1$, then

$$\begin{aligned}
\frac{2}{\delta(1-\kappa)}r^2 - \frac{4}{(1-\kappa)(1+\kappa)}r + \frac{2\delta}{(1+\kappa)} &= 0,\\
r^2 - \frac{2\delta}{(1+\kappa)}r + \frac{\delta^2(1-\kappa)}{(1+\kappa)} &= 0,\\
[r-\delta]\left[r - \frac{\delta(1-\kappa)}{(1+\kappa)}\right] &= 0.
\end{aligned}$$

Thus, for $\kappa \neq 0$ ($s \neq 1/2$) we have two solutions for r where

$$r_1 = \delta, \qquad r_2 = \tilde{\delta} = \frac{\delta(1-\kappa)}{(1+\kappa)}.$$

Hence the general solution of (4.19) is

$$\begin{aligned}
L_{k,1} &= K_1 r_1^k + K_2 r_2^k,\\
&= K_1\delta^k + K_2\tilde{\delta}^k,
\end{aligned} \tag{4.20}$$

for some constants K_1 and K_2. Further on, we now find the values of K_1 and K_2 in order to determine the measure of $L_{k,1}$ and $L_{k,2}$.

(i) First, we consider the case $s > 1/2$ (which implies that $-1 < \kappa < 0$). Note also that

$$L_{k,1} = \ell(B_{k,1}) = \ell(B \cap X_{k,1}) \leq \ell(X_{k,1}) = \frac{s(1-\delta)}{\delta}\delta^k \tag{4.21}$$

where $B_{k,1} = B \cap X_{k,1}$ and where $\frac{s(1-\delta)}{\delta}\delta^k$ is the area for the whole $X_{k,1}$. Since $L_{k,1}$ has the form as (4.20), therefore

$$K_1\delta^k + K_2\tilde{\delta}^k \leq \frac{s(1-\delta)}{\delta}\delta^k$$

which decays like δ^k as $k \to \infty$. Dividing each term by δ^k;

$$K_1 + K_2 \left(\frac{\tilde{\delta}}{\delta}\right)^k \leq \frac{s(1-\delta)}{\delta}.$$

We can see that from the above equation that the inequality is not satisfied since K_2 grows exponentially (unbounded) from $s(1-\delta)/\delta$. Therefore we must assume that $K_2 = 0$, and for this case of $\kappa < 0$, the only possible solution is $L_{k,1} = K_1\delta^k$. By comparing this to (4.21);

$$0 \leq L_{k,1} = K_1\delta^k \leq \frac{s(1-\delta)}{\delta}\delta^k,$$

then we have

$$0 \leq K_1 \leq \frac{s(1-\delta)}{\delta}.$$

For this case, if we consider $A = B_1 = \mathcal{B}(A_1)$ and we know the fact that all points in $X_{1,1}$ are definitely in B_1, i.e. $X_{1,1} \subseteq B_1$ where this means that $X_{1,1} = B_1 \cap X_{1,1}$. From the assumption, $B_1 \cap X_{1,1} = B_{1,1}$ and therefore $B_{1,1} = X_{1,1}$ which implies that $\ell(B_{1,1}) = \ell(X_{1,1})$, i.e. $L_{1,1} = \ell(X_{1,1})$.

Since $L_{1,1} = \ell(X_{1,1})$, therefore from (4.21),

$$L_{1,1} = \frac{s(1-\delta)}{\delta}\delta. \tag{4.22}$$

We know previously that $L_{k,1} = K_1\delta^k$, and so when $k = 1$, we have that $L_{1,1} = K_1\delta$. By comparing this with (4.22), we finally obtain that

$$K_1 = \frac{s(1-\delta)}{\delta}. \tag{4.23}$$

In general the solution for $L_{k,1}$ when $K_2 = 0$ and $\kappa < 0$ is

$$L_{k,1} = \frac{s(1-\delta)}{\delta}\delta^k = \ell(X_{k,1}) \text{ for } k \geq 1. \tag{4.24}$$

By substituting (4.24) into (4.18), we obtain the general solution for $L_{k,2}$;

$$L_{k,2} = \frac{(1-s)(1-\delta)}{\delta}\delta^k = \ell(X_{k,2}) \text{ for } k \geq 1. \tag{4.25}$$

By using the sum of a geometric progression, the sum of both $L_{k,1}$ and $L_{k,2}$ are

$$\sum_{k=1}^{\infty} L_{k,1} = \sum_{k=1}^{\infty} \frac{s(1-\delta)}{\delta}\delta^k = \frac{s(1-\delta)}{\delta}\frac{\delta}{1-\delta} = s$$

and

$$\sum_{k=1}^{\infty} L_{k,2} = \sum_{k=1}^{\infty} \frac{(1-s)(1-\delta)}{\delta}\delta^k = \frac{(1-s)(1-\delta)}{\delta}\frac{\delta}{1-\delta} = 1-s.$$

If we define $L_k = L_{k,1}+L_{k,2} = \ell(B\cap X_{k,1})+\ell(B\cap X_{k,2}) = \ell(B\cap(X_{k,1}\cup X_{k,2}) = \ell(B\cap X_k)$, then

$$\begin{aligned}\ell(B_1) &= \sum_{k=1}^{\infty} L_k, \\ &= s + (1-s), \\ &= 1.\end{aligned} \tag{4.26}$$

Therefore we have that $\ell(B_1) = 1$ Lebesgue full measure. Since one basin has full measure, then by Theorem 4.2, $\ell(B_0) = 0$.

(ii) Secondly, we consider the case $s < 1/2$ (which implies that $0 < \kappa < 1$). To find $L_{1,1}$, we recall that all points in $X_{1,1}$ will definitely go to A_1 (this follows from (4.6)) where A_1 is in B_1. We have obtained that the $L_{1,1} = \ell(X_{1,1})$ for previous case since $\ell(X_{1,1}\cap B_1) = \ell(X_{1,1})$. But if we consider $A = B_0$,

$$L_{i,j} = \ell(B_0 \cap X_{i,j})$$

then $L_{1,1} = 0$. Following from (4.20) for $k = 1$, we have that

$$K_1\delta + K_2\tilde{\delta} = 0$$

because $L_{1,1} = 0$. We can solve for K_2;

$$K_2 = \frac{-K_1\delta}{\tilde{\delta}}.$$

To solve K_1, we can take the largest possible set with asymptotically full measure from (4.21) such that

$$\frac{L_{k,1}}{\ell(X_{k,1})} \to 1 \text{ as } k \to \infty.$$

Note also from (4.21) that $\ell(X_{k,1}) = s(1-\delta)\delta^{k-1}$. Then

$$\begin{aligned}\frac{L_{k,1}}{s(1-\delta)\delta^{k-1}} &= \frac{K_1\delta^k + K_2\tilde{\delta}^k}{s(1-\delta)\delta^{k-1}}, \\ &= \frac{K_1\delta}{s(1-\delta)} + \frac{K_2\delta}{s(1-\delta)}\left(\frac{\tilde{\delta}}{\delta}\right)^k.\end{aligned}$$

Since $\tilde{\delta} < \delta$, as $k \to \infty$ then

$$\frac{K_1\delta}{s(1-\delta)} = 1.$$

Solving this we get

$$K_1 = \frac{s(1-\delta)}{\delta}.$$

Hence the general solution from (4.20) for $L_{k,1}$ in this case is

$$\begin{aligned} L_{k,1} &= \frac{s(1-\delta)}{\delta}\delta^k - \frac{s(1-\delta)}{\tilde{\delta}}\tilde{\delta}^k, \\ &= s(1-\delta)[\delta^{k-1} - \tilde{\delta}^{k-1}]. \end{aligned} \tag{4.27}$$

Now in order to find $L_{k,2}$, we need to substitute the above value of $L_{k,1}$ into (4.18)

$$L_{k,2} = (1-s)(1-\delta)\delta^{k-1} + \frac{s\delta - \tilde{\delta}}{\delta\tilde{\delta}}(1-\delta)\tilde{\delta}^k. \tag{4.28}$$

Thus the sum for L_k for this case is

$$\begin{aligned} \ell(B_0) &= \sum_{k=1}^{\infty} L_k, \\ &= \sum_{k=1}^{\infty} L_{k,1} + \sum_{k=1}^{\infty} L_{k,2}, \\ &= s - \frac{s(1-\delta)}{1-\tilde{\delta}} + (1-s) + \frac{(s\delta - \tilde{\delta})(1-\delta)}{\delta(1-\tilde{\delta})}, \\ &= 1 - \frac{\tilde{\delta}(1-\delta)}{\delta(1-\tilde{\delta})}, \\ &= \frac{2\kappa}{(1-\delta) + \kappa(1+\delta)}, \end{aligned} \tag{4.29}$$

where this shows that the values of $0 < \ell(B_0) < 1$ since $\kappa > 0$. Hence for $0 < \kappa < 1$, by Theorem 4.1, $0 < \ell(B_1) < 1$. For this case, A_0 is an attractor since it attracts a set of positive measure, i.e. $\ell(B_0) > 0$ (this satisfies the first condition for A_0 to be a Milnor attractor). ■

Recall we denote B_0 and B_1 the basins of A_0 and A_1 respectively. Next theorem proves that the basin of A_0 is riddled with basin of A_1. According to Alexander *et. al* [1], two steps are required to prove a basin is riddled:

(1) We must show that a set of positive measure is attracted to A_0.

(2) We must show that there are infinitely many points near the attractor A_0 repelled from it.

Whereas in this thesis, we divide our proof into 4 steps as discussed in the following theorem.

Theorem 4.4 *For any* $0 < \delta < 1$ *and* $s < 1/2$, B_0 *is riddled with* B_1.

Proof. To prove that B_0 is riddled with B_1, the following should be satisfied:

(i) $B_0 \cup B_1$ is full measure, i.e. $\ell(B_0 \cup B_1) = 1$ as proved in Theorem 4.2.

(ii) Both basins have positive measure, i.e. $\ell(B_0) > 0$ and $\ell(B_1) > 0$ where $B_0 \cap B_1 = \emptyset$ as proved in Theorem 4.3.

(iii) We need to show that B_1 is dense in $[0,1]^2$. For any point $\theta \in [0,1]$ with itinerary as in (4.8), there is a nearby point $\tilde{\theta}$ within any neighbourhood of θ such that $\tilde{\theta}$ ends with infinite number of 0s. Then by Lemma 4.3, $\lim_{N\to\infty} i_N(\theta)$ will converge to 0, which implies that $\lim_{N\to\infty} i_N(\theta)/N < 1/2$, which means that $\tilde{\theta}$ is in the zero set of the basin boundary. This means there are 'cusps' of instability at all points $(\tilde{\theta}, 0)$ on the θ-axis and this shows that B_1 is dense. Thus, this proves that B_1 is dense. We show the schematic of the cusps in Figure 4.5.

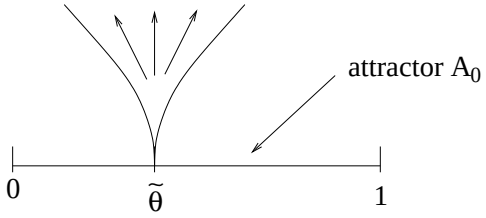

Figure 4.5 The schematic diagram showing the cusp at point $(\tilde{\theta}, 0)$ on the attractor A_0.

(iv) We need to show that B_1 has positive measure on any neighbourhood in $[0,1]^2$. The interior of $X_{1,1}$ is open and thus has positive Lebesgue measure. B_1 in fact the union of all the preimages of $X_{1,1}$. Therefore it contains open sets in any neighbourhood within $[0,1]^2$. Note that an orbit is in B_1 if and only if it ends in $X_{1,1}$ after some number of finite iterates. ■

4.4 Stability index for $(\theta, 0)$

From Theorem 4.4, we know that $\ell(B_0) > 0$ when $s < 1/2$ such that B_0 is a riddled basin. Thus we are interested to compute the stability index for this range to characterize the riddled basin for this system. Recall that we have defined the ergodic measures in Definition 2.27 and in this chapter we denote $\mathcal{E}(T_s)$ the set of all invariant ergodic measures for the map $T_s(\theta)$ such that $\mu \in \mathcal{P}(T_s)$. We note here

that there is a special case Lebesgue measure $\mu = \ell^1$. In fact we can relate the stability index with the Lyapunov exponents. In this section, we relate the stability index to the Lyapunov exponents.

We show the Lyapunov exponents for the map F at $(\theta, 0)$ as in the following lemmas.

Lemma 4.4 *Suppose* $t := \int_0^s d\mu(\theta)$ *for any* $\mu \in \mathcal{E}(T_s)$. *Then the Lyapunov exponent in the base direction is*

$$\lambda_{\|}(\theta) = -t \log s - (1-t)\log(1-s).$$

Proof. Note that as μ is a probability measure, we have that $1 - t = \int_s^1 d\mu(\theta)$. If μ is ergodic, then for μ-almost all θ,

$$\begin{aligned}
\lambda_{\|}(\theta) &= \lim_{N\to\infty} \frac{1}{N} \sum_{k=0}^{N-1} \log \frac{dT_s}{d\theta}(T_s^k(\theta)), \\
&= \int \log \frac{dT_s}{d\theta}(\theta)\ d\mu(\theta), \\
&= \int_{\theta=0}^{t} \log\left(\frac{1}{s}\right) d\mu(\theta) + \int_{\theta=t}^{1} \log\left(\frac{1}{1-s}\right) d\mu(\theta), \\
&= \log\left(\frac{1}{s}\right) \int_{\theta=0}^{t} d\mu(\theta) + \log\left(\frac{1}{1-s}\right) \int_{\theta=t}^{1} d\mu(\theta), \\
&= t \log\left(\frac{1}{s}\right) + (1-t)\log\left(\frac{1}{1-s}\right), \\
&= -t\log s - (1-t)\log(1-s). \ \blacksquare
\end{aligned} \tag{4.30}$$

Lemma 4.5 *Suppose* $t := \int_0^s d\mu(\theta)$ *for any* $\mu \in \mathcal{E}(T_s)$. *Then the Lyapunov exponent in the fibre direction is*

$$\lambda_{\perp}(\theta) = (1-2t)\log\delta.$$

Proof. If μ is ergodic, then for μ-almost all θ,

$$\begin{aligned}
\lambda_{\perp}(\theta) &= \lim_{N\to\infty} \frac{1}{N} \sum_{k=0}^{N-1} \log \frac{dh}{d\theta}(T_s^k(\theta)), \\
&= \int \log \frac{dh}{d\theta}(\theta)\ d\mu(\theta), \\
&= \int_{\theta=0}^{t} \log\left(\frac{1}{\delta}\right) d\mu(\theta) + \int_{\theta=t}^{1} \log\delta\ d\mu(\theta), \\
&= t\log\left(\frac{1}{\delta}\right) + (1-t)\log\delta, \\
&= -t\log\delta + (1-t)\log\delta, \\
&= (1-2t)\log\delta. \ \blacksquare
\end{aligned} \tag{4.31}$$

Note also that $\lambda_{\|}(\theta)$ is always positive but $\lambda_{\perp}(\theta)$ can be either positive or negative depending on the values of t. In particular, if $t < 1/2$, then $\lambda_{\perp}(\theta)$ is negative and if $t > 1/2$, then $\lambda_{\perp}(\theta)$ is positive.

Below we show the main result of stability index index at $(\theta, 0)$ in terms of the Lyapunov exponents.

Theorem 4.5 *For $s < 1/2$, any $0 < \delta < 1$ and any $\mu \in \mathcal{E}(T_s)$, for μ-almost all θ;*

$$\sigma(\theta,0) = \begin{cases} \frac{\log\tilde{\delta}-\log\delta}{\log\delta}\left(\frac{\lambda_{\|}(\theta)-\lambda_{\perp}(\theta)}{\lambda_{\|}(\theta)}\right) > 0 & \text{if } \lambda_{\|}(\theta)-\lambda_{\perp}(\theta) > 0, \\ \left(\frac{\lambda_{\|}(\theta)-\lambda_{\perp}(\theta)}{\lambda_{\|}(\theta)}\right) < 0 & \text{if } \lambda_{\|}(\theta)-\lambda_{\perp}(\theta) < 0, \end{cases} \tag{4.32}$$

where $\lambda_{\|}(\theta)$ and $\lambda_{\perp}(\theta)$ are the Lyapunov exponents in the base and fibre directions as defined in Lemma 4.4 and Lemma 4.5 respectively.

Proof. See Section 4.4.1. ■

The next theorem is a consequence of Theorem 4.5 for a special case $\mu = \ell^1$.

Theorem 4.6 *For $s < 1/2$, any $0 < \delta < 1$ and $\ell^1 \in \mathcal{E}(T_s)$,*

(i) For ℓ^1-almost all θ, we have θ with positive stability index, i.e. $\sigma(\theta, 0) > 0$,

(ii) There exists a θ with negative stability index (i.e. $\sigma(\theta, 0) < 0$) if and only if $\delta < s$.

Proof.

(i) If $0 < \delta < 1$ and $s < 1/2$, then for ℓ^1-almost all θ we have from (4.30) and (4.31) that

$$\lambda_{\|}(\theta) = -s\log s - (1-s)\log(1-s) > 0,$$

and

$$\lambda_{\perp}(\theta) = (1-2s)\log\delta < 0,$$

respectively, for $\mu = \ell^1$. Note that $t = \int_0^s d\ell = s$. So

$$\begin{aligned} \sigma(\theta,0) &= \frac{\log\tilde{\delta}-\log\delta}{\log\delta}\left(\frac{\lambda_{\|}(\theta)-\lambda_{\perp}(\theta)}{\lambda_{\|}(\theta)}\right), \\ &= \frac{\log\tilde{\delta}-\log\delta}{\log\delta}\cdot\frac{-s\log s-(1-s)\log(1-s)-(1-2s)\log\delta}{-s\log s-(1-s)\log(1-s)} > 0, \end{aligned} \tag{4.33}$$

where $\frac{\log\tilde{\delta}-\log\delta}{\log\delta} > 0$ since $\tilde{\delta} < \delta$. Then $\lambda_{\|}(\theta) - \lambda_{\perp}(\theta) > 0$ and therefore we will always have $\sigma(\theta, 0) > 0$.

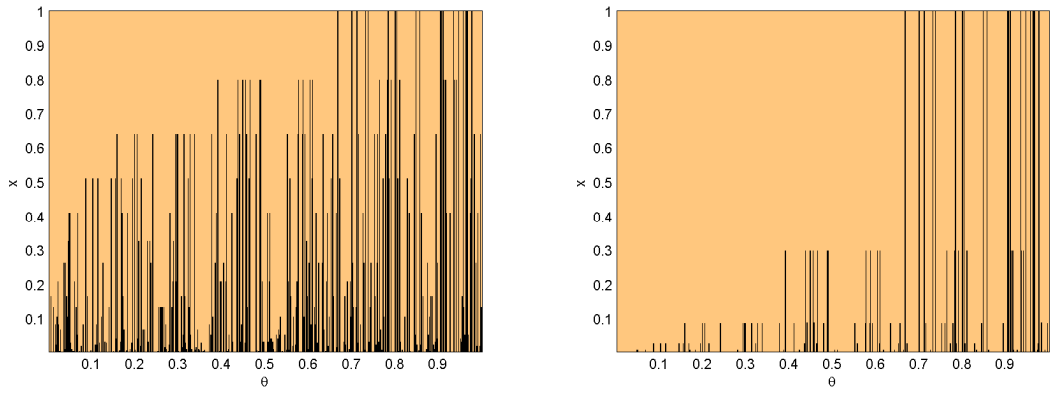

(a) (b)

Figure 4.6 The numerical approximation of riddled basin for model in (4.1). The black strips represent basin B_0 and the orange area is the basin B_1. (a) When $\delta = 0.8$ and $s = 0.49$, the stability index is positive for Lebesgue measure almost all θ. This corresponds to Case I in the proof of Theorem 4.5. (b) When $\delta = 0.3$ and $s = 0.49$, the stability index is negative for some points θ with the condition that $\delta < s$ (see Theorem 4.6). This corresponds to Case II in the proof of Theorem 4.5.

(ii) If $\lambda_{\|}(\theta) < \lambda_{\perp}(\theta)$ and $t := \int_0^s d\mu(\theta)$ for some $\mu \in \mathcal{E}(T_s)$, then

$$\begin{aligned}\sigma(\theta, 0) &= \left(\frac{\lambda_{\|}(\theta) - \lambda_{\perp}(\theta)}{\lambda_{\|}(\theta)}\right), \\ &= \frac{-t\log s - (1-t)\log(1-s) - (1-2t)\log\delta}{-t\log s - (1-t)\log(1-s)}. \end{aligned} \tag{4.34}$$

We wish to find a μ such that $\sigma(\theta, 0) < 0$ for μ-almost all θ. Note that

$$\inf_{0<t<1}(\lambda_{\|}(\theta) - \lambda_{\perp}(\theta)) = -\log s + \log\delta.$$

So, if $-\log s + \log\delta < 0$, we have $\log\delta < \log s$ if and only if $\delta < s$. Then this means that there are θ with $\sigma(\theta, 0) < 0$. ■

We show the riddled basins with the corresponding positive and negative stability indices in Figure 4.6 within the scale $(\theta, x) \in [0, 1] \times [0, 1]$. Moreover, we also plot the stability index for various $0 < \delta < 1$ in Figure 4.7. Our numerical result is indeed agrees with our proof in Theorem 4.6 where for ℓ^1-almost all θ, $\sigma(\theta, 0) > 0$ and for some θ, $\sigma(\theta, 0) < 0$ if and only if $\delta < s$ where $s = 0.49$. These positive and negative stability indices indicate that there are points $\tilde{\theta}$ within neighbourhood of θ that end up in B_1.

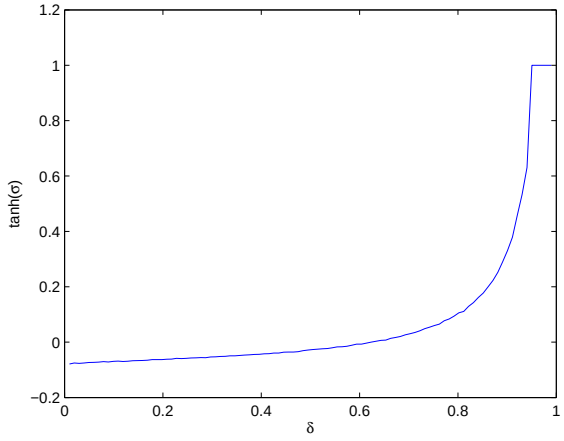

Figure 4.7 The stability index $\sigma(\theta, 0)$ for the piecewise linear map (4.1) over parameter $\delta = 0.01, \ldots, 0.99$ and fixed value $s = 0.49$ for a typical point $\theta = 0.9643$. The $\tanh(\theta) = 1$ here shows that $\sigma = +\infty$. The index increases from negative value monotonically to positive value then jumps to $+\infty$. Notice that there is no $\sigma(\theta, 0) = -\infty$ since we only consider the range $s < 1/2$ for which the riddled basin occurs such that the basin B_0 always has positive measure.

4.4.1 Proof of Theorem 4.5

Note that the computation of the above stability index is only for Lebesgue almost all θ. We can also compute for more general θ by also considering any other ergodic measures that is preserved by T_s, not only for the Lebesgue measure ℓ-almost all θ. There are uncountably many ergodic measures for this map, including the periodic measures (Dirac delta measures), Lebesgue measures, Bernoulli measures etc. This can be done by considering for example all possible Bernoulli measures μ_t.

In this section, we prove Theorem 4.5. The aim is to show that the first case gives positive stability index while the second case gives negative stability index. We also express the formulae for the stability indices in terms of the Lyapunov exponents of system F in (4.1).

For any point $\theta \in \mathbb{T}$, its orbit has the characteristic function as defined in (4.8). Now we take a nearby point $\tilde{\theta} \in \mathbb{T}$ within a neighbourhood of θ with the following itinerary function

$$n_k(\tilde{\theta}) := \begin{cases} 0 & \text{if } T_s^k(\tilde{\theta}) < s, \\ 1 & \text{if } T_s^k(\tilde{\theta}) \geq s. \end{cases}$$

If this nearby point $\tilde{\theta}$ has an orbit that always follow the orbit of θ, then we can define the following

$$I_N(\theta) := \{\tilde{\theta} \in \mathbb{T} : n_k(\tilde{\theta}) = n_k(\theta) \text{ for } k = 0, \ldots, N-1\}, \tag{4.35}$$

where we will have different $I_N(\theta)$ for different θ and N. Note that $T_s^k(I_N(\theta)) \subset I_{n_k(\theta)}$

for $k = 0, \ldots, N-1$ where $\begin{cases} I_0 &= [0, s), \\ I_1 &= [s, 1), \end{cases}$ and after Nth iterations $I_N(\theta)$ will be mapped to the whole of base space $\mathbb{T}$, i.e.,

$$T_s^N(I_N(\theta)) = \mathbb{T}.$$

Note also that $T_s^k|_{I_N(\theta)}$ is invertible for $k = 0, \ldots, N$, i.e.,

$$(T_s^N|_{I_N(\theta)})^{-1}(\mathbb{T}) = I_N(\theta). \tag{4.36}$$

We note that the 1-dimensional Lebesgue measure for any invariant set A under the skewed doubling map is

$$\ell^1(T_s(A)) = \begin{cases} \frac{\ell^1(A)}{s} & \text{if} \quad A \subset I_0, \\ \frac{\ell^1(A)}{1-s} & \text{if} \quad A \subset I_1, \end{cases}$$

where $1/s$ and $1/(1-s)$ are the slopes in I_0 and I_1 respectively. So, by using invertibility in (4.36), one can find the one-dimensional Lebesgue measure of the set $I_N(\theta)$ in (4.35) as

$$\begin{aligned} \ell^1(I_N(\theta)) &= s^{N-i_N(\theta)}(1-s)^{i_N(\theta)}\ell^1(\mathbb{T}) \\ &= s^{N-i_N(\theta)}(1-s)^{i_N(\theta)}, \end{aligned} \tag{4.37}$$

where $\ell^1(\mathbb{T}) = 1$, $(1-s)^{i_N(\theta)}$ describes number of times the orbit of θ lies in $[s, 1]$ (this follows from (4.9)) and $s^{N-i_N(\theta)}$ describes the number of times the orbit of θ lies in $[0, s]$.

Now we want to construct the neighbourhoods of point $(\theta, 0)$. From (4.37), we need to pick N such that

$$s^{N-i_N(\theta)}(1-s)^{i_N(\theta)} = 2\varepsilon \tag{4.38}$$

in the θ-direction. We can consider the neighbourhoods of $(\theta, 0)$ by

$$U_{N,M}(\theta) := \{(\tilde{\theta}, x) : \tilde{\theta} \in I_N(\theta), x < \delta^M\} \tag{4.39}$$

and $U_{N,M}(\theta) \approx B_\varepsilon(\theta, 0)$ if (4.38) is satisfied at $\delta^M = \varepsilon$ in x-direction, where $M = \frac{\log \varepsilon}{\log \delta}$. To put it simply, this means that the neighbourhood is 2ε in the θ-direction and ε in the x-direction.

First we consider for Case I. After N iterates, the neighbourhood $U_{N,M}(\theta)$ expands under the skew product transformation F such that

$$F^N(U_{N,M}(\theta)) = \mathbb{T} \times [0, \delta^{Q_\varepsilon(\theta)}], \tag{4.40}$$

for some $Q_\varepsilon(\theta)$, where this means that after Nth iterations, δ^M expands to $\delta^{Q_\varepsilon(\theta)}$ by considering the shrinking and expanding rates, i.e. $\delta^{i_N(\theta)}$ and $\left(\frac{1}{\delta}\right)^{N-i_N(\theta)}$ respectively. Hence we have

$$\begin{aligned}\delta^{Q_\varepsilon(\theta)} &= \delta^M \times \delta^{i_N(\theta)} \times \delta^{-N+i_N(\theta)}, \\ &= \delta^{M+2i_N(\theta)-N}.\end{aligned} \tag{4.41}$$

We show the sketch of $U_{N,M}(\theta)$ after N iterates in Figure 4.8.

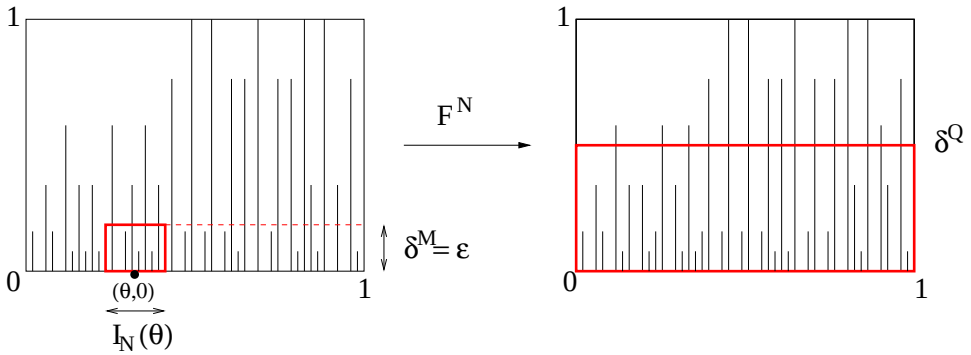

Figure 4.8 Case I: The schematic diagram showing the Nth iterates of $U_{N,M}(\theta)$ (red box) where δ^M expands to $\delta^{Q_\varepsilon(\theta)}$ and $I_N(\theta)$ to $\mathbb{T}$. The black strips denote the basin B_0.

From the above we consider for the case

$$Q_\varepsilon(\theta) = M + 2i_N(\theta) - N \geq 0. \tag{4.42}$$

Notice that from (4.40), the 2-dimensional Lebesgue measure for $U_{N,M}(\theta)$ after Nth iterations is

$$\ell^2(F^N(U_{N,M}(\theta))) = 1 \times \delta^{Q_\varepsilon(\theta)}.$$

Now from the above we want to find the 2-dimensional Lebesgue measure for $U_{N,M}(\theta)$. To measure this, we find the preimages of $F^N(U_{N,M}(\theta))$ such that

$$\begin{aligned}\ell^2(U_{N,M}(\theta)) &= 1 \times \delta^{Q_\varepsilon(\theta)} \times s^{N-i_N(\theta)} \times (1-s)^{i_N(\theta)} \times \delta^{-2i_N(\theta)+N}, \\ &= \delta^M \times s^{N-i_N(\theta)} \times (1-s)^{i_N(\theta)}.\end{aligned} \tag{4.43}$$

So far, we have computed $F^N(U_{N,M})$ and its measure $\ell^2(F^N(U_{N,M}))$. Now, in order to compute the stability index at point $(\theta, 0)$, we need to find the proportion of B_0 that is in $U_{N,M}(\theta)$. To compute this, we first use the results from Theorem 4.3 in the case of $s < 1/2$ where we refer $L_{k,1}$ in (4.27) and $L_{k,2}$ in (4.28) to find L_k. Recall

that $L_k = \ell_2(X_k \cap B_0)$ where $X_k = X_{k,1} \cup X_{k,2}$. We can find L_k by

$$\begin{aligned}
L_k &= L_{k,1} + L_{k,2}, \\
&= s(1-\delta)(\delta^{k-1} - \tilde{\delta}^{k-1}) + (1-s)(1-\delta)\delta^{k-1} + \frac{(s\delta - \tilde{\delta})(1-\delta)}{\delta}\tilde{\delta}^{k-1}, \\
&= s(1-\delta)\delta^{k-1} + s(1-\delta)\tilde{\delta}^{k-1} + (1-s)(1-\delta)\delta^{k-1} + \frac{(s\delta - \tilde{\delta})(1-\delta)}{\delta}\tilde{\delta}^{k-1}, \\
&= (1-\delta)\delta^{k-1}[s + 1 - s] + (1-\delta)\tilde{\delta}^{k-1}\left[-s + \frac{s\delta - \tilde{\delta}}{\delta}\right], \\
&= (1-\delta)\delta^{k-1} - (1-\delta)\tilde{\delta}^{k-1}\left(\frac{\tilde{\delta}}{\delta}\right), \\
&= (1-\delta)\left(\delta^{k-1} - \frac{\tilde{\delta}^k}{\delta}\right). \qquad (4.44)
\end{aligned}$$

Then we can find the sum of L_k from level $\delta^{Q_\varepsilon(\theta)}$ up to δ^k (for $k = Q_\varepsilon(\theta)+1, \ldots, \infty$) by

$$\begin{aligned}
L^+_{Q_\varepsilon(\theta)} = \ell^2(F^N(U_{N,M}(\theta) \cap B_0)) = \sum_{k=Q_\varepsilon(\theta)+1}^{\infty} L_k &= \sum_{k=Q_\varepsilon(\theta)+1}^{\infty} (1-\delta)\delta^{k-1} - \sum_{k=Q_\varepsilon(\theta)+1}^{\infty} \frac{(1-\delta)}{\delta}\tilde{\delta}^k, \\
&= \frac{(1-\delta)\delta^{Q_\varepsilon(\theta)}}{1-\delta} - \frac{(1-\delta)\tilde{\delta}^{Q_\varepsilon(\theta)+1}}{\delta(1-\tilde{\delta})}, \\
&= \delta^{Q_\varepsilon(\theta)} - \frac{(1-\delta)\tilde{\delta}^{Q_\varepsilon(\theta)+1}}{\delta(1-\tilde{\delta})}. \qquad (4.45)
\end{aligned}$$

So we obtain the proportion as

$$\begin{aligned}
\Sigma_\varepsilon(\theta, 0) &= \frac{\ell(U_{N,M}(\theta) \cap B_0)}{\ell(U_{N,M}(\theta))}, \\
&= \frac{\ell^2(F^N(U_{N,M}(\theta) \cap B_0))}{\ell^2(F^N(U_{N,M}(\theta))}, \\
&= \frac{L^+_{Q_\varepsilon(\theta)}}{\delta^{Q_\varepsilon(\theta)}}, \\
&= 1 - \left(\frac{1-\delta}{1-\tilde{\delta}}\right)\left(\frac{\tilde{\delta}}{\delta}\right)^{Q_\varepsilon(\theta)+1}. \qquad (4.46)
\end{aligned}$$

This means that as $\varepsilon \to 0$ we have that $M \to \infty$, hence $Q_\varepsilon(\theta) \to \infty$ and since $\tilde{\delta} < \delta$, $\lim_{\varepsilon \to 0} \Sigma_\varepsilon(\theta, 0) = 1$ and by Lemma 3.1(b) this implies that $\sigma_-(\theta, 0) = 0$. Meanwhile

$$1 - \Sigma_\varepsilon(\theta, 0) = \left(\frac{1-\delta}{1-\tilde{\delta}}\right)\left(\frac{\tilde{\delta}}{\delta}\right)^{Q_\varepsilon(\theta)+1}. \qquad (4.47)$$

Since $\sigma_-(\theta, 0) = 0$, from Lemma 3.1(b) we want to show that

$$1 - \Sigma_\varepsilon(\theta, 0) = \tilde{\Theta}(\varepsilon^{\sigma_+(\theta,0)}). \tag{4.48}$$

To prove the above, we need to find the values of $Q_\varepsilon(\theta)$ in (4.47) where $Q_\varepsilon(\theta)$ has been defined in (4.42). Previously, we know that $M = \log\varepsilon/\log\delta$. Let μ_t be the *Bernoulli measure* [2] such that the frequency of visiting the left interval is t, i.e.

$$t := \int_0^s d\mu_t(\theta) = \int_0^1 \chi_{[0,s)}(\theta) d\mu_t(\theta),$$

where $0 < t < 1$. We know from Birkhoff's Ergodic Theorem in (4.11) that for μ_t-almost all θ and for large N,

$$i_N(\theta) \approx (1-t)N.$$

By substituting this into (4.38);

$$\begin{aligned} 2\varepsilon &\approx s^{N-(1-t)N}(1-s)^{(1-t)N}, \\ &\approx s^{Nt}(1-s)^{N(1-t)}. \end{aligned}$$

By taking logs for small ε we have

$$\begin{aligned} \log\varepsilon &\approx Nt\log s + N(1-t)\log(1-s), \\ &\approx N(t\log s + (1-t)\log(1-s)). \end{aligned}$$

Therefore we obtain N as

$$N \approx \frac{\log\varepsilon}{t\log s + (1-t)\log(1-s)}.$$

Now substitute M and N into (4.42) to give

$$\begin{aligned} Q_\varepsilon(\theta) &:= \frac{\log\varepsilon}{\log\delta} + (1-2t)\frac{\log\varepsilon}{t\log s + (1-t)\log(1-s)}, \\ &:= \log\varepsilon\left(\frac{1}{\log\delta} + \frac{1-2t}{t\log s + (1-t)\log(1-s)}\right), \\ &:= \frac{\log\varepsilon}{\log\delta}\left(\frac{\lambda_\parallel(\theta) - \lambda_\perp(\theta)}{\lambda_\parallel(\theta)}\right). \end{aligned} \tag{4.49}$$

[2] Let $\sigma : \sum_2 \to \sum_2$ be a full shift on two symbols. Let $t = (t_1, t_2)$ be a probability vector (i.e. $t_1, t_2 \geq 0$ and $t_1 + t_2 = 1$) and let μ_t be the Bernoulli measure determined by t, i.e., on cylinder sets: $u_t[z_0, \ldots, z_{n-1}] = p_{z_0} \cdots p_{z_{n-1}}$ [60]. In this chapter, when $t = s$, the Bernoulli measure is equivalent to Lebesgue measure where we now have Bernoulli $(s, 1-s)$-measure.

Then from (4.47), we can define the constant $K = \frac{1-\delta}{1-\tilde{\delta}}$ and express it in logs' form;

$$\begin{aligned}
1 - \Sigma_\varepsilon(\theta, 0) &= K e^{\log\left(\frac{\tilde{\delta}}{\delta}\right)^{Q_\varepsilon(\theta)+1}}, \\
&= K e^{(Q_\varepsilon(\theta)+1)(\log\tilde{\delta} - \log\delta)}, \\
&= K e^{(\log\tilde{\delta} - \log\delta)} e^{(\log\tilde{\delta} - \log\delta)Q_\varepsilon(\theta)}, \\
&= \tilde{K} e^{(\log\tilde{\delta} - \log\delta)\frac{\log\varepsilon}{\log\delta}\left(\frac{\lambda_\parallel(\theta) - \lambda_\perp(\theta)}{\lambda_\parallel(\theta)}\right)}, \\
&= \tilde{K} e^{\left(\frac{\log\tilde{\delta} - \log\delta}{\log\delta}\right)\left(\frac{\lambda_\parallel(\theta) - \lambda_\perp(\theta)}{\lambda_\parallel(\theta)}\right)\log\varepsilon}, \\
&= \tilde{K} e^{\log\varepsilon^{\left(\frac{\log\tilde{\delta} - \log\delta}{\log\delta}\right)\left(\frac{\lambda_\parallel(\theta) - \lambda_\perp(\theta)}{\lambda_\parallel(\theta)}\right)}}, \\
&= \tilde{K} \varepsilon^{\left(\frac{\log\tilde{\delta} - \log\delta}{\log\delta}\right)\left(\frac{\lambda_\parallel(\theta) - \lambda_\perp(\theta)}{\lambda_\parallel(\theta)}\right)}, \qquad (4.50)
\end{aligned}$$

where $\tilde{K} = K e^{(\log\tilde{\delta} - \log\delta)}$. Therefore by comparing the above with (4.48), we have

$$\sigma_+(\theta, 0) = \left(\frac{\log\tilde{\delta} - \log\delta}{\log\delta}\right)\left(\frac{\lambda_\parallel(\theta) - \lambda_\perp(\theta)}{\lambda_\parallel(\theta)}\right), \quad \sigma_-(\theta, 0) = 0.$$

Thus as long as $Q_\varepsilon(\theta) \geq 0$, the stability index at point $(\theta, 0)$ is

$$\begin{aligned}
\sigma(\theta, 0) &= \sigma_+(\theta, 0) - \sigma_-(\theta, 0), \\
&= \left(\frac{\log\tilde{\delta} - \log\delta}{\log\delta}\right)\left(\frac{\lambda_\parallel(\theta) - \lambda_\perp(\theta)}{\lambda_\parallel(\theta)}\right), \qquad (4.51)
\end{aligned}$$

where $\lambda_\parallel(\theta)$ and $\lambda_\perp(\theta)$ are as obtained in (4.30) and (4.31) respectively. For this case, this index is always positive since A_0 is an attractor. $Q_\varepsilon(\theta) \to \infty$ as $\varepsilon \to 0$ if and only if from (4.49) we have that $\lambda_\parallel(\theta) - \lambda_\perp(\theta) > 0$ i.e. $\lambda_\parallel(\theta) > \lambda_\perp(\theta)$.

Now, we consider for Case II. On the other hand, for this case we consider for

$$Q_\varepsilon(\theta) = M + 2i_N(\theta) - N < 0.$$

The Nth iterates for $U_{N,M}(\theta)$ now is

$$F^N(U_{N,M}(\theta)) = \mathbb{T} \times [0, 1].$$

The mapping is just $\mathbb{T} \times [0, 1]$ since we have assume for this model that everything that is larger than 1 (i.e. $x > 1$) will be mapped to A_1. In particular,

$$F^N : I_N(\theta) \times [0, \delta^{M - Q_\varepsilon(\theta)}] \to \mathbb{T} \times [0, 1],$$

and

$$F^N : I_N(\theta) \times [\delta^{M - Q\varepsilon(\theta)}, \delta^M] \to \mathbb{T} \times \{1\} = A_1.$$

We show the the sketch of $U_{N,M}(\theta)$ for this case in Figure 4.9.

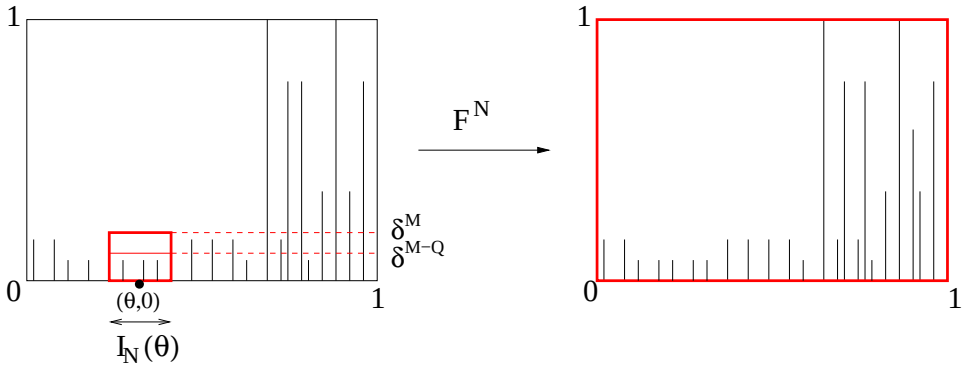

Figure 4.9 Case II: The schematic diagram showing the Nth iterates of $U_{N,M-Q_\varepsilon(\theta)}(\theta) = I_N(\theta) \times [0, \delta^{M-Q_\varepsilon(\theta)}]$ (lower red box) where it mapped to $\mathbb{T} \times [0,1]$. The Nth iterates of the upper red box is just $A_1 = \mathbb{T} \times \{1\}$.

To compute the proportion of B_0 that is in the $U_{N,M}(\theta)$, we use (4.45) to compute L_0^+ from level $\delta^0 = 1$ up to δ^k (for $k = 1, \ldots, \infty$);

$$L_0^+ = \ell^2(F^N(U_{N,M}(\theta) \cap B_0)) = \sum_{k=1}^{\infty} L_k = 1 - \left(\frac{1-\delta}{1-\tilde{\delta}}\right)\left(\frac{\tilde{\delta}}{\delta}\right).$$

Then the proportion is

$$\begin{aligned}
\Sigma_\varepsilon(\theta, 0) &= \frac{\ell^2(U_{N,M-Q_\varepsilon(\theta)}(\theta) \cap B_0)}{\ell^2(U_{N,M}(\theta))}, \\
&= \frac{\ell^2(U_{N,M-Q_\varepsilon(\theta)}(\theta) \cap B_0)}{\ell^2(U_{N,M-Q_\varepsilon(\theta)}(\theta))} \cdot \frac{\ell^2(U_{N,M-Q_\varepsilon(\theta)}(\theta)}{\ell^2(U_{N,M}(\theta))}, \\
&= \frac{\ell^2(F^N(U_{N,M-Q_\varepsilon(\theta)}(\theta) \cap B_0))}{\ell^2(F^N(U_{N,M-Q_\varepsilon(\theta)}(\theta))} \cdot \frac{I_N(\theta) \times \delta^{M-Q_\varepsilon(\theta)}}{I_N(\theta) \times \delta^M}, \\
&= \frac{L_0^+}{1}\delta^{-Q_\varepsilon(\theta)}, \\
&= L_0^+ \delta^{-Q_\varepsilon(\theta)}, \\
&= \hat{K}\delta^{-Q_\varepsilon(\theta)}, \qquad (4.52)
\end{aligned}$$

where $\hat{K} = L_0^+ = 1 - \left(\frac{1-\delta}{1-\tilde{\delta}}\right)\left(\frac{\tilde{\delta}}{\delta}\right)$. Note that from the above $\ell^2(U_{N,M-Q_\varepsilon(\theta)}(\theta) \cap B_0) \approx \ell^2(F^N(U_{N,M-Q_\varepsilon(\theta)}(\theta) \cap B_0))$ and $\ell^2(U_{N,M-Q}(\theta)) \approx \ell^2(F^N(U_{N,M-Q_\varepsilon(\theta)}(\theta))$ since F^N is linear and invertible on $U_{N,M}(\theta)$. It is clear from (4.52) that $\Sigma_\varepsilon(\theta, 0)$ does not converge to 1, i.e. we can show that

$$\Sigma_\varepsilon(\theta, 0) = \tilde{\Theta}(\varepsilon^{\sigma_-(\theta,0)}).$$

To prove this, we use the values of $Q_\varepsilon(\theta)$ in (4.49) into (4.52);

$$\begin{aligned}
\Sigma_\varepsilon(\theta,0) \approx \hat{K}\delta^{-Q_\varepsilon(\theta)} &= \hat{K}e^{\log\delta^{-Q_\varepsilon(\theta)}}, \\
&= \hat{K}e^{-Q_\varepsilon(\theta)\log\delta}, \\
&= \hat{K}e^{-\log\delta\frac{\log\varepsilon}{\log\delta}\left(\frac{\lambda_\parallel(\theta)-\lambda_\perp(\theta)}{\lambda_\parallel(\theta)}\right)}, \\
&= \hat{K}e^{-\left(\frac{\lambda_\parallel(\theta)-\lambda_\perp(\theta)}{\lambda_\parallel(\theta)}\right)\log\varepsilon}, \\
&= \hat{K}e^{\log\varepsilon^{-\left(\frac{\lambda_\parallel(\theta)-\lambda_\perp(\theta)}{\lambda_\parallel(\theta)}\right)}}, \\
&= \hat{K}\varepsilon^{-\left(\frac{\lambda_\parallel(\theta)-\lambda_\perp(\theta)}{\lambda_\parallel(\theta)}\right)}.
\end{aligned}$$

Therefore we have

$$\sigma_-(\theta,0) = -\left(\frac{\lambda_\parallel(\theta)-\lambda_\perp(\theta)}{\lambda_\parallel(\theta)}\right).$$

By Lemma 3.1(c)), $1-\Sigma_\varepsilon \to 1$ as $\varepsilon \to 0$ and this implies that $\sigma_+(\theta,0)=0$. Thus as long as $Q_\varepsilon(\theta)<0$, the stability index at point $(\theta,0)$ now is

$$\sigma(\theta,0) = \sigma_+(\theta,0) - \sigma_-(\theta,0) = \left(\frac{\lambda_\parallel(\theta)-\lambda_\perp(\theta)}{\lambda_\parallel(\theta)}\right),$$

since $\sigma_+(\theta,0)=0$. For this case, as $Q\to-\infty$ and as $\varepsilon\to 0$, we have from (4.49) that $\lambda_\parallel(\theta)-\lambda_\perp(\theta)<0$ i.e. $\lambda_\perp(\theta)>\lambda_\parallel(\theta)$. This index now is always negative. ■

In fact, the proof of Theorem 4.5 can be related to Lemma 4.2 where Lemma 4.2 describes the behaviour of (θ_N, x_N). In the first case, if $x_N<1$, then it will stay inside $\mathbb{T}\times[0,1]$. Thus by Theorem 4.5 this corresponds that x_N will be within $\delta^{Q_\varepsilon(\theta)}<1$ as $Q_\varepsilon(\theta)\to\infty$. From the calculation of the stability index in the proof, the point (θ_N, x_N) has positive stability index.

On the other hand, for the second case, by Lemma 4.2, if $x_N>1$, then it will be mapped just to $\mathbb{T}\times\{1\}$. By Theorem 4.5, now $\delta^{Q_\varepsilon(\theta)}>1$ as $Q_\varepsilon(\theta)\to-\infty$. From the calculation of stability index in the proof, the point (θ_N, x_N) has negative stability index.

4.5 Stability index for the attractor

In Section 4.4, we have proved the stability index at point $(\theta,0)$ where for almost all θ, they have positive stability index, while for some θ, they can have negative stability index. Besides calculating this index for a point $(\theta,0)$, in this section we also formulate the stability index for the whole attractor $A_0=[0,1]\times\{0\}$. This means that we are no longer considering a specific θ. Our next result, Theorem 4.7,

can be related to that of Theorem 4.5.

Theorem 4.7 *For $s < 1/2$, any $0 < \delta < 1$ and $\varepsilon > 0$,*

$$\sigma(A_0) = \frac{\log\tilde{\delta} - \log\delta}{\log\delta},$$

where A_0 is the attractor at the baseline.

Proof. Since for this case we consider for the A_0, then we have for the θ-direction that

$$I_0(\theta) = \mathbb{T}.$$

Then the neighbourhood of A_0 is

$$U_{0,M} = \{(\tilde{\theta}, x) : \tilde{\theta} \in I_0(\theta), x < \delta^M\},$$

where $U_{0,M} \approx B_\varepsilon(A_0)$ which also satisfies at $\delta^M = \varepsilon$, i.e. $M = \frac{\log\varepsilon}{\log\delta}$. This means that the area of $U_{0,M}$ is

$$V_m = \ell(B_\varepsilon(A_0)) = 1 \times \delta^M = \delta^M.$$

We show the sketch of $U_{0,M}$ in Figure 4.10.

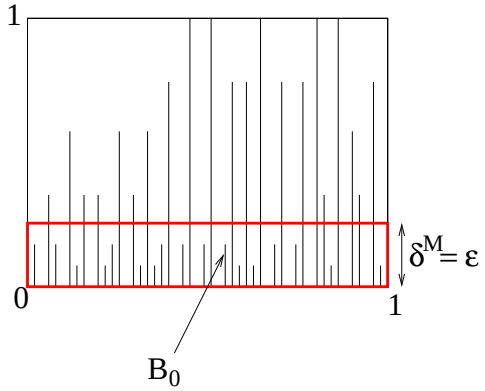

Figure 4.10 The schematic diagram showing the neighbourhood of the attractor $A_0 = [0,1] \times \{0\}$ represented by the red box $U_{0,M} = \mathbb{T} \times [0, \delta^M]$. We recall that the black strips B_0 is the basin of A_0.

Now, to determine the measure of B_0 that is in $U_{0,M}$, we use (4.45) to find the area from level δ^M to δ^k (for $k = M+1, \ldots, \infty$) which gives

$$\begin{aligned} L_m^+ &= \ell(B_\varepsilon(A_0) \cap B_0), \\ &= \sum_{k=M+1}^{\infty} L_k, \\ &= \delta^M - \left(\frac{1-\delta}{1-\tilde{\delta}}\right) \cdot \frac{\tilde{\delta}^{M+1}}{\delta}. \end{aligned}$$

Then the proportion is

$$\Sigma_\varepsilon(A_0) = \frac{L_m^+}{V_m} = \frac{\delta^M - \left(\frac{1-\delta}{1-\tilde{\delta}}\right)\cdot\frac{\tilde{\delta}^{M+1}}{\delta}}{\delta^M},$$
$$= 1 - \left(\frac{1-\delta}{1-\tilde{\delta}}\right)\left(\frac{\tilde{\delta}}{\delta}\right)^{M+1}.$$

From the above, as $M \to \infty$ and since $\tilde{\delta} < \delta$, $\Sigma_\varepsilon(\theta, 0)$ converges to 1 and by Lemma 3.1(b) this implies that $\sigma_-(A_0) = 0$. Therefore

$$1 - \Sigma_\varepsilon(A_0) = \left(\frac{1-\delta}{1-\tilde{\delta}}\right)\left(\frac{\tilde{\delta}}{\delta}\right)^{M+1},$$
$$= \overline{K}\varepsilon^{\sigma_+(A_0)},$$

where $\overline{K} = \left(\frac{1-\delta}{1-\tilde{\delta}}\right)e^{(\log\tilde{\delta}-\log\delta)}$ is the constant and where $e^{M\log\left(\frac{\tilde{\delta}}{\delta}\right)} = e^{\frac{\log\varepsilon}{\log\delta}(\log\tilde{\delta}-\log\delta)}$, then we have

$$\sigma_+(A_0) = \frac{\log\tilde{\delta} - \log\delta}{\log\delta}.$$

Since $\sigma_-(A_0) = 0$, then the stability index for the attractor A_0 is as follows

$$\sigma(A_0) = \sigma_+(A_0) - \sigma_-(A_0),$$
$$= \frac{\log\tilde{\delta} - \log\delta}{\log\delta}. \blacksquare \tag{4.53}$$

By comparing with Theorem 4.5, we have the following corollary.

Corollary 4.8 *For $s < 1/2$, any $0 < \delta < 1$ and any $\mu \in \mathcal{E}(T_s)$, for μ-almost all θ;*

$$\sigma(\theta, 0) = \begin{cases} \sigma(A_0)\cdot\frac{\lambda_\parallel(\theta)-\lambda_\perp(\theta)}{\lambda_\parallel(\theta)} > 0 & \text{if } \lambda_\parallel(\theta) - \lambda_\perp(\theta) > 0, \\ \frac{\lambda_\parallel(\theta)-\lambda_\perp(\theta)}{\lambda_\parallel(\theta)} < 0 & \text{if } \lambda_\parallel(\theta) - \lambda_\perp(\theta) < 0, \end{cases} \tag{4.54}$$

where $\sigma(A_0)$ is the stability index of A_0.

Notice that the formula for $\sigma(A_0)$ in (4.53) does not depend on θ while $\sigma(\theta, 0)$ depends on θ. This result was inspired by Keller's result in [44] which will be discussed in Chapter 5.

4.6 Criteria for non-convergence of the stability index

In the previous section, we have proved that the stability index exists for almost all θ. This is due to the fact that the limit $\lim_{N\to\infty} i_N(\theta)/N$ in (4.10) converges to some value. However, there are some points for which such limit does not converge and therefore we discuss the non-convergence of the stability index in this section. For this case, the stability index will oscillates between the lim inf and lim sup. To be more precise;

Theorem 4.9 *Suppose θ is such that*

$$\limsup_{N\to\infty} \frac{i_N(\theta)}{N} \neq \liminf_{N\to\infty} \frac{i_N(\theta)}{N}.$$

Then $\sigma(\theta, 0)$ will not converge.

Proof. From (4.42) if the limit $\lim_{N\to\infty} \frac{i_N(\theta)}{N}$ does not converge, then we have

$$\bar{t} = \limsup_{N\to\infty} \frac{i_N(\theta)}{N},$$

and

$$\underline{t} = \liminf_{N\to\infty} \frac{i_N(\theta)}{N}.$$

According to the stability index's formula, we have from (4.50) that

$$\frac{\log(1-\Sigma(\theta,0))}{\log\varepsilon} = \log\tilde{K} + \frac{Q_\varepsilon(\theta)}{\log\varepsilon}\left(\frac{\log\tilde{\delta}-\log\delta}{\log\delta}\right). \tag{4.55}$$

Let us denote

$$q(\theta) := \lim_{\varepsilon\to 0} \frac{Q_\varepsilon(\theta)}{\log\varepsilon},$$

where $Q_\varepsilon(\theta)$ is as in (4.49). If $q(\theta)$ does not converge, then $\sigma(\theta, 0)$ does not converge as well. In particular, if we denote

$$\bar{q}(\theta) := \limsup_{\varepsilon\to 0} \frac{Q_\varepsilon(\theta)}{\log\varepsilon},$$

and

$$\underline{q}(\theta) := \liminf_{\varepsilon\to 0} \frac{Q_\varepsilon(\theta)}{\log\varepsilon},$$

then from (4.55) we have either

$$\limsup_{\varepsilon\to 0} \frac{\log(1-\Sigma(\theta,0))}{\log\varepsilon} = \log\tilde{K} + \bar{q}(\theta)\left(\frac{\log\tilde{\delta}-\log\delta}{\log\delta}\right),$$

or

$$\liminf_{\varepsilon\to 0}\frac{\log(1-\Sigma(\theta,0))}{\log\varepsilon}=\log\tilde{K}+\underline{q}(\theta)\left(\frac{\log\tilde{\delta}-\log\delta}{\log\delta}\right).$$

This means that $\sigma_+(\theta,0)$ oscillates between the lim inf and lim sup. The same also true for $\sigma_-(\theta,0)$. Thus, this proved that $\sigma(\theta,0)$ does not converge when the $\lim_{N\to\infty}\frac{i_N(\theta)}{N}$ does not converge. ■

In fact, Jordan *et al.* [40] have discussed about the non-convergence of the limit of $i_N(\theta)/N$ and presented some examples for sequence of θ for which the limit does not converge.

Example 4.6.1 ([40]) *Consider the sequence starting with 0, followed by 2 ones, followed by 2^2 zeros, followed by 2^3 ones, and so on, i.e.*

$$\{\theta_n\}=0,1,1,0,0,0,0,1,1,1,1,1,1,1,1,\ldots.$$

For this example, the limis set of $i_N(\theta)/N$ is $[1/3,2/3]$.

5 Stability index $\sigma(v)$ for Keller's map

In this chapter, we study a skew product map proposed by Keller [44]. We first investigate behaviour of the invariant graph as we vary parameter r in the system. For this map, Keller has computed a stability index (though not in our sense) for map F. However, in our study we compute the stability index for the inverse map F^{-1} where the attractor in F become a repellor and is a boundary between the basins of attraction. Thus, the existence of more than one basin shows that we again have a riddled basin. This enables us to compute the stability index for this system which has riddled basin of attraction.

5.1 The model

Keller [44] considers a skew product system where the base map $\hat{S} : \Theta \to \Theta$ is hyperbolic, with fibre maps of the form $x \mapsto \hat{g}(\theta)h(x)$ where $\hat{g} : \Theta \to (0, \infty)$ is a measurable map and $h : I \to \mathbb{R}_+$ is a strictly increasing, concave function with $h(0) = 0$ and $h'(0) = 1$. He considers the baker transformation as the base map for this system. Let $\Theta = [0, 1)^2$ and $\hat{S} : \Theta \to \Theta$ be the base map which is defined by

$$\hat{S}(\theta) = \hat{S}(u, v) = \begin{cases} \left(\frac{u}{s}, sv\right) & \text{if } u < s, \\ \left(\frac{u-s}{1-s}, s + (1-s)v\right) & \text{if } u \geq s, \end{cases} \tag{5.1}$$

where $s \in (0, 1)$. Meanwhile the fibre maps $F_\theta : I \to I$ are defined by

$$F_\theta(x) = \hat{g}(\theta)h(x), \tag{5.2}$$

where $\hat{g}(\theta) = \hat{g}(u, v) = g(\Pi(u, v)) = g(v)$ for some $g : \mathbb{T} \to (0, \infty)$. The skew product system is the transformation

$$F : \Theta \times I \to \Theta \times I,$$

defined by

$$F(\theta, x) = (\hat{S}(\theta), F_\theta(x)). \tag{5.3}$$

We can generate a dynamical system from (5.3) by iterating the map F. Thus, after n-iterations we will have that

$$F^n(\theta, x) = (\hat{S}^n(\theta), F^n_\theta(x))$$

for $(\theta, x) \in \Theta \times I$ and $n \in \mathbb{N}_0$ and where F_θ is a *cocycle* over the map $\hat{S}$ and we can compute that

$$\begin{aligned} F^n_\theta(x) &= F_{\hat{S}^{n-1}\theta} \circ \cdots \circ F_\theta(x), \\ F^0_\theta(x) &= x, \end{aligned}$$

for all $n \in \{1, 2, 3, \ldots\}$, $\theta \in \Theta$ and $x \in I$.

Furthermore, for the skew product system in (5.3), Keller assumes that there exists a Markov map $S : \mathbb{T} \to \mathbb{T}$ which is a factor map of $\hat{S}^{-1}$ defined by

$$S(v) = \begin{cases} \frac{v}{s} & \text{for } v < s, \\ \frac{v-s}{1-s} & \text{for } v \geq s, \end{cases} \tag{5.4}$$

with $\mathbb{T} = [0, 1]$. Note that this map is called the skewed doubling map in Subsection 2.6.3.

5.1.1 Invariant graphs

Recall that we have introduced the invariant graphs in Section 1.1. In this chapter, we differentiate two notations of invariant graphs, namely $\hat{\varphi}_\infty(\theta)$ and $\varphi_\infty(v)$.

For the skew product system in (5.3), the global attractor is given as:

$$K = \{(\theta, x) \in \Theta \times I : 0 \leq x \leq \hat{\varphi}_\infty(\theta)\}, \tag{5.5}$$

where $\hat{\varphi}_\infty : \Theta \to I$ is the *maximal invariant graph* which satisfies the following invariance property

$$F(\theta, \hat{\varphi}_\infty(\theta)) = (\hat{S}(\theta), \hat{\varphi}_\infty(\hat{S}(\theta))), \tag{5.6}$$

or equivalently,

$$F_\theta(\hat{\varphi}_\infty(\theta)) = \hat{\varphi}_\infty(\hat{S}(\theta))$$

for all $\theta \in \Theta$. We show action of the skew product F (5.6) schematically in Figure 5.1.

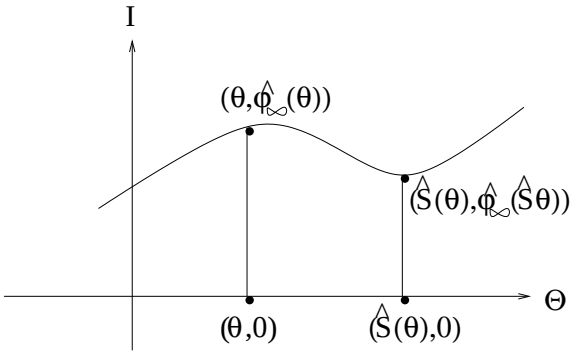

Figure 5.1 The schematic diagram showing the action of skew product F on the two invariant graphs, given by $\hat{\varphi}_\infty$ and 0.

The function $\hat{\varphi}_\infty(\theta)$ is defined as in Keller and Otani [46, Lemma 1] and the proof showing that this function is invariant is given in Keller [42, p.144-145].

Lemma 5.1 *The maximal F-invariant function $\hat{\varphi}_\infty : \Theta \to I$ is defined by*

$$\hat{\varphi}_\infty(\theta) = \lim_{n\to\infty} \hat{\varphi}_n(\theta) = \inf_n \hat{\varphi}_n(\theta),$$

where $\hat{\varphi}_n(\theta) = F^n_{\hat{S}^{-n}\theta}(a)$.

Proof. Define for $n \in \mathbb{N}$,

$$\hat{\varphi}_n : \Theta \to I,$$

$$\hat{\varphi}_n(\theta) = F^n_{\hat{S}^{-n}\theta}(a)$$

where $a = \sup_{(\theta,x)} F_\theta(x)$. Then

$$\hat{\varphi}_{n+1}(\theta) = F^n_{\hat{S}^{-n}\theta}(F_{\hat{S}^{-(n+1)}\theta}(a)).$$

Therefore we can conclude that

$$\hat{\varphi}_{n+1}(\theta) \le F^n_{\hat{S}^{-n}\theta}(a) = \hat{\varphi}_n(\theta).$$

Since the above sequence is decreasing and bounded below by 0, then by the Monotone Convergence Theorem, the limit of a decreasing sequence is its infimum. Hence

$$\hat{\varphi}_\infty(\theta) = \lim_{n\to\infty} \hat{\varphi}_n(\theta) = \inf_n \hat{\varphi}_n(\theta)$$

is well-defined. ■

Moreover, the function $\hat{\varphi}_\infty$ is always invariant. We can define the following:

(a) the *baseline* of the skew product system

$$\Phi_0 = \{(\theta, 0) : \theta \in \Theta\} \tag{5.7}$$

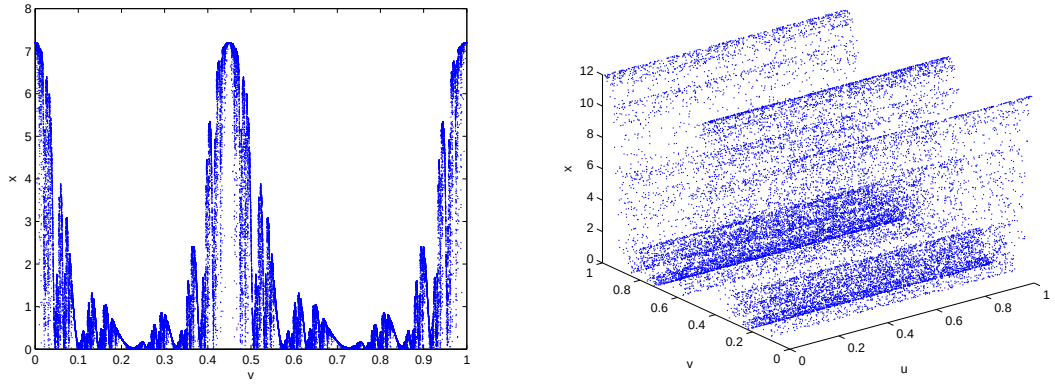

(a) (b)

Figure 5.2 (a) The two-dimensional attractor which is the invariant graph $\varphi_\infty(v)$ for the Keller's map (5.3) for $r = 2.5$. (b) The three-dimensional invariant graph for the baker map on (u, v, x)-axis.

(b) and the nontrivial invariant graph

$$\Phi_+ = \{(\theta, \varphi_\infty) : \theta \in \Theta\}. \tag{5.8}$$

Both Φ_0 and Φ_+ have been proved to be invariant in [46].

We note from [44] that since $\hat{g}$ depends only on $\Pi(\theta)$, then the graph $\hat{\varphi}_\infty(\theta)$ also depends on $\Pi(\theta)$ such that $\hat{\varphi}_\infty(\theta) = \varphi_\infty(\Pi(\theta)) = \varphi_\infty(v)$ for a measurable function $\varphi_\infty : \mathbb{T} \to I$.

From (5.3), the mapping of the Keller's map is as follows:

$$F \begin{pmatrix} u \\ v \\ x \end{pmatrix} \to \begin{pmatrix} \hat{S} \begin{pmatrix} u \\ v \end{pmatrix} \\ g(v)h(x) \end{pmatrix}, \tag{5.9}$$

with $\hat{S} = \hat{S}_1(u, v) = (\frac{u}{s}, sv)$ if $0 \le u < s$, $\hat{S} = \hat{S}_2(u, v) = (\frac{u-s}{1-s}, s+(1-s)v)$ if $s \le u < 1$, $g(v) = r \cdot (1 + \epsilon + \cos(2\pi v))$, $h(x) = \arctan(x)$, where $s = 0.45, \epsilon = 0.01, r = 2.5$. In order to plot the invariant graph $\varphi_\infty(v)$, we choose a random point (u_0, v_0, x_0) and iterate it for several thousands times to remove any transient point. Then we plot several hundred thousands iterations for two-dimensional (v_n, x_n) and three-dimensional (u_n, v_n, x_n). The figures for the invariant graph are shown in Figure 5.2.

5.1.2 Critical values of parameter r for invariant graph

In this section, we show the invariant graph for different values of parameter r as depicted in Figure 5.3. We can clearly see from this figure that there is transition of the invariant graph from $\varphi_\infty(v) = 0$ to $\varphi_\infty(v) > 0$. There are 3 critical parameters for this invariant graph. In this section we explain about these critical parameters.

We denote the set of S-invariant Borel probability measures and its subset of ergodic measures by $\mathcal{P}(S)$ and $\mathcal{E}(S)$ respectively. S is the Markov map as in (5.4) and here we consider

$$G(\mu) = \int \log g \; d\mu \;\; \text{such that } \mu \in \mathcal{P}(S). \tag{5.10}$$

Notice that $\{G(\mu) : \mu \in \mathcal{P}(S)\} \subseteq \mathbb{R}$. Therefore, we can define for measures μ_+, μ_{ac} and μ_- respectively as:

$$G(\mu_+) = \sup\{G(\mu) : \mu \in \mathcal{P}(S)\} = \sup_{\mu\in\mathcal{P}(S)} G(\mu), \tag{5.11}$$

$$G(\mu_{ac}) = G(\ell) \text{ where } \ell \text{ is the Lebesgue measure,} \tag{5.12}$$

$$G(\mu_-) = \inf\{G(\mu) : \mu \in \mathcal{P}(S)\} = \inf_{\mu\in\mathcal{P}(S)} G(\mu). \tag{5.13}$$

Note that the $G(\mu_{ac})$ in (5.12) needs to be defined since it is a well-known fact that S has a unique invariant probability measure μ_{ac} absolutely continuous w.r.t. ℓ on $\mathbb{T}$ [44].

Assuming that these three quantities are not equal, there exist 4 possible cases which are:

(i) $G(\mu_-) < G(\mu_{ac}) < G(\mu_+) < 0$.

(ii) $G(\mu_-) < G(\mu_{ac}) < 0 < G(\mu_+)$.

(iii) $G(\mu_-) < 0 < G(\mu_{ac}) < G(\mu_+)$.

(iv) $0 < G(\mu_-) < G(\mu_{ac}) < G(\mu_+)$.

In this study, we consider for all the cases above. Therefore, to find the critical values, we characterize them in terms of μ_+, μ_{ac} and μ_- and by referring the above cases, we obtain that there are value $r_{c_1}, r_{c_2}, r_{c_3}$ such that

(i) when $r = r_{c_1}$, $G(\mu_+) = 0$,

(ii) when $r = r_{c_2}$, $G(\mu_{ac}) = 0$,

(iii) when $r = r_{c_3}$, $G(\mu_-) = 0$.

From numerical approximation as we will show in Chapter 6, we obtained the critical values as follow:

(i) $r_{c_1} \leq 0.49751$,

(ii) $r_{c_2} = 1.7364$,

(iii) $r_{c_3} \geq 3.5441$.

Note that our numerical computations suggest that we have equalities in both (i) and (iii) above. We need these values in this chapter in order to compute the stability index for the inverse of this skew product map, that is to detect the range of parameters r for which that riddled basin exists.

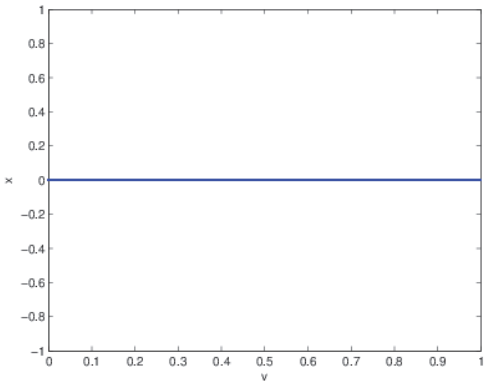

(a) $r = 0.2$

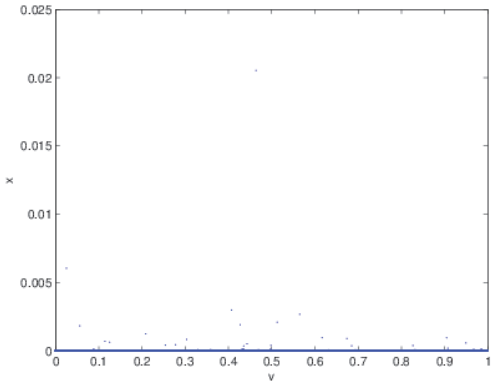

(b) $r = 1.7$

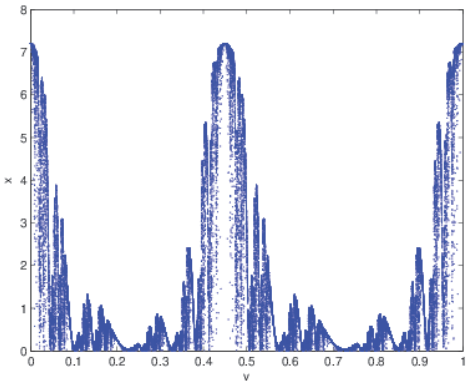

(c) $r = 2.5$

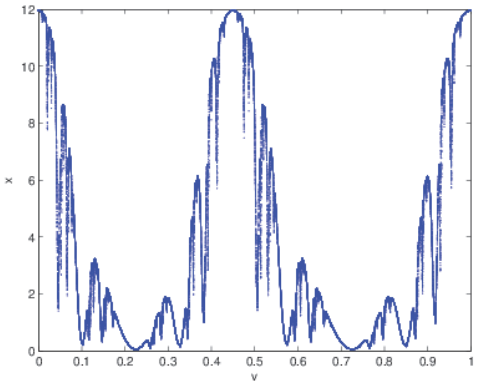

(d) $r = 4$

Figure 5.3 The invariant graphs on (v, x)-axis for various r. For (a), when $r < r_{c_1}$, the invariant graph is zero everywhere, i.e. $\varphi_\infty(v) = 0$ for all v. In (b), some points in the invariant set start to diverge away from $x = 0$. In (c), when $r_{c_1} \leq r \leq r_{c_2}$, $\varphi_\infty(v) > 0$ for almost all v and in (d), the invariant graph is strictly positive for all v.

5.2 Keller's stability index for F

Keller [44] picks a point $(v, 0)$ on the baseline $x = 0$ under the invariant graph and defines a local stability index $\sigma(v)$ in the following way:

$$\sigma(v) = \sigma_+(v) - \sigma_-(v),$$

where

$$\sigma_-(v) = \lim_{\varepsilon \to 0} \frac{\log \Sigma_\varepsilon(v)}{\log \varepsilon}, \quad \sigma_+(v) = \lim_{\varepsilon \to 0} \frac{\log(1 - \Sigma_\varepsilon(v))}{\log \varepsilon},$$

with

$$\Sigma_\varepsilon(v) = \frac{1}{\varepsilon |U_\varepsilon(v)|} \int_{U_\varepsilon(v)} \min\{\varphi_\infty(t), \varepsilon\} dt$$

and

$$1 - \Sigma_\varepsilon(v) = \frac{1}{\varepsilon |U_\varepsilon(v)|} \int_{U_\varepsilon(v)} (\varepsilon - \varphi_\infty(t))^+ dt,$$

where $U_\varepsilon(v) = (v - \varepsilon, v + \varepsilon)$ are neighbourhoods with size 2ε. **Note that this definition is not the stability index as we define in Chapter 3; in this case there is a single attractor**. Since Keller's map has only one attractor, everything that is in $[0, 1] \times \mathbb{R}^+$ in Figure 5.2(a) is in fact the basin of attraction for the attractor. He computes the stability index by taking a point on the baseline and estimates the area under the invariant graph to obtain the following proportion:

$$\Sigma_\varepsilon(v) = \frac{\ell((U_\varepsilon(v) \times [0, \varepsilon]) \cap N)}{\ell(U_\varepsilon(v) \times [0, \varepsilon])},$$

where $N = \{(t, x) : 0 \leq x \leq \varphi_\infty(t)\}$. Note that N is not simply the basin of an attractor. In our case, we will invert Keller's map and obtain two attractors where each of them has its own basin of attraction, namely one attractor is at $x = 0$ and the other is at $x = 1$. We show that N is the basin of the attractor in $x = 0$ for inverse map. We will compute the stability index by taking a point on the attractor at $x = 0$ and then within a neighbourhood of the point we find the proportion of points that are attracted to this attractor. Keller has chosen a point under the invariant graph (attractor), whereas in our case we choose a point on the attractor as defined in Definition 3.1.

Keller then formulated his main results of the stability index at point v as follows [44, Theorem 2.5].

Theorem 5.1 *Let $v \in \mathbb{T}^1$ and any $\mu \in \mathcal{E}(S)$, for μ-almost all v;*

$$\sigma(v) = \begin{cases} s_* \cdot \frac{\Gamma(v)+\Lambda(v)}{\Lambda(v)} > 0 & \text{if } \Gamma(v) + \Lambda(v) > 0, \\ \frac{\Gamma(v)+\Lambda(v)}{\Lambda(v)} < 0 & \text{if } \Gamma(v) + \Lambda(v) < 0, \end{cases} \tag{5.14}$$

where $s_* > 0$ is the Loynes' exponent obtained from a certain thermodynamic pressure function, $\Gamma(v)$ and $\Lambda(v)$ are local Lyapunov exponents for F (5.3), in particular for the fibre map and base map respectively.

If we compare the theorem above with our result in Corollary 4.8 in the previous chapter, it suggests that s_* is in fact the stability index for the attractor A_0 in our system in (4.1). Note that Keller defined the s_* using concepts from the thermodynamic formalism whereas the stability index for the attractor can be defined purely in geometric terms.

5.3 Inverse of Keller's map

Keller [44] computed the stability index for the invariant graph for the skew product system F. In this thesis, we use a different approach to compute the stability index, which is by considering the basins of attraction for system F. To obtain these basins we need to invert map F and by doing this, the invariant graph for F become a boundary of the basins in F^{-1}.

Let $F(u, v, x) \to (u', v', x')$, therefore $F^{-1}(u', v', x') \to (u, v, x)$, i.e.,

$$F^{-1}\begin{pmatrix} S\begin{pmatrix} u \\ v \end{pmatrix} \\ g(v)h(x) \end{pmatrix} \to \begin{pmatrix} u \\ v \\ x \end{pmatrix},$$

Hence for the following two cases;

(i) For $0 \leq v < s$;

$$F^{-1}\begin{pmatrix} \frac{u}{s} \\ sv \\ g(v)\arctan(x) \end{pmatrix} \to \begin{pmatrix} su' \\ \frac{v'}{s} \\ \tan(\frac{x'}{g(v)}) \end{pmatrix},$$

i.e.,

$$F^{-1}\begin{pmatrix} \frac{u}{s} \\ sv \\ g(v)\arctan(x) \end{pmatrix} \to \begin{pmatrix} su' \\ \frac{v'}{s} \\ \tan(\frac{x'}{g(\frac{v'}{s})}) \end{pmatrix}.$$

(ii) For $s \leq v < 1$;

$$F^{-1}\begin{pmatrix} \frac{u-s}{1-s} \\ s + (1-s)v \\ g(v)\arctan(x) \end{pmatrix} \to \begin{pmatrix} (1-s)u' + s \\ \frac{v'-s}{1-s} \\ \tan(\frac{x'}{g(v)}) \end{pmatrix},$$

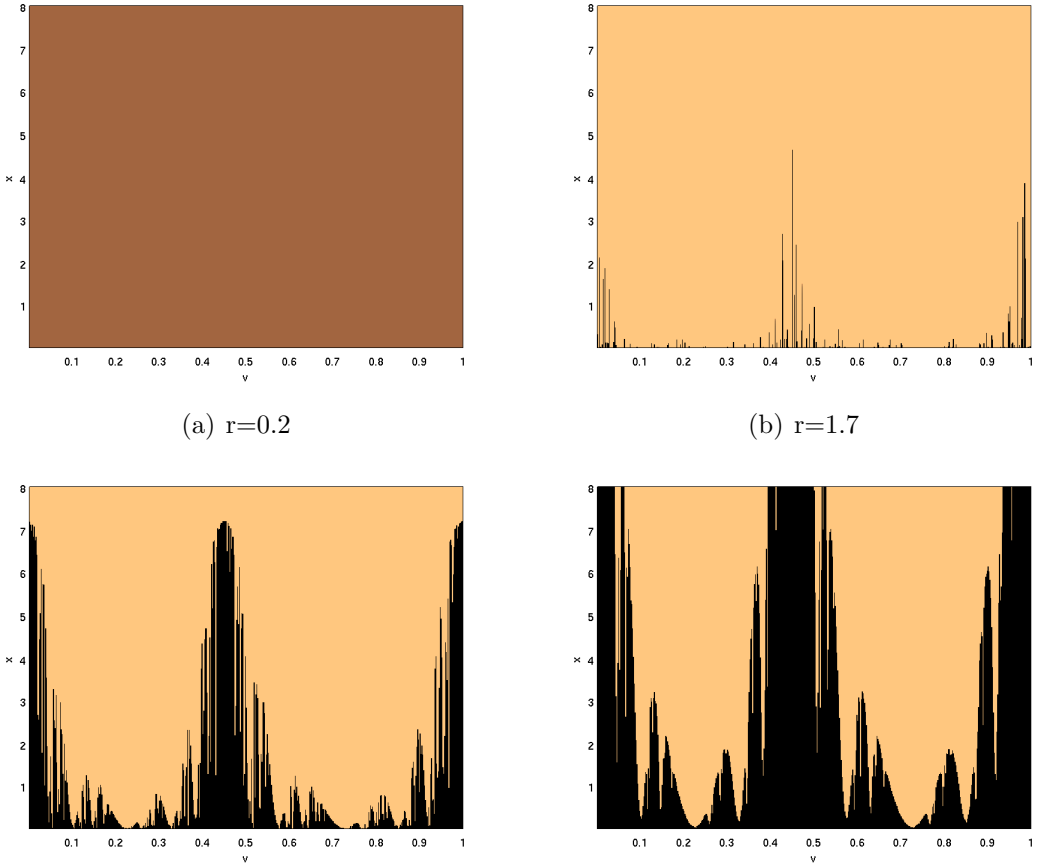

(a) r=0.2 (b) r=1.7

(c) r=2.5 (d) r=4.0

Figure 5.4 The basin of attraction for the inverse map $G(u, v, x)$ (5.15) for various r on (v, x)-plane. The black area represents the basin where the points go to $x = 0$ (denoted as $\mathcal{B}(v, 0)$) and the orange area represents the basin for the points go to $x = \infty$ (denoted as $(\mathcal{B}(v, 0))^c$). Note that the black area is in fact the area under the invariant graph while the orange area is the area above the invariant graph.

i.e.,

$$F^{-1}\begin{pmatrix} \frac{u-s}{1-s} \\ s+(1-s)v \\ g(v)\arctan(x) \end{pmatrix} \to \begin{pmatrix} (1-s)u'+s \\ \frac{v'-s}{1-s} \\ \tan(\frac{x'}{g(\frac{v'-s}{1-s})}) \end{pmatrix}.$$

In summary, let $G = F^{-1}$ and by ignoring the $(')$ sign above, the inverse map is as follows:

$$G(u,v,x) = \begin{cases} \left(su, s^{-1}v, \tan\left(\frac{x}{g(\frac{v}{s})}\right)\right) & \text{if } 0 \le v < s, \\ \left((1-s)u+s, (1-s)^{-1}(v-s), \tan\left(\frac{x}{g(\frac{v-s}{1-s})}\right)\right) & \text{if } s \le v < 1. \end{cases} \tag{5.15}$$

Using this inverse map, we obtain the basins of attraction for the map F. These basins are depicted as in Figure 5.4 where the black area denotes the basin of attraction for the points go to $x = 0$ and the orange area shows the basin of attraction for the points move away to $x = \infty$.

5.4 Numerical computation of stability index for F^{-1}: results and discussion

Here we discuss difference appearance of Figure 5.2(a) and Figure 5.4. Figure 5.2(a) shows that the blue points represent the invariant graph $\varphi_\infty(v)$ which is also the attractor. As we said earlier, to plot the map F, we pick a random point (u_0, v_0, x_0) and iterate it for a while to remove transient points. Then we iterate more to obtain (u_n, v_n, x_n), i.e., let

$$F : [0,1)^2 \times \mathbb{R}^+ \to [0,1)^2 \times \mathbb{R}^+,$$

$\varphi_\infty(v)$ is the attractor and suppose that

$$(u_n, v_n, x_n) = F^n(u_0, v_0, x_0).$$

Then $|\varphi_\infty(v_n) - x_n| \to 0$ as $n \to \infty$ for almost all (u_0, v_0) and all $x_0 > 0$. The invariant graph has been plotted in Figure 5.2(a) for points (v_k, x_k).

On the other hand, by finding the inverse for Keller's map, we obtained the basin of attraction as in Figure 5.4 where the attracting invariant graph for F has become the repellor for F^{-1} and plays a role as the boundary of the basins of attraction. As we iterate backward, the point will either goes to 0 or ∞. If the point started below the invariant graph, then it will go to 0, otherwise if the point started above the invariant graph, it will end up goes to ∞, i.e., let

$$G : [0,1)^2 \times \mathbb{R}^+ \to [0,1)^2 \times \mathbb{R}^+,$$

and let $G = F^{-1}$ be the inverse map. Suppose that

$$(\tilde{u}_n, \tilde{v}_n, \tilde{x}_n) = G^n(\tilde{u}_0, \tilde{v}_0, \tilde{x}_0).$$

Therefore,

(i) if $0 < \tilde{x}_0 < \varphi_\infty(\tilde{v})$, then $\tilde{x}_n \to 0$ as $n \to -\infty$, or

(ii) if $\tilde{x}_0 > \varphi_\infty(\tilde{v})$, then $\tilde{x}_n \to \infty$ as $n \to -\infty$,

for almost all $(\tilde{u}_0, \tilde{v}_0)$ and all $x_0 \neq \varphi_\infty(\tilde{v})$. Note that for both maps F and G, if $x_0 = 0$ then $x_n = 0$ as $x = 0$ is the invariant set for both fibre maps in (5.2) and (5.15). We show schematically comparison between Keller's map F and the inverse map G in Figure 5.5.

Recall that for Keller's map, the stability index was estimated by taking an individual point v on the baseline $x = 0$ and compute the fraction of $\Sigma_\varepsilon(v, 0)$ by considering

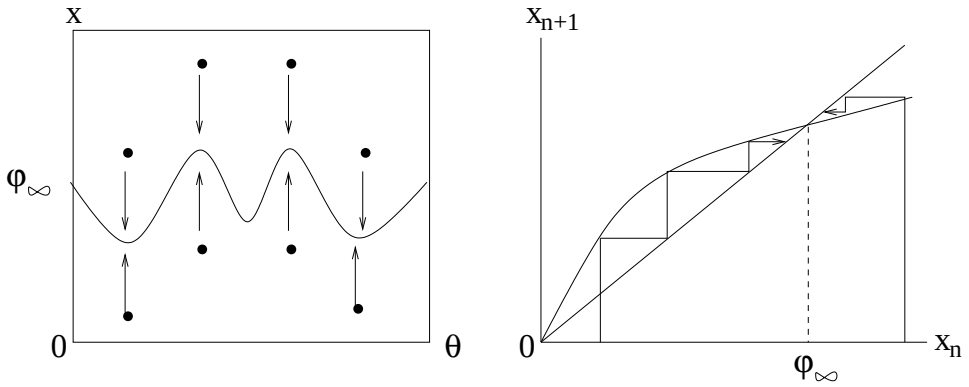

(a) Map F

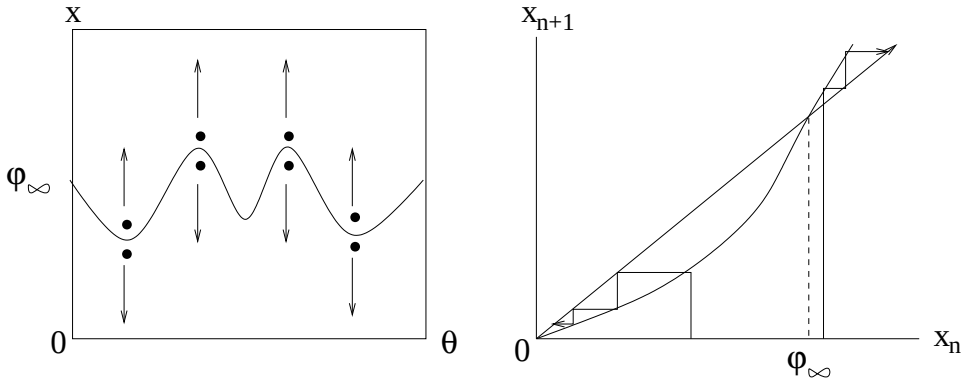

(b) Map G

Figure 5.5 The mechanisms in map F (5.9) and map G (5.15). In (a), all points $x > 0$ in $[0, 1] \times [0, 8]$ attracted to φ_∞ and from the sketch of x_{n+1} versus x_n, points x_0 that start both from left or right of φ_∞ will go to one number only, i.e. to φ_∞. In (b), points x that start from below φ_∞ will attracted to the baseline $x = 0$ while points start from above φ_∞ will go to $x = \infty$. This can be seen clearly in the sketch of x_{n+1} versus x_n where for two points start from left or right of φ_∞, one will go to 0 and the other will diverge away to ∞.

the area under the invariant graph $\varphi_\infty(v)$ [45]. We have stated the stability index for Keller's map in Section 5.2.

In our case, we use Definition 3.1 to compute the stability index $\sigma((v,0),\mathcal{B}(v,0))$ for the point $(v,0)$ in the basin of attraction of the attractor at $x=0$ where the basin for the inverse map F^{-1} is obtained as in Figure 5.4.

We denote $B_\varepsilon(v,0)$ the ε-neighbourhood of point $(v,0)$ and $\mathcal{B}(v,0)$ the basin of attraction for $(v,0)$. We take a point $(v,0)$ in the basin $\mathcal{B}(v,0)$ and define that

$$\Sigma_\varepsilon(v,0) = \tfrac{\ell(B_\varepsilon(v,0)\cap\mathcal{B}(v,0))}{\ell(B_\varepsilon(v,0))},$$

i.e.,

$$1-\Sigma_\varepsilon(v,0) = \tfrac{\ell(B_\varepsilon(v,0)\cap(\mathcal{B}(v,0))^c)}{\ell(B_\varepsilon(v,0))}.$$

Then the stability index for the point $(v,0)$ is

$$\sigma((v,0),\mathcal{B}(v,0)) = \sigma_+((v,0),\mathcal{B}(v,0)) - \sigma_-((v,0),\mathcal{B}(v,0)), \tag{5.16}$$

which exists when the following converge:

$$\sigma_-((v,0),\mathcal{B}(v,0)) = \lim_{\varepsilon\to 0}\frac{\log(\Sigma_\varepsilon(v,0))}{\log\varepsilon},\quad \sigma_+((v,0),\mathcal{B}(v,0)) = \lim_{\varepsilon\to 0}\frac{\log(1-\Sigma_\varepsilon(v,0))}{\log\varepsilon}.$$

To compute the fraction of $\Sigma_\varepsilon(v,0)$, we first transform the basin of attraction in Figure 5.4 to the basin using the random number generator (RNG) in Matlab. Thus, we show the random basin in Figure 5.6. In fact, the measure ℓ is computed by counting the random points generated in $B_\varepsilon(v,0)$. Now the proportion $\Sigma_\varepsilon(v,0)$ can be calculated as follows:

$$\Sigma_\varepsilon(v,0) = \frac{\#\text{ of blue points in the } B_\varepsilon(v,0)}{\#\text{ of blue and yellow points in the } B_\varepsilon(v,0)}. \tag{5.17}$$

First, we compute the proportion of (5.17) for the blue points over the whole points (blue points and yellow points) as we increase the parameter r in the fibre map of F. From Figure 5.7, we can see that the proportion increases as we increase the parameter r. This is due to the increasing number of blue points when r is increased from 0 to larger values. Figure 5.7 is produced for fixed size of ε-neighbourhood for $r=0,\ldots,4$.

Secondly, from Figure 5.6, we pick a particular random point $(v,0)$ in the basin and take a neighbourhood around this point to plot how the proportion varies when we decrease the size of the ε-neighbourhood. The result is shown as in Figure 5.8. From this figure, it shows that as $\varepsilon\to 0$, $\Sigma_\varepsilon(v,0)\to 1$. For $r=0.2$, the proportion is zero

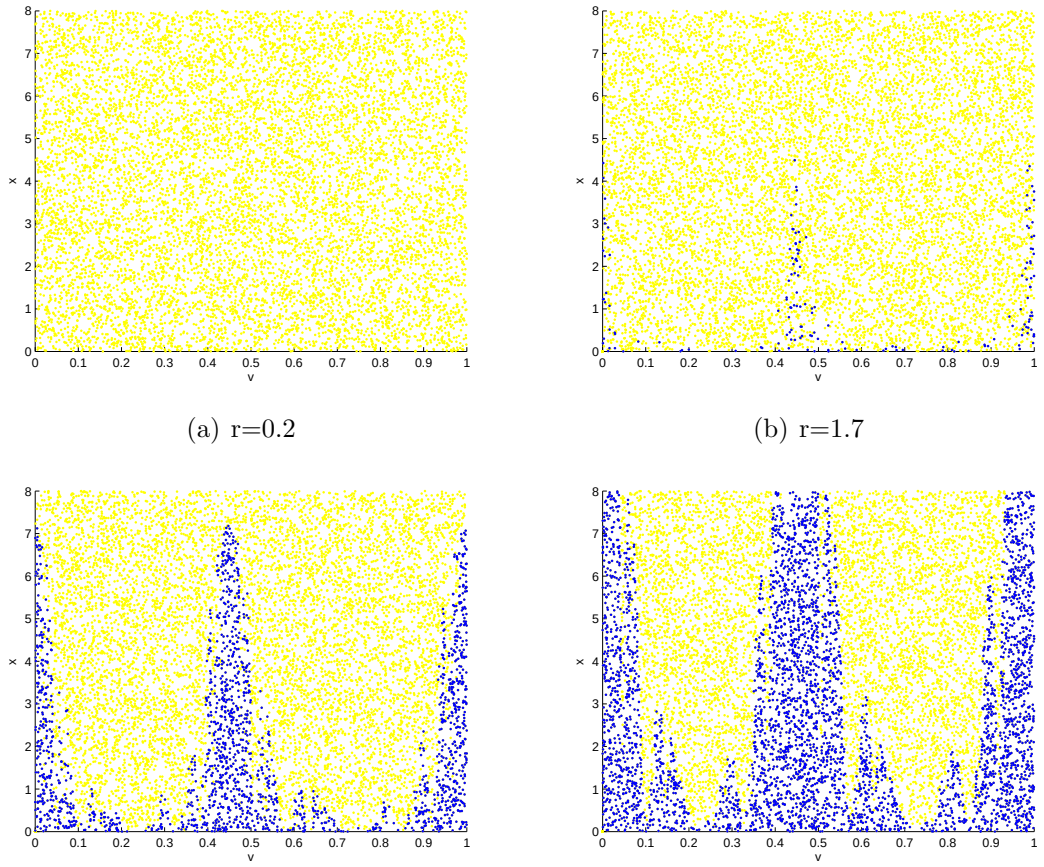

(a) r=0.2

(b) r=1.7

(c) r=2.5

(d) r=4.0

Figure 5.6 The basin of attraction generated using random number generator for $G(u, v, x)$ (5.15) for various r. The blue points represent the basin $\mathcal{B}(v, 0)$ and the yellow points represent $(\mathcal{B}(v, 0))^c$. We can see that the number of blue dots increasing as we increase r since the proportion of the black region of the basin of attraction in Figure 5.4 increases as we increase r as well.

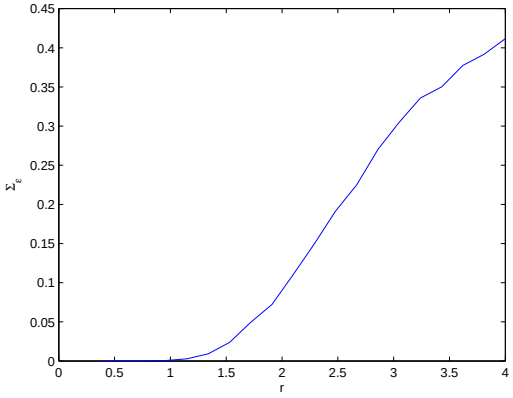

Figure 5.7 The proportion of the blue dots over the whole image from Figure 5.6 for the inverse map $G(u, v, x)$ (5.15). This proportion starts from 0 then increases monotonically as r increases where $\Sigma_\varepsilon(v, 0) = 0$ means that all the points are in $(\mathcal{B}(v, 0))^c$, i.e. the yellow dots.

everywhere since there are no points that go to $x = 0$ (i.e. no blue points). Besides, we can also see that as r increases, $\Sigma_\varepsilon(v, 0) \to 1$ much faster than the lower r.

Then according to the stability index formula in (5.16), we can compute $\sigma_-((v, 0), \mathcal{B}(v, 0))$ from the slope of the graph of $\log(\Sigma_\varepsilon(v))$ against $\log(\varepsilon)$ and for $\sigma_+((v, 0), \mathcal{B}(v, 0))$, we find the slope of $\log(1 - \Sigma_\varepsilon(v))$ against $\log(\varepsilon)$. The result is depicted as in Figure 5.9 for example for $r = 2.5$. From this figure, since $\sigma_-((v, 0), \mathcal{B}(v, 0)) = 0$ and $\sigma_+((v, 0), \mathcal{B}(v, 0)) = \infty$, the stability index for $r = 2.5$ is ∞.

We also compute the stability index for various r in Figure 5.10. Our numerical computation shows that the index increases monotonically from $-\infty$ to ∞. For lower r, $\sigma((v, 0), \mathcal{B}(v, 0)) = -\infty$ indicates that $\ell(\mathcal{B}(v, 0)) = 0$ since all points in the ε-neighbourhood of $(v, 0)$ are attracted to $(\mathcal{B}(v, 0))^c$. This corresponds to the case where $\varphi_\infty(v) = 0$ for all v. Then for larger r, we can see that the index varies from 0 to positive values, where this means that the basin $\mathcal{B}(v, 0)$ is riddled with $(\mathcal{B}(v, 0))^c$. There are points nearby within the neighbourhood of $(v, 0)$ that are in $(\mathcal{B}(v, 0))^c$. Further increasing r, we have $\sigma((v, 0), \mathcal{B}(v, 0)) = \infty$ which shows that the basin $\mathcal{B}(v, 0)$ has full measure such that all points in the ε-neighbourhood are attracted to $x = 0$. This corresponds that $\varphi_\infty(v)$ is strictly positive for all v.

We compare our result on stability index on the riddled basin with Keller's result [44] for the same map where we agree that the index is positive for ℓ-almost all v.

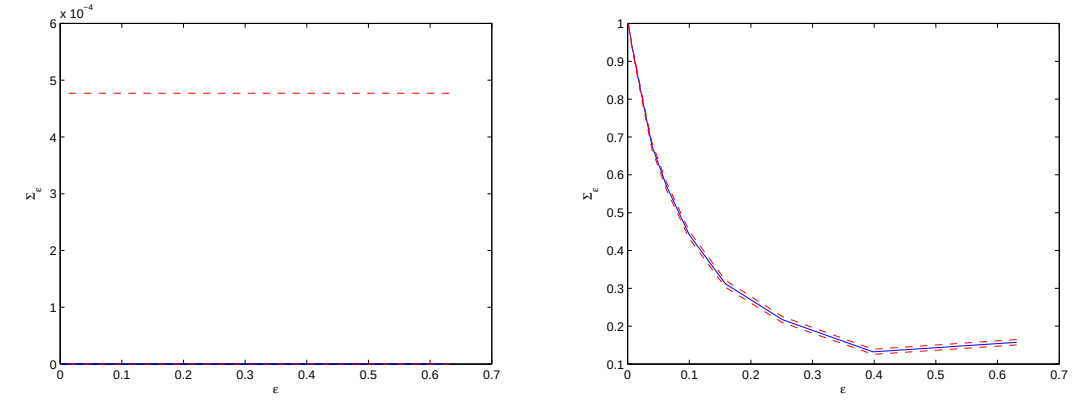

(a) r=0.2 (b) r=1.7

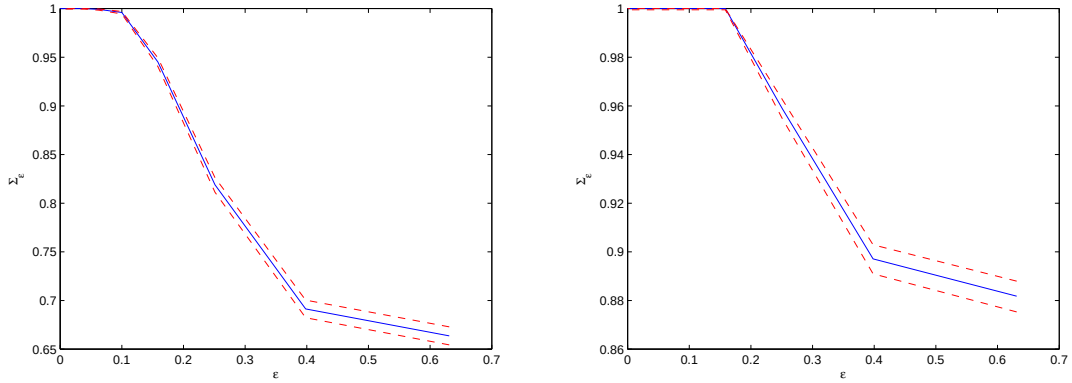

(c) r=2.5 (d) r=4.0

Figure 5.8 The proportion of the blue points over the ε for $G(u, v, x)$ (5.15). When $r < r_{c_1}$, the proportion is zero everywhere since all points are in $(\mathcal{B}(v, 0))^c$, i.e. no blue points. When $r \geq r_{c_1}$, $\Sigma_\varepsilon(v, 0) \to 1$ as $\varepsilon \to 0$ where for higher value of r, $\Sigma_\varepsilon(v, 0)$ converges to 1 faster than the lower r. This is due to the increasing number of blue points as we decrease the size of ε-neighbourhood.

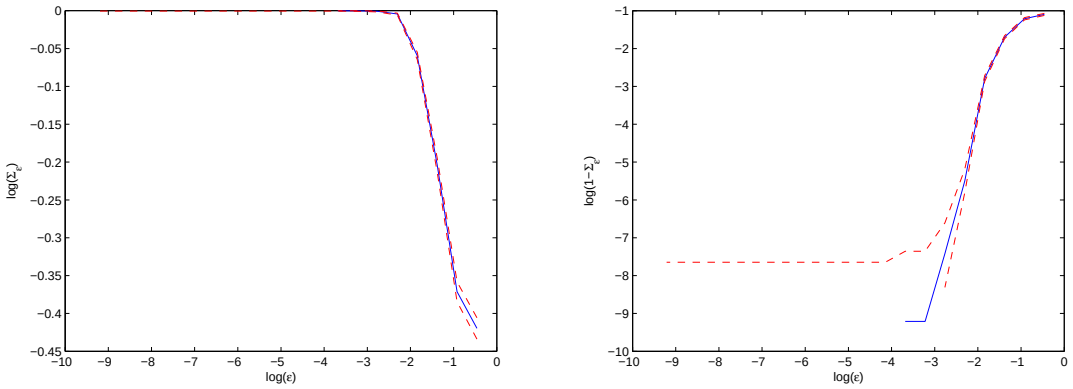

(a) (b)

Figure 5.9 Computation of the stability index for $G(u, v, x)$ (5.15) for $r = 2.5$. (a) $\sigma_-((v, 0), \mathcal{B}(v, 0))$: $\log(\Sigma_\varepsilon(v, 0))$ versus $\log(\varepsilon)$ where the slope is 0. (b) $\sigma_+((v, 0), \mathcal{B}(v, 0))$: $\log(1 - \Sigma_\varepsilon(v))$ versus $\log(\varepsilon)$ where the slope is ∞.

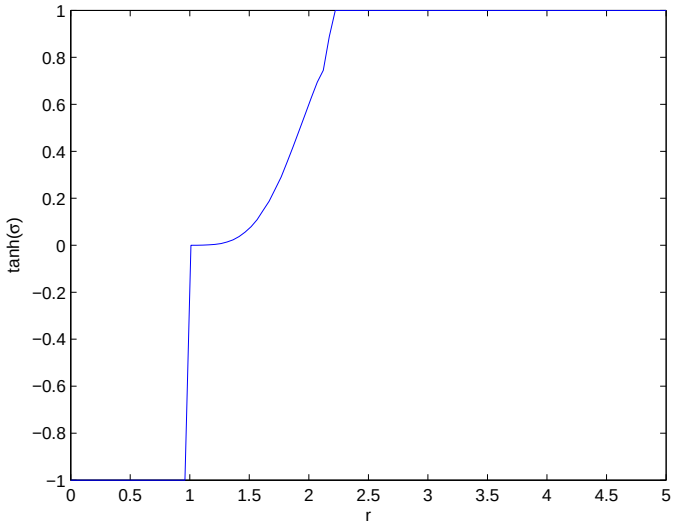

Figure 5.10 The stability index $\sigma((v,0),\mathcal{B}(v,0))$ for the inverse map $G(u,v,x)$ (5.15) over parameter $r=0,\ldots,5$ for the typical point $v=0.7927$. Here -1 and 1 represent that the indices are $-\infty$ and ∞ respectively. When $0<r<r_{c_2}$, $\sigma((v,0),\mathcal{B}(v,0))=-\infty$ since the proportion of points that are in $\mathcal{B}(v,0)$ is zero for all v. When $r_{c_2}<r<r_{c_3}$, the index starts from 0 and increases monotonically to positive value where in this range the riddled basin occurs. As r increases in this range, there are less and less nearby points within the neighbourhood of $(v,0)$ that belong to $(\mathcal{B}(v,0))^c$. Then as $r>r_{c_3}$, $\sigma((v,0),\mathcal{B}(v,0))=\infty$ since all points in the ε-neighbourhood of $(v,0)$ attracted to the attractor in $\mathcal{B}(v,0)$.

6 Birkhoff averages for periodic orbits and the zero set of the invariant graph

This chapter is a continuation from the previous chapter. We will look in much more depth into the system, not just the typical points as in previous chapter, but also at all possible values of v by looking at the dimension of a set. First, we will compute averages of periodic points for the skewed doubling map used in Keller's paper [44] where its periodic points are computed using the method of symbolic dynamics. These averages are computed using Birkhoff averages. Next, we will also be looking at the size of zero and nonzero sets of the invariant graph in terms of the Hausdorff dimension. To do this, we define these sets and discuss some of their basic properties. We make a conjecture to improve Theorem 2 from Keller and Otani [46] for a complete range of parameter r.

6.1 Birkhoff averages for periodic points

In this section, we study the behaviour of the orbits of periodic points in the Markov map S in (5.4). Such orbits are characterized by their symbolic sequences which are generated by the Markov partition. Our aim is to compute the maximum and minimum averages for the periodic points obtained where we associate this to the maximum and minimum measures for system F in (5.3).

6.1.1 Computations of periodic points using symbolic dynamics

To study the behaviour of the orbits of the periodic points, we use the method of symbolic dynamics which we mainly refer to Glendinning's book [29]. This method uses some symbols to represent the sequence of orbits in the interval map. Therefore to set up the symbolic dynamics for this map, we must first define what is meant by

a *partition*. Strictly speaking, a partition is a division of the interval into pairwise disjoint subintervals.

For the map S, we divide its interval $\mathbb{T} = [0, 1]$ into two subintervals. Hence, we can write $\mathbb{T} = [0, s) \cup (s, 1] = I_0 \cup I_1$ and for the coding we use the binary symbols '0' for I_0 which is for the left interval and '1' for I_1 which is for the right interval of the map such that

$$n_k(v) = \begin{cases} 0 & \text{if } S^k(v) \in I_0, \\ 1 & \text{if } S^k(v) \in I_1, \end{cases} \tag{6.1}$$

for $k = 0, \ldots, N-1$. Furthermore, the orbit of the point v can be found using the transformation S. In fact, the role of S is to shift the sequence of binary digits one place to the left. In particular, if a point v has a binary sequence 001, then the effect of S is 001, 010, 100. Also if v has a binary sequence 011, then the effect of S is 011, 110, 101. We can clearly seen that each number in the sequence moves one step to the left after each iteration.

Moreover, in the case of periodic orbit, for each period n, S has 2^n periodic points since there are 2^n different sequences of 0s and 1s of period n. For instance, period 3 has $2^3 = 8$ possible finite binary sequences which are 000, 001, 010, 011, 100, 101, 110, 111. Given a point $v_0 \in \mathbb{T}$, we can consider the orbit of this point as

$$\{v_0, S(v_0), S^2(v_0), \ldots\},$$

which is obtained by iterating the map S. In this map, we can find more than one periodic point. For this map, v_0 is periodic if

$$S^n(v_0) = v_0.$$

The points obtained are denoted as $\{v_0, v_1, v_2, \ldots, v_{n-1}\}$. This means that after nth iteration, the last point is in fact the starting point v_0. We find the periodic points for the Markov map according to the chosen number of periodic orbit and further we also show how to measure the integral over the delta functions for all of the periodic points.

For example, Keller has chosen a period-3 orbit $\overline{001}$ for the Markov map S and the points obtained are at $v_0 = 0.10255$, $v_1 = 0.22788$ and $v_2 = 0.50640$ with $s = 0.45$. Here we would like to verify the computation for these periodic points. Since our $v_0 = 0.10255 < s$, therefore the first condition in (5.4) is used;

$$\begin{aligned} S(0.10255) &= \frac{0.10255}{0.45} \\ &= 0.22788. \end{aligned}$$

We denote this last number as $v_1 = 0.22788$ and since this v_1 is smaller than s as well, hence

$$\begin{aligned} S(0.22788) &= \frac{0.22788}{0.45} \\ &= 0.50640. \end{aligned}$$

Now we denote $v_2 = 0.50640 > s$, so we use the second condition in (5.4) and get:

$$\begin{aligned} S(0.50640) &= \frac{0.50640 - 0.45}{1 - 0.45} \\ &= 0.10255. \end{aligned}$$

Notice that the last number is same as v_0 after three iterations and therefore this proved that those three points satisfy the period-3-orbit. In fact, we can simplify the computations above as:

$$\begin{aligned} S(v_0) &= v_1 \\ S(v_1) &= v_2 \\ S(v_2) &= v_0. \end{aligned}$$

We show this period-3 orbit on the Markov map in Figure 6.1.

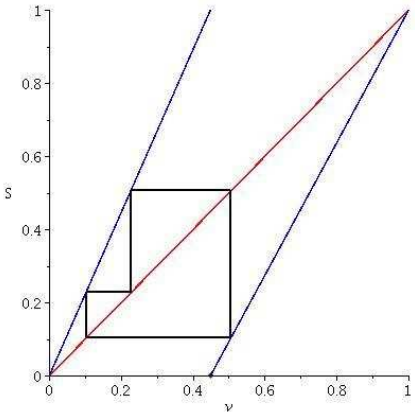

Figure 6.1 The iterations for period-3-orbit $\overline{001}$ on the Markov map (5.4).

6.1.2 Examples of more periodic orbits

We also show the results for more periodic points that can be obtained from the Markov map (5.4) in Figure 6.2. Keller has used $\overline{001}$ and the sequence is 001001001 . . . .

In addition, the sequences in the caption of Figure 6.2 have the following meanings:

$$\overline{01} = 0101010101\ldots$$
$$\overline{011} = 011011011\ldots$$
$$\overline{0001} = 000100010001\ldots$$
$$\overline{001100} = 001100001100001100\ldots.$$

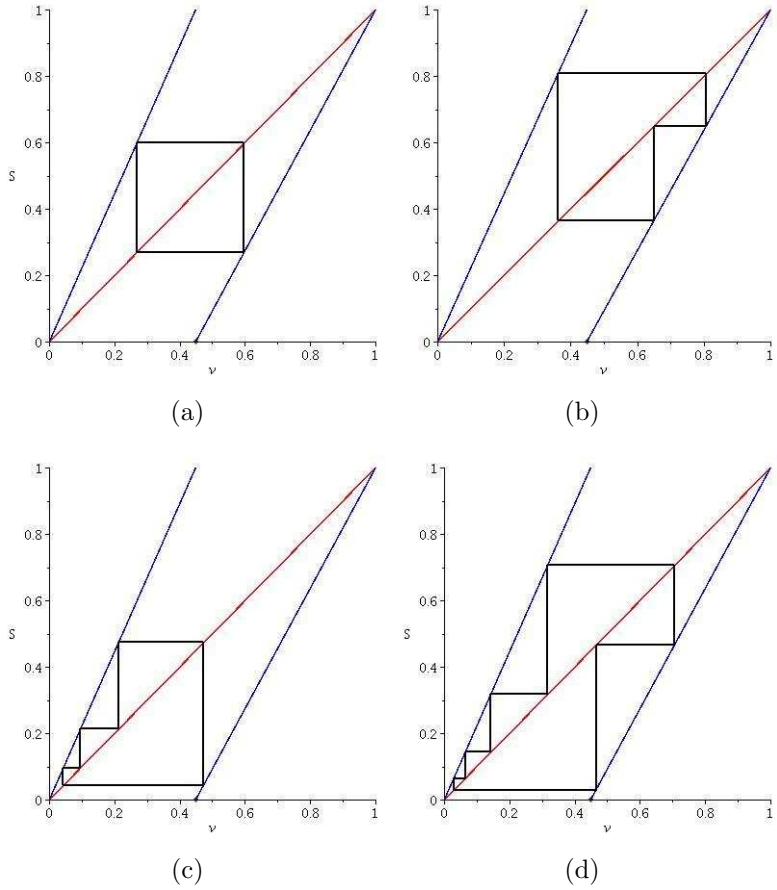

Figure 6.2 The iterations for Markov map (5.4) for various number of periodic orbits. (a) The period-2 orbit for $\overline{01}$. (b)The period-3 orbit for $\overline{011}$. (c) The period-4 orbit for $\overline{0001}$. (d)The period-6 orbit for $\overline{001100}$.

6.1.3 Results: maximum and minimum averages

In this section, we compute the averages of $G(\mu_+)$, $G(\mu_{ac})$ and $G(\mu_-)$ as defined in (5.11), (5.12) and (5.13) respectively. Therefore, to compute the averages for periodic points, we use the Birkhoff averages from the left hand side of (2.13), in particular

$$\frac{1}{n}\sum_{i=0}^{n-1}\log g(v_i) = \frac{1}{n}\sum_{i=0}^{n-1}\log(r\times(1+\epsilon+\cos(2\pi v_i))),$$

where n is the number of period to return to v_0. We note that the quantity $\int \log g \, d\mu$ in (5.10) is in fact the Lyapunov exponent in fibre direction at $(v, 0)$ for map F, obtained from (5.2).

From (2.14), we have defined that the Dirac delta measure is supported on the points in a given periodic orbits in general. In this case, we will define such measure on the periodic points v in Keller's map. For instance, for the period-1 orbit at points $v = 0$ and $v = 1$, we define the Dirac delta measures at 0 and 1 by $\mu_+ = \delta_0$, then $G(\mu_+)$ has the following average:

$$\begin{aligned} G(\mu_+) &= \int_A \log g(v) \; d\mu_+, \\ &\geq \int_A \log g(v) \; \delta_0(v) \; dv, \\ &= \log g(0), \\ &= \log r \times (1 + \epsilon + \cos(2\pi(0))), \\ &= \log(r \times 2.01). \end{aligned} \tag{6.2}$$

The same is also true for $v = 1$ where the average is $\log(r \times 2.01)$. Meanwhile, since $G(\mu_{ac})$ is absolutely continuous w.r.t. Lebesgue measure ℓ, therefore the measure is defined as $\mu_{ac} = \ell$, then $G(\mu_{ac})$ has the following average:

$$\begin{aligned} G(\mu_{ac}) &= \int_A \log g(v) \; d\ell, \\ &= \int_0^1 \log g(v) \; dv, \\ &= \int_0^1 \log[r \times (1 + \epsilon + \cos(2\pi(v))] \; dv, \\ &= \int_0^1 \log r \; dv + \int_0^1 \log(1 + \epsilon + \cos(2\pi(v)) \; dv, \\ &= \log r - 0.551843, \\ &= \log r + \log e^{-0.551843}, \\ &= \log(r \times e^{-0.551843}), \\ &= \log(r \times 0.57589). \end{aligned} \tag{6.3}$$

For the period-3 orbit $\overline{001}$ at points $v_0 = 0.10255$, $v_1 = 0.22788$ and $v_2 = 0.50640$, we define the Dirac delta measures at v_0, v_1 and v_2 as

$$\mu_- = \frac{1}{3}(\delta_{v_0} + \delta_{v_1} + \delta_{v_2}).$$

Then the average of $G(\mu_-)$ is

$$\begin{aligned} G(\mu_-) &= \int_A \log g(v)\ d\mu_-, \\ &\leq \int_A \log g(v) \left(\frac{1}{3}(\delta_{v_0} + \delta_{v_1} + \delta_{v_2})dv \right), \\ &= \frac{1}{3}(\log g(v_0) + \log g(v_1) + \log g(v_2)), \\ &= \log(g(v_0)g(v_1)g(v_2))^{\frac{1}{3}}, \qquad (6.4) \\ &= \log(r^3 \times (1+\epsilon+\cos(2\pi(v_0))(1+\epsilon+\cos(2\pi(v_1))(1+\epsilon+\cos(2\pi(v_2)))^{\frac{1}{3}}, \\ &= \log(r \times 0.28216). \qquad (6.5) \end{aligned}$$

In fact, by equating (6.2), (6.3) and (6.4) to zero, one obtains the values of r_{c_1}, r_{c_2} and r_{c_3} respectively. We show the plots of $\log g$ corresponding for these three averages in Fig. 6.3.

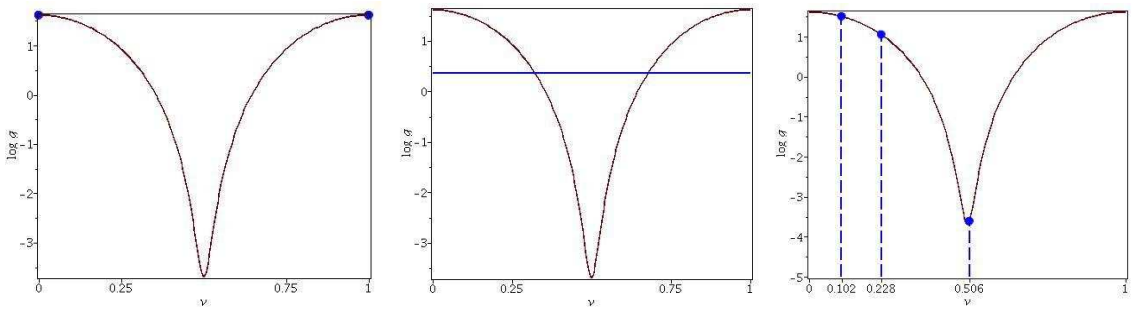

(a) (b) (c)

Figure 6.3 Plots of $\log g$ over $v = 0, \ldots 1$ for $r = 2.5$. (a) The period-1 points at $v = 0$ and $v = 1$. (b) Absolutely continuous w.r.t. Lebesgue measure means integration of the $\log g$ for the whole $v = 0 \ldots, 1$. (c) The period-3 points.

As a result, we plot the average of $\log g$ against the periodic points for fixed $r = 2.5$ for variety number of periodic points in Figure 6.4. Clearly we obtained that for each period, it has its own average, and what is more, different period gives different values of averages. To exemplify, for the case of $r = 2.5$, period-1 which contains $v = 0$ and $v = 1$ has average 1.6144, period-2 $\overline{01}$ which consists of points $v = 0.26910$ and $v = 0.5980$ has average 0.0374, period-3 $\overline{001}$ which has points at $v = 0.10255, 0.22788$ and 0.50640 has average of -0.3490, period-3 $\overline{011}$ which has points at $v = 0.36333, 0.80741$ and 0.64983 has average of 0.38769, period-4 $\overline{0001}$ which has points at $v = 0.04317, 0.09593, 0.21318$ and 0.47374 has average of 0.35459 and so on. To put it simply, for a particular value of parameter r, it will gives a set of periodic points with particular value of their averages. Our numerical computations suggest that for $r = 2.5$, period-1 gives maximum average which corresponds to maximum average for $G(\mu)$ while period-3 $\overline{001}$ gives minimum average which corresponds to minimum average for $G(\mu)$.

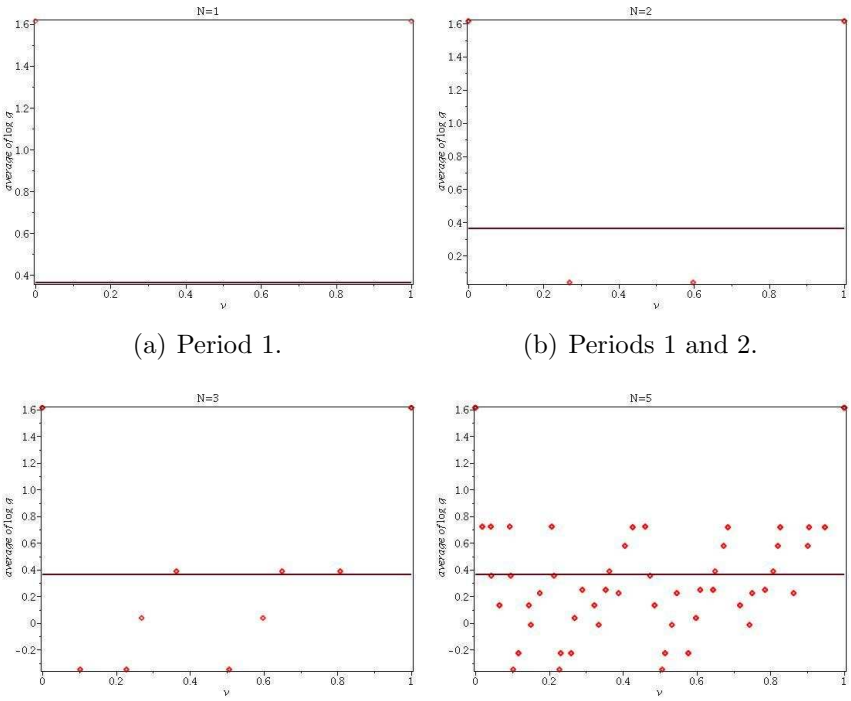

(a) Period 1.

(b) Periods 1 and 2.

(c) Periods 1, 2 and 3.

(d) Periods 1, 2, 3, 4 and 5.

Figure 6.4 The distribution of the average of $G(\mu)$ for $r = 2.5$ for different number of periodic points N. The red circles denote the periodic points while the vertical lines represent the $G(\mu_{ac}) = 0.36445$ for all N, absolutely continuous w.r.t. Lebesgue measure.

Moreever, as we vary r, we still have the same periodic points for each period, except that this time their averages are different (See Figure 6.5). This is due to the quantity of $\log(r \cdot (1 + \epsilon + \cos(2\pi v)))$. From this figure, we notice that as we increase r, the averages are also increase. Note also that the plots of Figure 6.5(a), 6.5(b), 6.5(c) and 6.5(d) are corresponding to cases (i), (ii), (iii) and (iv) respectively from Section 5.1.2. In fact, case (i) implies that $\varphi_\infty(v) = 0$ since $G(\mu) < 0$ for all S-invariant probability measures μ and case (iv) implies that $\varphi_\infty(v) > 0$ since $G(\mu) > 0$ for all such μ. Our numerical results also indicate that the measure $\mu_+ = \delta_0$ for the period-1 orbit always maximizes $G(\mu)$ while the measure μ_- for the period-3 orbit $\overline{001}$ always minimizes the $G(\mu)$ for all $N \geq 1$ where these results have been obtained by Keller in his paper [44]. Thus, this means that the result obtained by him is verified here by our numerical computations.

6.2 Properties of the zero set of the invariant graph

This section is devoted to investigating the "size" of zero set of the invariant graph $\varphi_\infty(v)$ for Keller's map in terms of Hausdorff dimension $\dim_H$. In particular, we will study the changes of the size of this set which is influenced by the parameter

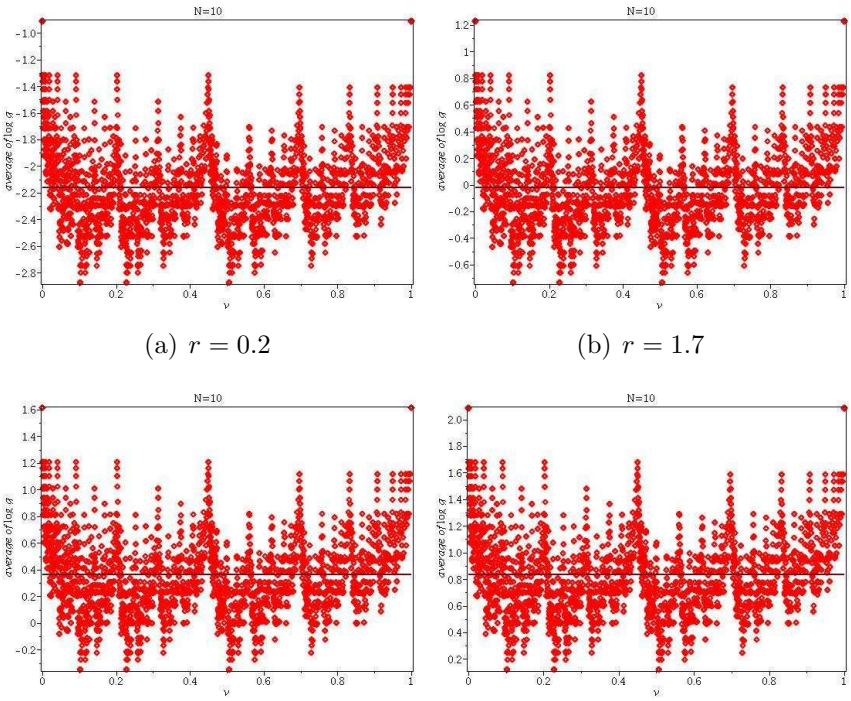

(a) $r = 0.2$ (b) $r = 1.7$

(c) $r = 2.5$ (d) $r = 4$

Figure 6.5 Comparisons for $N = 10$ and various r where the horizontal lines represent $G(\mu_{ac})$. Notice that the location of $G(\mu_{ac})$ changes from negative to positive as we change r. The top two points in each figure represent $G(\mu_+)$ where they are always maximum for all r, i.e. at $v = 0$ and $v = 1$. Meanwhile the lowest three points for the period-3 orbit $\overline{001}$ at $v = 0.10255$, 0.22788 and 0.5064 are always minimum for all r. From Section 5.1.2 (a) corresponds to case (i) with $G(\mu_{ac}) = -2.16128$, (b) corresponds to case (ii) with $G(\mu_{ac}) = -0.646154$, (c) corresponds to case (iii) with $G(\mu_{ac}) = 0.36445$ and (d) corresponds to case (iv) with $G(\mu_{ac}) = 0.83445$.

r in the fibre maps in the skew product system in [44]. We denote $\varphi_{\infty,r}(v)$ to show dependency of the invariant graph on r. In fact, Keller and his coworker have studied the transition from $\varphi_{\infty,r}(v) = 0$ to $\varphi_{\infty,r}(v) > 0$ in terms of Hausdorff dimension [46]. Their results show that for r smaller than r_{c_1}, $\varphi_{\infty,r}(v) = 0$, while for r larger than r_{c_3}, $\varphi_{\infty,r}(v) > 0$. To study this transition, both zero and non-zero sets of $\varphi_{\infty}(v)$ need to be defined. We refer to Keller *et al.* [45] and Keller and Otani [46] for their definitions.

The zero set is defined by

$$N_r = \{\theta \in \Theta : \varphi_{\infty,r}(v) = 0\}. \tag{6.6}$$

whereas for the nonzero set;

$$N_r^c = \Theta \setminus N_r = \{\theta \in \Theta : \varphi_{\infty,r}(v) > 0\}. \tag{6.7}$$

Below we show some basic properties of the zero set [46, Remark 2]:

(a) N_r is invariant under the skew product map F (5.3).

(b) For $r < s$, we have $\varphi_{\infty,r}(\theta) \leq \varphi_{\infty,s}(\theta)$ for all $\theta \in \Theta$. Hence $N_r \supseteq N_s$.

In property (a), the zero set N_r is obtained when the baseline collides with the nontrivial invariant graph, i.e.

$$N_r = \Phi_0 \cap \Phi_+$$

where Φ_0 and Φ_+ have been defined in (5.7) and (5.8) respectively. Since both Φ_0 and Φ_+ are invariant, then the intersection is also an invariant. We prove this in the following theorem.

Lemma 6.1 *Let $A, B \subseteq \Theta \times I$. If $F(A) = A$ and $F(B) = B$, and F is invertible, then $F(A \cap B) = A \cap B$.*

Proof. The sets $(\theta, x) \in A$ if and only if $F(\theta, x) \in A$ and so $(\theta, x) \in B$ if and only if $F(\theta, x) \in B$. Then $F(A \cap B) = A \cap B = F^{-1}(A \cap B)$ since F is also invertible. ■

For the property (b), if $r < s$, then

$$\begin{aligned}
r \cdot (1 + \epsilon + \cos(2\pi v)) \cdot h(x) &< s \cdot (1 + \epsilon + \cos(2\pi v)) \cdot h(x), \\
F_{\theta,r}(x) &< F_{\theta,s}(x), \\
F^n_{\hat{S}^{-n}\theta,r}(x) &< F^n_{\hat{S}^{-n}\theta,s}(x), \\
\lim_{n\to\infty} F^n_{\hat{S}^{-n}\theta,r}(x) &\leq \lim_{n\to\infty} F^n_{\hat{S}^{-n}\theta,s}(x), \\
\lim_{n\to\infty} \hat{\varphi}_{n,r}(\theta) &\leq \lim_{n\to\infty} \hat{\varphi}_{n,s}(\theta), \\
\hat{\varphi}_{\infty,r}(\theta) &\leq \hat{\varphi}_{\infty,s}(\theta), \\
N_r &\supseteq N_s.
\end{aligned}$$

This means that N_r has bigger zeros (larger size of zero set) than N_s when $r < s$.

6.2.1 Dimension of the zero set of the invariant graph, from Keller and Otani [46]

Previously, we have shown that there are three critical values for parameter r, namely at r_{c_1}, r_{c_2} and r_{c_3} in Chapter 5. In here, we are interested to estimate the dimensions for both N_r and N_r^c for all values of r in terms of Hausdoff dimension analytically. In Keller and Otani [46], they consider the dimension for both sets on the open interval (r_{c_1}, r_{c_3}). However, in this study, we would like to extend their results by

also looking at what happen to the dimension outside (r_{c_1}, r_{c_3}) as well as at the boundaries, i.e. at r_{c_1} and r_{c_3}. We discuss this as in the following conjecture which relies on the results in [46, Theorem 2], but here we also clarify the dimension at the boundaries.

Conjecture 6.1 *There is a real continuous function* $D : [r_{c_1}, r_{c_3}] \to [0, 1]$ *that is analytic on* (r_{c_1}, r_{c_3}) *such that*

(i) $D(r_{c_2}) = 1$, $D''(r_{c_2}) < 0$

(ii) $D'(r) \left\{ \begin{array}{c} < \\ > \end{array} \right\} 0$ *for* $r \left\{ \begin{array}{c} > \\ < \end{array} \right\} r_{c_2}$.

(iii)
$$\dim_H(N_r) = \begin{cases} 2 & \text{for } r \le r_{c_2}, \\ D(r) + 1 & \text{for } r_{c_2} \le r \le r_{c_3}, \\ 0 & \text{for } r > r_{c_3}. \end{cases}$$

$$\dim_H(N_r^c) = \begin{cases} 0 & \text{for } r \le r_{c_1}, \\ D(r) + 1 & \text{for } r_{c_1} < r \le r_{c_2}, \\ 2 & \text{for } r \ge r_{c_2}. \end{cases}$$

From the above conjecture, we consider a function D from the closed interval $[r_{c_1}, r_{c_3}]$ that maps to $[0, 1]$. Statements (i) and (ii) have already been proved in [46, Theorem 2]. In (i) they proved that the function D is a unimodal map on the interval (r_{c_1}, r_{c_3}) and has a critical point at r_{c_2}, D is monotone increasing on the left of r_{c_2} and monotone decreasing on the right of r_{c_2}. In (ii), the first derivative $D'(r)$ is positive shows that the function D is increasing for $r_{c_1} < r < r_{c_2}$ and the first derivative $D'(r)$ is negative shows that the function D is decreasing for $r_{c_2} \le r \le r_{c_3}$.

In (iii), we first consider for the zero set N_r as defined in (6.6). Note that we use the dimension 2 instead of 1 since we consider the two-dimensional (u, v). When $r \le r_{c_2}$, we observe that N_r has dimension 2 since the zero set of invariant graph $\varphi_{\infty,r}(v)$ stays along the $x = 0$ for all u and v. Next, when $r_{c_2} \le r \le r_{c_3}$, we are using the result in [46, Theorem 2] that the dimension of N_r now is less than 2 since the size of N_r decreases as r increases. We also observe that the dimension of N_r decreases monotonically from 2 to 1 as shown in Figure 6.6. Finally, when $r > r_{c_3}$, the dimension of N_r is 0 as there is no more N_r on (u, v)-axis.

Secondly, we also consider for nonzero set N_r^c as defined in (6.7). When $r \le r_{c_1}$, we can see from the Figure 5.3(a) that there is no N_r^c on $x = 0$, i.e., there is no $\varphi_{\infty,r}(v) > 0$ for all u and v and therefore the dimension is 0. Next, when $r_{c_1} < r \le r_{c_2}$, we use the result in [46, Theorem 2] that the dimension is now between 1 and 2 but this time the dimension of N_r^c increases monotonically from 1

to 2 since the size of N_r^c increases as r increases (See Figure 6.6). Finally, as $r \geq r_{c_2}$, N_r^c has the dimension 2 for all u and v since $\varphi_{\infty,r}(v)$ now is strictly positive.

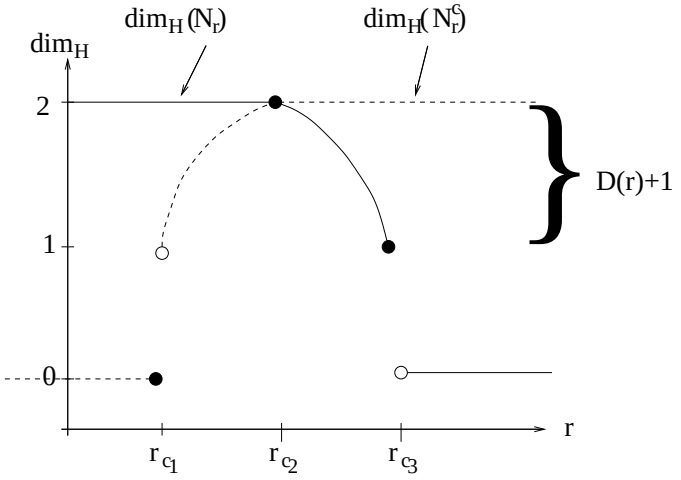

Figure 6.6 The schematic diagram showing Hausdorff dimension dim_H for both zero set N_r and non-zero set N_r^c as r varies from small values to large values. The solid lines represent the dimension of N_r while the dashed lines represent the dimension of N_r^c. The maximum dimension 2 is achieved when $r \leq r_{c_2}$ since the set N_r occupies along the baseline $x = 0$ for all v. As r is increased from r_{c_2} to r_{c_3}, the size of N_r decreased and so its dimension. As $r > r_{c_3}$, the dimension is zero for all v. Meanwhile the non-zero set N_r^c has dimension 0 when $r \leq r_{c_1}$ since $\varphi_{\infty,r}(v) = 0$ for all v and thus no non-zero set within this range. Further as r_{c_1} increases to r_{c_2}, its dimension increasing monotonically from 1 to 2 as more and more points escape from the invariant set $x = 0$. Finally it attains the maximum dimension at 2 as there are dense set of non-zero set of $\varphi_{\infty,r}(v)$ when $r \geq r_{c_2}$.

6.3 Summary for results on the stability index $\sigma((v,0),\mathcal{B}(v,0))$ and $\dim_H(N_r)$

We recall that the invariant graph $\varphi_\infty(v)$ is the attractor for F (5.3). In this section, we summarize the stability index for the basin of the attractor (obtained in Chapter 5) and the dimension of the zero set of the attractor in Table 6.1 for different range of parameter r. We note that the riddled basin occurs within $r_{c_2} \leq r \leq r_{c_3}$. In fact, at $r = r_{c_1}$ and at $r = r_{c_3}$, these correspond to the extremal period-3 orbit and period-1 orbit respectively. From Conjecture 6.1, when $r = r_{c_3}$, $\dim_H(N_r) = 1$ can possibly be justified by noting that the extremal period-1 orbit is still nonlinearly stable.

Range of r	$\sigma((v,0),\mathcal{B}(v,0))$	$\dim_H(N_r)$
$r \leq r_{c_2}$	$-\infty$	2
$r_{c_2} \leq r \leq r_{c_3}$	positive	monotonic decreasing from 2 to 1
$r > r_{c_3}$	∞	0

Table 6.1 This table shows summary for stability index for the basin of the attractor $\varphi_\infty(v)$ and the dimension for the zero set of $\varphi_\infty(v)$.

7 Stability index $\sigma(A)$ for a set and attractor in Ashwin's model

In both chapters 4 and 5, we have computed the stability index for a class of skew product systems which exhibit the riddled basins. In this chapter, we compute the stability index for a non-skew product map which also has a riddled basin. We consider a map proposed in Ashwin *et al.* [6; 7] where it is a coupled identical chaotic electronic circuits system. This map has two Milnor attractors, one at baseline $x_2 = 0$ and the other at infinity.

We observe that geometry of the basins of attraction changes as we vary a parameter in this map. The riddled basin happens within a certain range of this parameter. To compute the stability index for such basin, we also use the random number generator in MATLAB for the purpose of counting the number of points that are in the basins of attraction of the attractor A. In this chapter we compute the stability index for the attractor using the concept of stability index defined for a set as we introduce in Definition 3.2.

We first discuss about the global geometry of the basins of attraction for this map and secondly to concentrate on the computation of stability index for the local geometry of these basins of attraction by considering a neighbourhood of the attractor A.

7.1 The model

We consider the following: Suppose that $f_{\alpha,\nu,\epsilon} : M \to M$ is a smooth mapping where M is a compact subset of X such that $f_{\alpha,\nu,\epsilon}$ has an invariant subspace $N \subset M$. Let A be an invariant set which is an attractor when the dynamics is restricted to N.

Let $f_{\alpha,\nu,\epsilon}$ be a three-parameter map of $\mathbb{R}^2$ to itself that is equivariant under $\mathbb{Z}_2$

generated by $(x_1, x_2) \mapsto (-x_1, x_2)$ given by

$$f_{\alpha,\nu,\epsilon}\begin{pmatrix} x_1 \\ x_2 \end{pmatrix} = \begin{pmatrix} \frac{3\sqrt{3}}{2}x_1(x_1^2 - 1) + \epsilon x_1 x_2^2 \\ \nu e^{-\alpha x_1^2} x_2 + x_2^3 \end{pmatrix} \tag{7.1}$$

where α, ν, ϵ are three *normal parameters* [3] restricted to N and ν is a bifurcation parameter. This map is in fact an extension of a cubic logistic equation $h : \mathbb{R} \to \mathbb{R}$ which is given by

$$h(x) = \frac{3\sqrt{3}}{2}x(x^2 - 1). \tag{7.2}$$

Note that on the invariant subspace N, i.e. when $x_2 = 0$, h has an asymptotically stable attractor $A = [-1, 1] \times \{0\}$ which is independent of α, ν and ϵ. In this study, the values of $\alpha = 0.7$ and $\epsilon = 0.5$ are fixed and the parameter ν is varied. These values of α and ϵ are chosen based on the work by [6; 7].

It also has been calculated that for this map the transitions of the attractor A from one behaviour to another behaviour were investigated by varying ν which happen at the following values [6; 7]:

(a) When $\nu = 1$, the attractor A looses its asymptotic stability.

(b) When $\nu = 1.285$, A experiences a blowout bifurcation.

(c) When $\nu = 1.538$, there is a bifurcation to normal repulsion.

We redepict from [7] the three critical curves above in Figure 7.1.

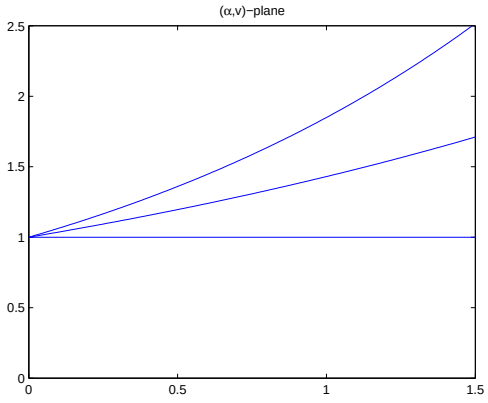

Figure 7.1 The plot of the three critical curves on (α, ν)-plane: the lower line $\nu = 1$ represents the value where A looses its asymptotic stability while the upperline $\nu = 1.538$ is where the bifurcation to the normal repulsion occurs. The middle line $\nu = 1.285$ is where the blowout bifurcation takes place.

7.2 Behaviour of map $f_{\alpha,\nu,\epsilon}$

In this section, we study behaviour of the map $f_{\alpha,\nu,\epsilon}$ by varying the value of ν and fixing parameters α and ϵ. The changes of these behaviour are in fact dependent on the geometry of the basins of attraction of A. The theorem below shows different behaviour for different ranges of ν with fixed $\alpha = 0.7$ and $\epsilon = 0.5$.

Theorem 7.1 [7] *The behaviour of the map $f_{\alpha,\nu,\epsilon}$ is as follows:*

(a) When $0 \leq \nu < 1$, A is an asymptotically stable attractor.

(b) When $1 < \nu < 1.285$, A is a Milnor attractor whose basin is riddled with that of the attractor at infinity.

(c) When $1.285 < \nu < 1.538$, A is a chaotic saddle.

(d) When $\nu > 1.538$, A is a normally repelling chaotic saddle.

Proof. See [7].

Recall that from previous section, the blowout bifurcation happens when $\nu = 1.285$. From the above theorem, this means that the basin is riddled before the blowout bifurcation takes place.

7.2.1 Geometry of basins of attraction by varying ν

In this section, we show the basins of attraction for the map $f_{\alpha,\nu,\epsilon}$ for $\alpha = 0.7$, $\epsilon = 0.5$ and various ν in Figure 7.2. The black area denotes the basin of attraction, $\mathcal{B}(A)$, i.e. the points that are attracted to the baseline $x_2 = 0$ and all the figures are shown in the rectangle $(x_1, x_2) \in [-1.5, 1.5] \times [-1.1, 1.1]$. Meanwhile, the orange area indicates the complement of the basin of attraction, $\mathcal{B}(A)^c$ for the points that are attracted to ∞. We can see that the area of basin $\mathcal{B}(A)$ shrinks as we increase the parameter.

From the above theorem, when $0 < \nu < 1$, the attractor A is asymptotically stable. This means that all the points in ε-neighbourhood of A are attracted to $A = [-1, 1] \times \{0\}$, i.e. $\ell(\mathcal{B}(A)) = 1$. The geometry for basins of attraction within this range is corresponds to Figure 7.2(a). When $1 < \nu < 1.285$, A is no longer stable where it is now a Milnor attractor with riddled basin such that there are nearby points in the ε-neighbourhood of A belong to $\mathcal{B}(A)^c$. From Definition 2.22 we have $\ell(\mathcal{B}(A)) > 0$ and $\ell(\mathcal{B}(A)^c) > 0$. This is corresponds to Figure 7.2(b).

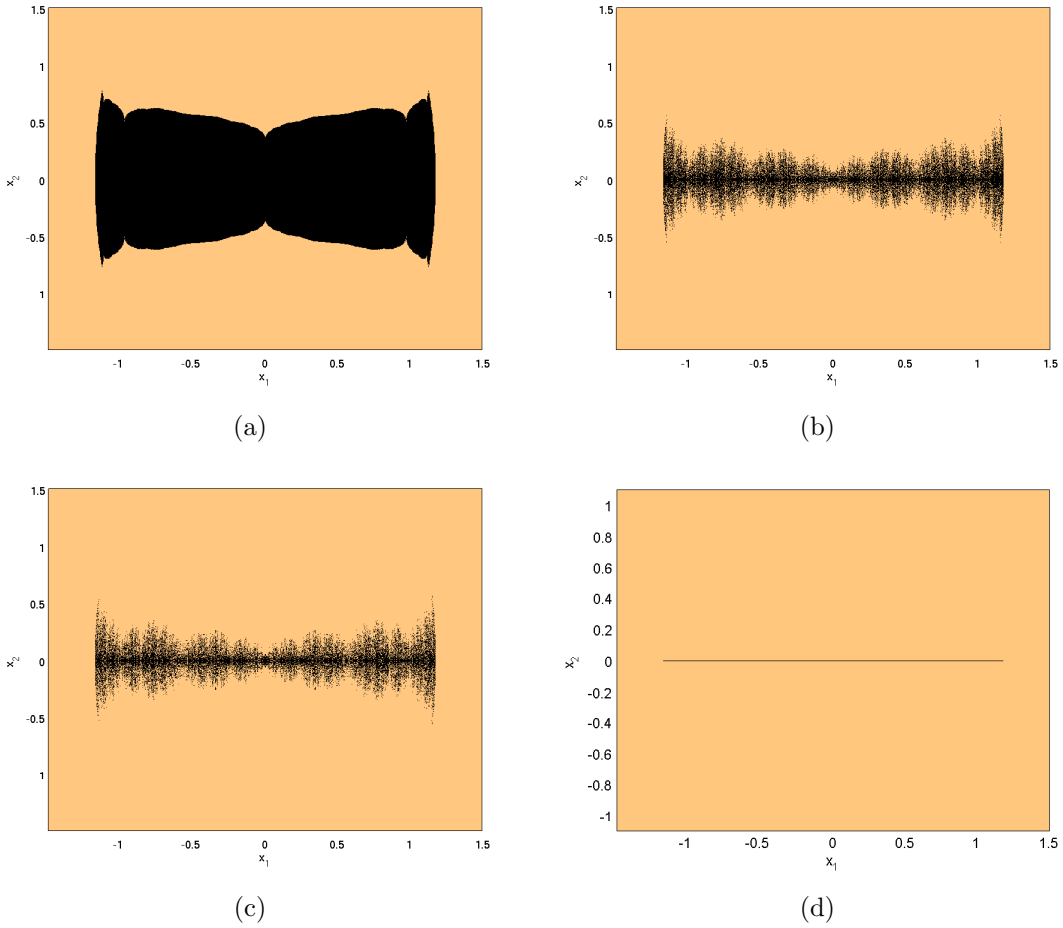

Figure 7.2 The basins of attraction for $f_{\alpha,\nu,\epsilon}$ with $\alpha = 0.7, \epsilon = 0.5$ and various ν. The black region corresponds to basin of attraction where the initial conditions are attracted to $x_2 = 0$ ($\mathcal{B}(A)$) while orange region corresponds to basin of attraction where the initial conditions attracted to $x_2 = \pm\infty$ ($\mathcal{B}(A)^c$). (a) For $\nu = 0.9$, the attractor A is asymptotically stable. (b) For $\nu = 1.28$, A is a Milnor attractor with riddled basin where the basin $\mathcal{B}(A)$ is riddled the basin at ∞. Here both $\mathcal{B}(A)$ and $\mathcal{B}(A)^c$ have positive measure. (c) For $\nu = 1.285$, the blowout bifurcation occurs. (d) For $\nu = 1.48$, A is a chaotic saddle where the basin $\mathcal{B}(A)$ has zero measure.

Further, when $\nu > 1.285$, all the points in the ε-neighbourhood of A are now attracted to the attractor at ∞ in $\mathcal{B}(A)^c$ where A now is a chaotic saddle. The corresponding basin is shown in Figure 7.2(d). Since there is no orbit attracted to A, this implies that $\ell(\mathcal{B}(A)) = 0$.

7.3 Approximating Lebesgue measure for a set $\ell(A)$

Before we compute the stability index for the attractor A, we first need to transform the basins of attraction images in Figure 7.2 to dots points images to calculate the proportions in (3.6) and (3.7). To do this, we use RNG in MATLAB to generate

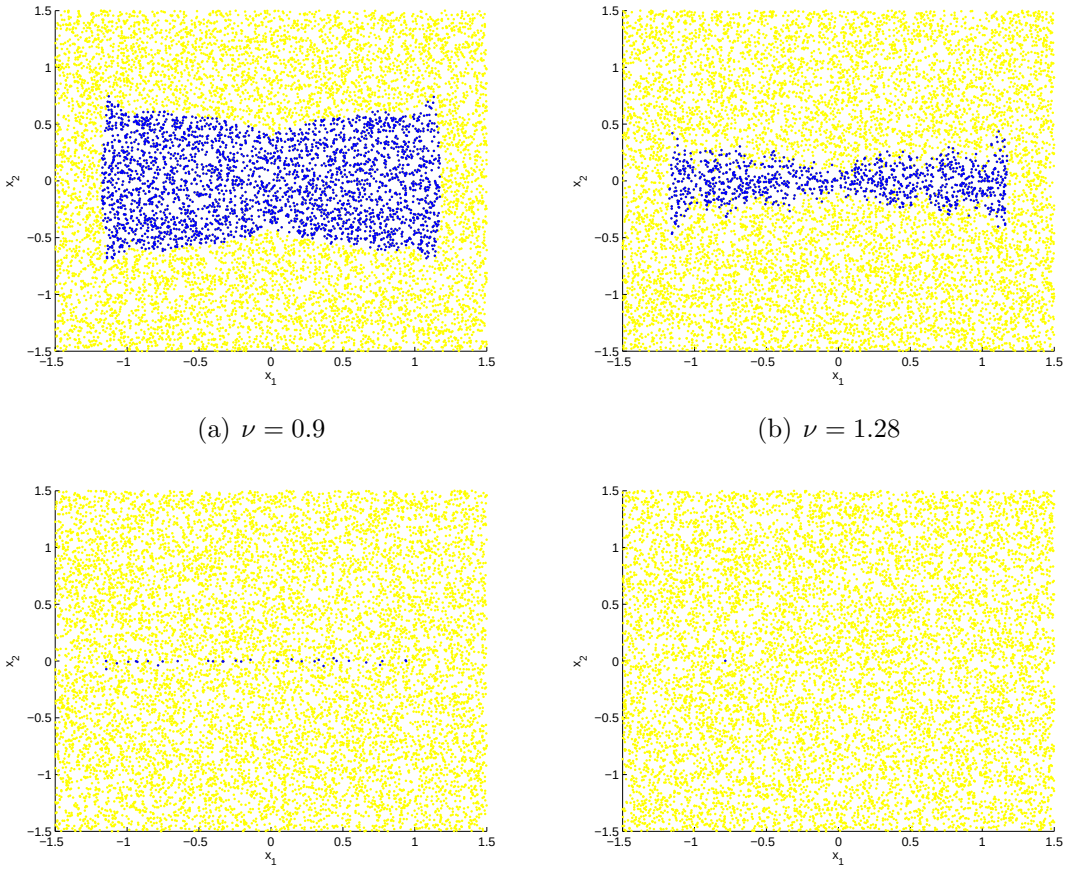

(a) $\nu = 0.9$ (b) $\nu = 1.28$

(c) $\nu = 1.48$ (d) $\nu = 1.6$

Figure 7.3 The images of basins of attraction which are transformed from Figure 7.2 using RNG. The blue points represent the points that go to $x_2 = 0$ and this corresponds to $\mathcal{B}(A)$. While the yellow points represent for the points that repelled away to $x_2 = \infty$ and this corresponds to $\mathcal{B}(A)^c$.

random points thoroughout the images.

By using the RNG, we use two 'for' loops; the first loop is to test whether the point is in $\mathcal{B}(A)$ by iterating the point several thousands times. We encode *nits* to represent the number of iterations needed in the MATLAB codes. The second loop is to produce points that are in the ε-neighbourhood of the attractor A where we encode this number in MATLAB as *nii*.

Therefore, as a result, we show the basins of attraction generated by using RNG in Figure 7.3. In this figure, the blue points represent $\mathcal{B}(A)$ which corresponds to the black area in Figure 7.2, while the yellow points represent $\mathcal{B}(A)^c$ which corresponds to the orange area in Figure 7.2. By obtaining these random basins, it make it possible to measure ℓ by counting the blue and yellow points.

By using the results in Figure 7.3, we would like to investigate how the proportion of the image that is in $\mathcal{B}(A)$ varies with parameter ν in (7.1) looks like. To do this, we fix $nits = 20$ and $nii = 2500$ for various ν. This is shown in Figure 7.4

where the results indicate that the proportion $\Sigma_\varepsilon(A)$ decreases as ν increases. This is because the number of blue points over the yellow points in Figure 7.3 decreases as ν increases. Further, we also vary the *nits* and *nii* to see how the convergence of $\Sigma_\varepsilon(A)$ looks like. This is depicted in Figure 7.5. We notice that by increasing *nits*, $\Sigma_\varepsilon(A)$ converges to 0 faster than lower *nits*. While by varying *nii*, it gives the results that are approximately same with each other.

In fact, we can rewrite the proportions (3.6) and (3.7) as:

$$\Sigma_\varepsilon(A) = \frac{\#\text{ of blue points inside the } \varepsilon\text{-neighbourhood of } A}{\#\text{ of blue and yellow points inside the } \varepsilon\text{-neighbourhood of } A} \tag{7.3}$$

and

$$1 - \Sigma_\varepsilon(A) = \frac{\#\text{ of yellow points inside the } \varepsilon\text{-neighbourhood of } A}{\#\text{ of blue and yellow points inside the } \varepsilon\text{-neighbourhood of } A}. \tag{7.4}$$

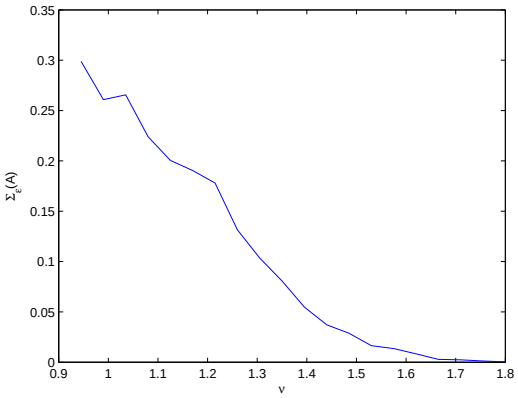

Figure 7.4 The proportion $\Sigma_\varepsilon(A)$ as in (3.6) versus $\nu = 0.9, ..., 1.8$ with $nits = 20$ and $nii = 2500$. The proportion decreases as we increase ν since the black region becomes smaller and smaller as we increase ν. This corresponds to Figure 7.2.

In the next section, we will focus on the local geometry of the basins of attraction as depicted in Figure 7.2 where we will compute the stability index for the attractor A.

7.4 Computations of $\sigma(A, \mathcal{B}(A))$

To compute this index, we divide into several steps. According to the stability index's formula in Definition 3.5, we need to choose an ε-neighbourhood around the attractor A. We already know that $A = [-1, 1] \times \{0\}$. In our study, we choose the ε-neighbourhood on the x_1-axis as $[-1 - \varepsilon, 1 + \varepsilon]$ and $[-\varepsilon, \varepsilon]$ on the x_2-axis.

First, we compute $\Sigma_\varepsilon(A)$ by changing the size of the ε-neighbourhood. Therefore,

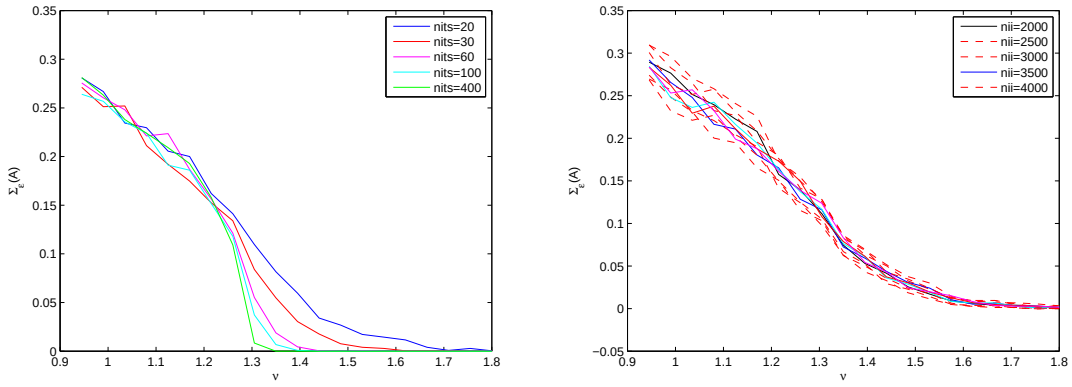

(a) (b)

Figure 7.5 The patterns of proportion by varying the (a) *nits* with $nii = 2500$. As we increase *nits*, $\Sigma_\varepsilon(A)$ converges to 0 faster than the lower *nits*. (b) *nii* with $nits = 20$. The patterns do not change much for all the *nii* chosen.

the result is as in Figure 7.6 where generally, $\Sigma_\varepsilon(A) \to 1$ as $\varepsilon \to 0$. In particular, when $\nu < 1$, there is a critical ε_c where the proportion Σ_ε increases and finally hits 1 as $\varepsilon \to 0$, see Figure 7.6(a). When $\Sigma_\varepsilon(A) = 1$, this means that the ε-neighbourhood only filled with the points that go to the baseline $x_2 = 0$ (i.e. the blue points).

When $1 < \nu < 1.285$, $\Sigma_\varepsilon(A) \to 1$ as $\varepsilon \to 0$ but never reaches 1. This proportion increases as more and more points that go to the baseline occupy in the ε-neighbourhood around A (see Figure 7.6(b)). When $\nu > 1.285$, all points are now go to ∞ and stay in $\mathcal{B}(A)^c$. Thus this means that $\ell(\mathcal{B}(A)) = 0$ and therefore the proportion $\Sigma_\varepsilon(A)$ is zero everywhere for all ε (see Figure 7.6(c)).

Next, in order to obtain $\sigma_-(A)$ from (3.9), we plot $\log(\Sigma_\varepsilon(A))$ versus $\log \varepsilon$ where the slope of the curve gives the values of $\sigma_-(A)$. We show the results for $\nu = 0.9, 1.28, 1.48$ in Figure 7.7. Here the slopes are $\sigma_-(A) = 0, 0, \infty$ respectively. We also do the plot for $\sigma_+(A)$ by plotting $\log(1 - \Sigma_\varepsilon(A))$ versus $\log \varepsilon$ where the slope gives the values of $\sigma_+(A)$. We plot this for the same values of ν in Figure 7.8 and now $\sigma_+(A) = \infty, 0.52, 0$ respectively. To compute the slopes, we fit the data points obtained in Figure 7.7 and 7.8 with regression lines. Therefore from (3.8), $\sigma(A, \mathcal{B}(A)) = \infty, 0.52, -\infty$ for $\nu = 0.9, 1.28, 1.48$ respectively.

Follows from this, we also compute $\sigma(A, \mathcal{B}(A))$ for $\nu = 1.2, \ldots, 1.4$ and see how the pattern of stability index looks like as we vary ν. We observe that $\sigma(A, \mathcal{B}(A))$ varies continuously and monotonically decreases from ∞ to $-\infty$. See Figure 7.9. Based on Figure 7.9, the index varies with ν as follows:

(a) When $0 < \nu < 1$, $\sigma(A, \mathcal{B}(A)) = \infty$.

(b) When $1 < \nu < 1.285$, $\sigma(A, \mathcal{B}(A)) > 0$.

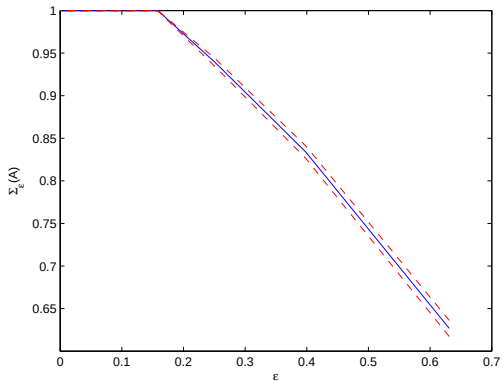

(a) $\nu = 0.9$

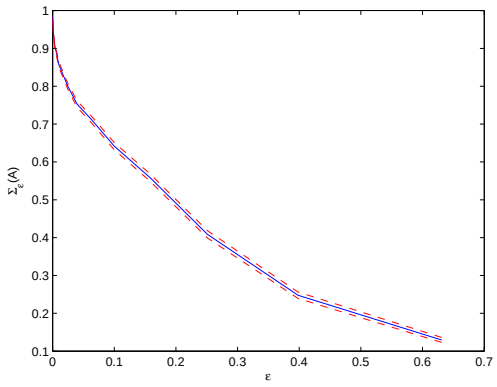

(b) $\nu = 1.28$

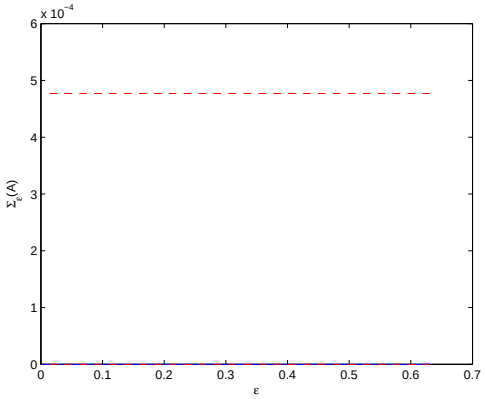

(c) $\nu = 1.48$

Figure 7.6 The proportion $\Sigma_\varepsilon(A)$ of the points that go to the baseline $x_2 = 0$ (refer to the blue points in Figure 7.3). (a) As $\varepsilon \to 0$, the proportion of the blue points over the whole points in the ε-neighbourhood increases and finally hits 1 as the ε-neighbourhood only filled with the blue points. There is a critical $\varepsilon_c = 1.585$ that changes from lower positive value to 1. (b) The proportion increases but never hits 1 as $\varepsilon \to 0$. Note that the initial values of the proportion at this stage are less than (a) since the area of the blue points smaller when ν decereases. (c) At this stage, the blue points only stay on the invariant set A, not lingering around in the basin $\mathcal{B}(A)$, therefore since there are no points inside $\mathcal{B}(A)$, $\Sigma_\varepsilon(A) = 0$ for all ε.

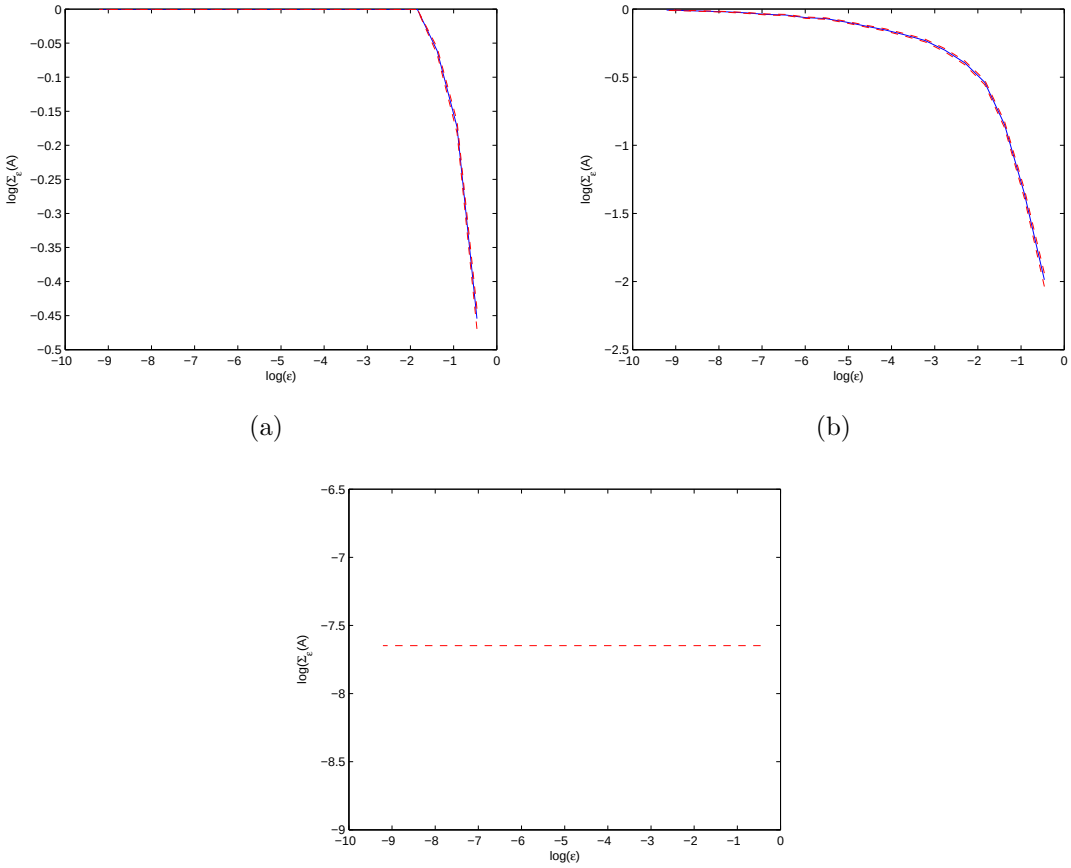

Figure 7.7 Computation of $\sigma_{-}(A)$ for $f_{\alpha,\nu,\epsilon}$: $\log(\Sigma_{\varepsilon}(A))$ versus $\log(\varepsilon)$. (a) For $\nu = 0.9$, the slope is 0. (b) For $\nu = 1.28$, the slope is 0. (c) For $\nu = 1.48$, the slope is ∞.

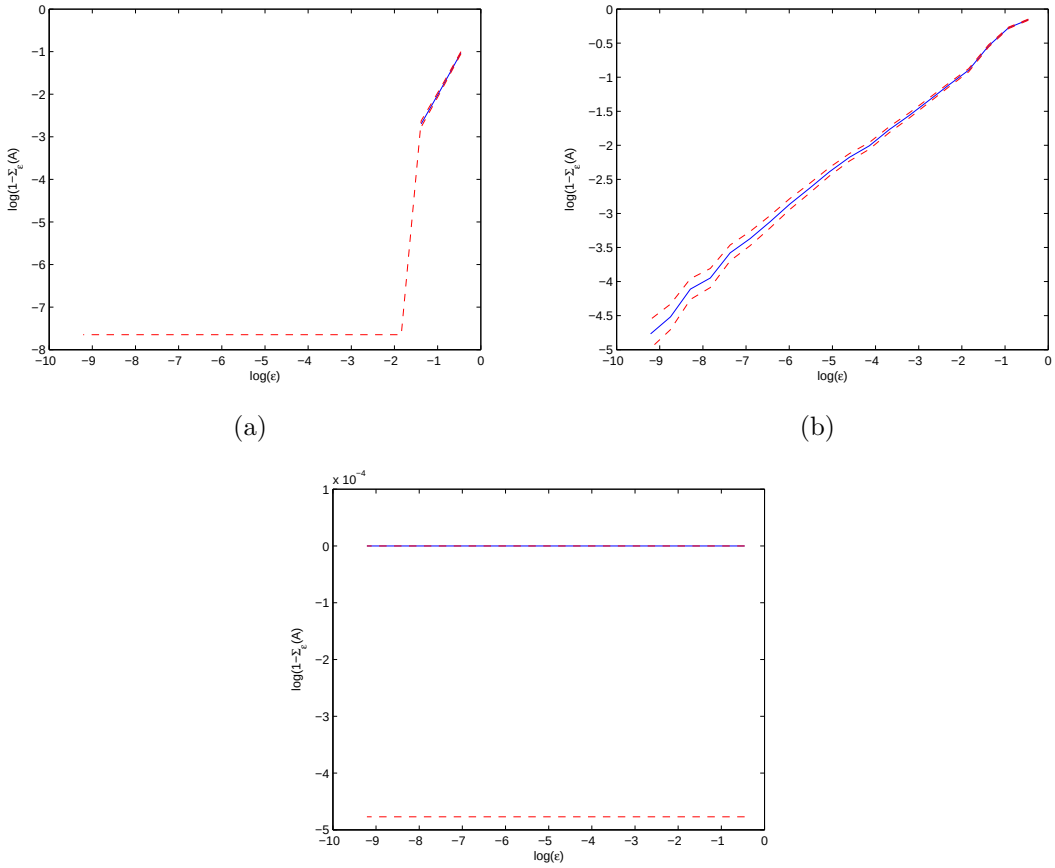

(a) (b)

(c)

Figure 7.8 Computation of $\sigma_+(A)$ for $f_{\alpha,\nu,\epsilon}$: $\log(1-\Sigma_\varepsilon(A))$ versus $\log(\varepsilon)$. (a) For $\nu = 0.9$, the slope is ∞. (b) For $\nu = 1.28$, the slope is 0.52. (c) For $\nu = 1.48$, the slope is 0.

(c) When $\nu > 1.285$, $\sigma(A, \mathcal{B}(A)) = -\infty$.

The result in (b) above also agrees with Theorem 4.6(i) and Keller's result [44] where for ℓ-almost all points x_1, the stability index $\sigma(A, \mathcal{B}(A))$ is positive when the riddled basin occurs.

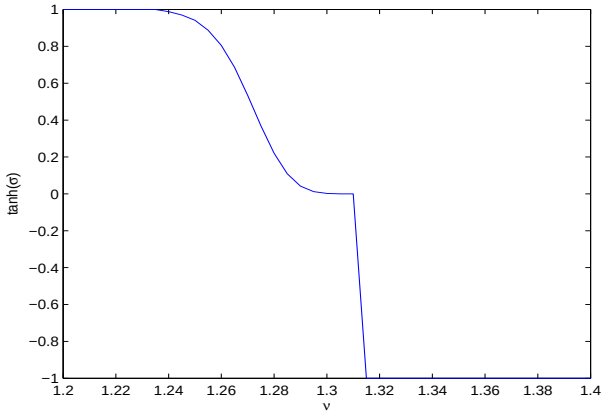

Figure 7.9 The numerical approximation of stability index $\sigma(A, \mathcal{B}(A))$ (3.8) for the attractor $A = [-1, 1] \times \{0\}$ for $f_{\alpha,\nu,\epsilon}$ by varying ν. The values of 1 and -1 represent that the indices are $+\infty$ and $-\infty$ respectively. When $0 < \nu < 1$, $\sigma(A, \mathcal{B}(A)) = \infty$ since all points in the ε-neighbourhood of A belong to $\mathcal{B}(A)$. When $1 < \nu < 1.285$, $\sigma(A, \mathcal{B}(A))$ decreases from positive value down to 0 since more and more points belong to $\mathcal{B}(A)^c$. Then at $\nu = 1.285$, it jumps straight to $-\infty$. For $\nu \geq 1.285$, $\sigma(A, \mathcal{B}(A)) = -\infty$ because all the points in the ε-neighbourhood of A are in $\mathcal{B}(A)^c$.

8 Discussion and conclusions

This thesis is devoted to an investigation of the structure of invariant sets of riddled basins of attraction in discrete dynamical systems. The stability index is used to describe the local structure of the riddled basins. Our numerical calculation of the stability index shows that this index depends on the local structure of the basins of attraction of the invariant sets. We have considered the stability index for both points and attractors in this thesis.

In Chapter 3, we have discussed the basic properties of stability index using stronger notion than [59] where we have shown that $\varepsilon^{\sigma_-(x)}$ and $\varepsilon^{\sigma_+(x)}$ are exponentially asymptotically tight bounds for the proportions $\Sigma_\varepsilon(x)$ and $1-\Sigma_\varepsilon(x)$ respectively. We also pointed out the relation between stability index with local dimension of measures in Theorem 3.3 using the restriction of Lebesgue measure to any measurable set N. Another significant contribution in this chapter is that we also defined the stability index for a set as well as for a point [59].

We first applied the stability index to a simple example of a piecewise linear skew product system in Chapter 4. In the first part of this chapter, we have proved in Theorem 4.4 that there exists a riddled basin for this map. In the second part, we have shown that in the case of riddled basin,

1. For Lebesgue almost all points in the invariant set, the stability indices are positive.

2. There may be some points in the invariant set that have negative stability index.

These results depend on the values of parameters δ and s as shown in Theorem 4.6; for example the stability index is negative when $\delta < s$. Moreover, Corollary 4.8 states that the stability index of a point can be computed in terms of Lyapunov exponents and the stability index for a set (which plays as Loynes' exponent in Keller's paper [44]). However, there are also some points for which the limits of stability indices do no converge. We showed some sufficient conditions for the non-convergence of the stability index in Theorem 4.9.

Recall that we have considered Keller's map [44] in both Chapter 5 and Chapter

6. Before we compute the stability index numerically, we compared Keller's result on stability index in Theorem 5.1 with our result in Conjecture 4.8. We observed that the stability index for the attractor in our piecewise linear map is in fact the Loynes' exponent in Keller's map. We define our stability index for the attractor purely in terms of geometry whereas Keller defines the Loynes' exponent in terms of thermodynamic pressure function. Although Keller's definition of stability index is not the same as ours, we can relate this by noting that the stability index of Keller correponds to our stability index for the inverse of Keller's map. In fact, Keller's map has only one attractor while the inverse map has two attractors, namely at zero and ∞.

In Chapter 6, we numerically verified the maximum and minimum invariant probability measures μ obtained in Keller's paper [44]. This was done by computing the Birkhoff averages on the periodic points in the skewed doubling map. The results show that period-1 orbit always gives maximum measure μ for all r while period-3 orbit always gives minimum measure μ for all r. We also discussed the result of Keller and Otani [46] on the dimension of zero and non-zero sets of invariant graph by including the dimensions at the critical values r_{c_1} and r_{c_3}. We present this in Conjecture 6.1. We believe that it is also possible to compute stability indices for the periodic points since from Figure 6.5, every period-n point has its own average. This means that limit of i_N/N exists and implies that limit of stability index converges to some value. Besides, we know exactly the value of the proportion of time whether the orbit lands on left or right intervals. For example, for the period-3 $\overline{001}$, the proportion of time that the orbit lands on the left interval is $2/3$ and $1/3$ on the right interval. We can then use the formula of stability index for a point as obtained in (4.32) to compute the stability indices for the periodic orbits.

Chapter 7 is the only chapter which considers a non-skew product map; we have computed the stability index for a riddled basin attractor of such a map. However, as we notice in this chapter, the basin boundary need not be an invariant graph as in chapters 4 and 5. One of advantages of having an invariant graph is that we can characterize the convergence of orbits of points whether they start from above or below the invariant graph. With this convergence of the orbits, we are able to identify the riddled basin where such basin is characterized by the stability index. This is not possible in this case.

Alongside the numerical computations of σ in Chapter 5 and 7, we noticed that the values of σ are different from the theoretical values. An exact σ from numerical computations is impossible to obtain although we would like to understand the sources of the errors. Some questions include: How many iterations ($nits$) should be used to test whether a point is in the basin or not? How many points (nii) should be produced in the ε-neighbourhood around the point of the attractor to get more

exact proportions? How to characterize whether a point is in the riddled basin or not?

Currently, the analytical results for the stability indices that we give in this thesis are restricted to one example of a piecewise linear map, as obtained in Chapter 4. In this thesis we have compared our result with Keller's stability index. We notice that his result is more general in the sense that he uses the powerful techniques of thermodynamic formalism to obtain the stability index. It would be of interest to see whether these techniques can be generalized to understand stability index in other (e.g. non-skew product) cases.

Appendices

A Asymptotic notations

We give a brief review of definitions of several types of asymptotic notation and properties of O, Ω, Θ and $\tilde{\Theta}$ as $\epsilon \to 0$. The notation of O, Ω and Θ have been introduced by Knuth [47] in 1976.

Big oh (O)

Definition A.1 *Let $f(\epsilon)$ and $g(\epsilon)$ be two functions. The set $O(g(\epsilon))$ is defined as*

$$O(g(\epsilon)) = \{f(\epsilon) |\ \exists\ c, \epsilon_0 > 0, \forall\ 0 < \epsilon \leq \epsilon_0 : 0 \leq f(\epsilon) \leq cg(\epsilon)\}.$$

We say that $g(\epsilon)$ is *asymptotic upper bound* for $f(\epsilon)$.

Big omega (Ω)

Definition A.2 *Let $f(\epsilon)$ and $g(\epsilon)$ be two functions. The set $\Omega(g(\epsilon))$ is defined as*

$$O(g(\epsilon)) = \{f(\epsilon) |\ \exists\ c, \epsilon_0 > 0, \forall\ 0 < \epsilon \leq \epsilon_0 : 0 \leq cg(\epsilon) \leq f(\epsilon)\}.$$

Here we say that $g(\epsilon)$ is *asymptotic lower bound* for $f(\epsilon)$.

Big theta (Θ)

Definition A.3 *Let $f(\epsilon)$ and $g(\epsilon)$ be two functions. The set $\Theta(g(\epsilon))$ is defined as*

$$\Theta(g(\epsilon)) = \{f(\epsilon) |\ \exists\ c_1, c_2, \epsilon_0 > 0, \forall\ 0 < \epsilon \leq \epsilon_0 : 0 \leq c_1 g(\epsilon) \leq f(\epsilon) \leq c_2 g(\epsilon)\}.$$

Here we write $f(\epsilon) = \Theta(g(\epsilon))$ and $g(\epsilon)$ is said to be an *asymptotically tight bound* for $f(\epsilon)$, i.e. $f(\epsilon)$ has both upper and lower bounds. This can also be written as:

$$f(\epsilon) = \Theta(g(\epsilon)) = O(g(\epsilon)) \cap \Omega(g(\epsilon)).$$

Big theta 'tilde'($\tilde{\Theta}$)

From our personal communication with Professor Quentin F. Stout from University of Michigan and by referring to a book by Crandall and Pomerance [22], we introduce a new notation of $\tilde{\Theta}(g(\epsilon))$ where we define as:

$$\tilde{\Theta}(g(\epsilon)) = \{f(\epsilon) | \, \forall \, \delta > 0, \exists c_1, c_2, \epsilon_0 > 0, \forall \, 0 < \epsilon \leq \epsilon_0 : 0 \leq c_1 \epsilon^{\delta} g(\epsilon) \leq f(\epsilon) \leq c_2 \epsilon^{-\delta} g(\epsilon)\},$$

where we can see that the upper bound is of the form $c_2\epsilon^{-\delta}g(\epsilon)$ and $c_1\epsilon^{\delta}g(\epsilon)$ for the lower bound, i.e., $f(\epsilon) = \tilde{\Theta}(g(\epsilon))$ means $f \in \Omega(g(\epsilon)\epsilon^{\delta})$ and $f \in O(g(\epsilon)\epsilon^{-\delta})$ for $\delta > 0$ which Stout calls it as "soft theta". In this thesis, we call $\tilde{\Theta}$ as *exponentially asymptotically tight bound*.

Lemma A.1 *Suppose* $f(\epsilon) = \tilde{\Theta}(g(\epsilon))$ *and* $h(\epsilon) = \tilde{\Theta}(j(\epsilon))$. *Then*

$$f(\epsilon) \cdot h(\epsilon) = \tilde{\Theta}(g(\epsilon) \cdot j(\epsilon)),$$

and

$$\frac{f(\epsilon)}{h(\epsilon)} = \tilde{\Theta}\left(\frac{g(\epsilon)}{j(\epsilon)}\right).$$

Proof. From the above definition, $f(\epsilon) = \tilde{\Theta}(g(\epsilon))$ means $f(\epsilon) = O(g(\epsilon).\epsilon^{-\delta})$ and $f(\epsilon) = \Omega(g(\epsilon).\epsilon^{\delta})$ while $h(\epsilon) = \tilde{\Theta}(j(\epsilon))$ means $h(\epsilon) = O(j(\epsilon).\epsilon^{-\delta})$ and $h(\epsilon) = \Omega(j(\epsilon).\epsilon^{\delta})$. For the upper bound, for all $\delta > 0$, there exist $c_1 > 0$, $c_2 > 0$, $\epsilon_1 > 0$, $\epsilon_2 > 0$ such that

$$\begin{aligned} f(\epsilon) &\leq c_1 \cdot \epsilon^{-\delta} \cdot g(\epsilon) \quad \text{for } \epsilon \leq \epsilon_1, \\ h(\epsilon) &\leq c_2 \cdot \epsilon^{-\delta} \cdot j(\epsilon) \quad \text{for } \epsilon \leq \epsilon_2. \end{aligned} \tag{A.1}$$

Let $\epsilon_0 = \max(\epsilon_1, \epsilon_2)$ and $c_0 = c_1 \cdot c_2$. Consider the product $f(\epsilon) \times h(\epsilon)$ for $\epsilon \leq \epsilon_0$:

$$\begin{aligned} f(\epsilon) \times h(\epsilon) &\leq c_1 \cdot \epsilon^{-\delta} \cdot g(\epsilon) \times c_2 \cdot \epsilon^{-\delta} \cdot j(\epsilon) \\ &\leq c_0(\epsilon^{-\delta} \cdot g(\epsilon) \times \epsilon^{-\delta} \cdot j(\epsilon)). \end{aligned} \tag{A.2}$$

Thus, $f(\epsilon) \cdot h(\epsilon) = O(\epsilon^{-\delta} \cdot g(\epsilon) \times \epsilon^{-\delta} \cdot j(\epsilon))$.

For the lower bound, for all $\delta > 0$, there exist $c_3 > 0$, $c_4 > 0$, $\epsilon_3 > 0$, $\epsilon_4 > 0$ such that

$$\begin{aligned} f(\epsilon) &\geq c_3 \cdot \epsilon^{\delta} \cdot g(\epsilon) \quad \text{for } \epsilon \leq \epsilon_3, \\ h(\epsilon) &\geq c_4 \cdot \epsilon^{\delta} \cdot j(\epsilon) \quad \text{for } \epsilon \leq \epsilon_4. \end{aligned} \tag{A.3}$$

Let $\epsilon_0 = \max(\epsilon_3, \epsilon_4)$ and $c_0 = c_3 \cdot c_4$. Consider the product $f(\epsilon) \times h(\epsilon)$ for $\epsilon \leq \epsilon_0$:

$$\begin{aligned} f(\epsilon) \times h(\epsilon) &\geq c_3 \cdot \epsilon^{\delta} \cdot g(\epsilon) \times c_4 \cdot \epsilon^{\delta} \cdot j(\epsilon) \\ &\geq c_0(\epsilon^{\delta} \cdot g(\epsilon) \times \epsilon^{\delta} \cdot j(\epsilon)). \end{aligned} \tag{A.4}$$

Thus, $f(\epsilon) \cdot h(\epsilon) = \Omega(\epsilon^{\delta} \cdot g(\epsilon) \times \epsilon^{\delta} \cdot j(\epsilon))$. Therefore, $f(\epsilon) \cdot h(\epsilon) = \tilde{\Theta}(g(\epsilon) \cdot j(\epsilon))$.

For the second part, for upper bound, from (A.1), $f(\epsilon)/h(\epsilon)$ can be both

$$\frac{f(\epsilon)}{h(\epsilon)} \leq \frac{c_1 \cdot \epsilon^{-\delta} \cdot g(\epsilon)}{c_2 \cdot \epsilon^{-\delta} \cdot j(\epsilon)},$$

or

$$\frac{f(\epsilon)}{h(\epsilon)} \geq \frac{c_1 \cdot \epsilon^{-\delta} \cdot g(\epsilon)}{c_2 \cdot \epsilon^{-\delta} \cdot j(\epsilon)},$$

since $\frac{1}{h(\epsilon)} \geq \frac{1}{c_2 \cdot \epsilon^{-\delta} \cdot j(\epsilon)}$. This means that $\frac{f(\epsilon)}{h(\epsilon)} = O\left(\frac{\epsilon^{-\delta} \cdot g(\epsilon)}{\epsilon^{-\delta)} \cdot j(\epsilon)}\right)$ or $\frac{f(\epsilon)}{h(\epsilon)} = \Omega\left(\frac{\epsilon^{-\delta} \cdot g(\epsilon)}{\epsilon^{-\delta} \cdot j(\epsilon)}\right)$. Similar things happen for lower bound where from (A.3), since $\frac{1}{h(\epsilon)} \geq \frac{1}{c_2 \cdot \epsilon^{-\delta} \cdot j(\epsilon)}$,

$$\frac{f(\epsilon)}{h(\epsilon)} \geq \frac{c_3 \cdot \epsilon^{\delta} \cdot g(\epsilon)}{c_4 \cdot \epsilon^{\delta} \cdot j(\epsilon)},$$

or

$$\frac{f(\epsilon)}{h(\epsilon)} \leq \frac{c_3 \cdot \epsilon^{\delta} \cdot g(\epsilon)}{c_4 \cdot \epsilon^{\delta} \cdot j(\epsilon)},$$

i.e., $\frac{f(\epsilon)}{h(\epsilon)} = \Omega\left(\frac{\epsilon^{\delta} \cdot g(\epsilon)}{\epsilon^{\delta} \cdot j(\epsilon)}\right)$ or $\frac{f(\epsilon)}{h(\epsilon)} = O\left(\frac{\epsilon^{\delta} \cdot g(\epsilon)}{\epsilon^{\delta} \cdot j(\epsilon)}\right)$. Therefore, it is proved that $\frac{f(\epsilon)}{h(\epsilon)} = \tilde{\Theta}\left(\frac{g(\epsilon)}{j(\epsilon)}\right)$. ■

B MATLAB codes for Chapter 4

Codes for Figure 4.6

```
%% plot basins for PWL map
%% black = basin B_0
%% orange = basin B_1

%% test for 3 cases: i) delta = 0.8, s = 0.49 (riddled, sigma>0 for almost all points)
%%                   ii) delta = 0.8, s = 0.51 (no basin)
%%                   iii) delta = 0.3, s = 0.49 (riddled,sigma<0 at some points)

clear all;
%% parameters
delta=0.8
s=0.49

%% number of iterations for every points to test whether in B_0
nits=10000;
xx=zeros(nits,2);

%% iterations
ntheta=500;
nx=500;

%% axis
thetamin=0;
thetamax=1;
xmin=0;
xmax=1;

%% To set the size of vector
yy=zeros(ntheta,nx);
ytheta=zeros(ntheta,nx);
yx=zeros(ntheta,nx);


for itheta=1:ntheta
```

```
    xx(1,1)=(thetamax-thetamin)*(itheta/ntheta)+thetamin;
    for ix=1:nx
        xx(1,2)=(xmax-xmin)*(ix/nx)+xmin;

        ytheta(itheta,ix)=xx(1,1);
            yx(itheta,ix)=xx(1,2);

        for i=2:nits
            theta=xx(i-1,1);
                x=xx(i-1,2);
            %% apply PWL map
            if x<1
                if theta<s
                    xx(i,1)=theta/s;
                    xx(i,2)=(1/delta)*x;
                else
                    xx(i,1)=(theta-s)/(1-s);
                    xx(i,2)=delta*x;
                end
            else
                xx(i,2)=1;
            end
        end
        yy(itheta,ix)=min(abs(x),1);
    end
end

%% create figure graphics objects
figure(1);
clf;

%% creates a pseudocolor plot with colors are determined by yy. The
    minimum and maximum of yy are assigned the first and last colors in
     the colormap. This is a two-dimensional plot.
pcolor(ytheta,yx,yy);

%% set color shading properties. Besides 'flat', can also use 'faceted'
     or 'interp'.
shading flat
%% label for x-axis and y-axis.
xlabel('\theta');
ylabel('x');

%% 'colormap' set the color for pcolor. 'copper' varies smoothly from
    black to bright copper, can also use other commands such as 'winter
    ', 'autumn', 'grey', etc.
%% if the last point gives value 0, then color black; if the value is
    1, then color orange
colormap copper;
```

```
%% to show color scale
%colorbar

hold on
y2=rectangle('position',[0.3,0.0,0.2,0.1],'EdgeColor','m');
plot(ytheta,y2);

keyboard;
```

Codes for Figure 4.7

```
%% stability index vs delta for PWL map

clear all;

%% parameter
s=0.49

%% periodic point, select random point between 0 and 1
thetaperiod =  0.9643

%% number of iterations for every points
nits=5000;

%% number of epsilon values used
np=20;

%% number and range of values for parameter scan in delta
ndelta=100;
deltamin=0.01;
deltamax=0.99;

%% number of points sampled in delta-neighbourhood of attractor
nii=10000;

%% Scans over range of parameter delta
for idelta=1:ndelta
    %% set value of parameter
    delta=(deltamax-deltamin)*(idelta-1)/(ndelta-1)+deltamin
    deltaval(idelta)=delta;

    xx=zeros(nits,2);
    pp=zeros(1,np);
    yp=zeros(1,np);

    %% scan through values of epsilon for fixed delta
    for id=1:np
        epsilon=10^(-id/5)
```

```
38          %% define neighbourhood of B_0
39          thetamin=thetaperiod-epsilon;
40          thetamax=thetaperiod+epsilon;
41          xmin=0;
42          xmax=epsilon;
43
44          %% number of points in the basin of attraction B_0
45          nb=0;
46
47          %xx(1,1)=0.48932792356723;
48          for ii=1:nii
49              xx(1,1)=(thetamax-thetamin)*rand+thetamin; %initial
50              xx(1,2)=(xmax-xmin)*rand+xmin; %initial
51
52              ytheta(ii)=xx(1,1);
53              yx(ii)=xx(1,2);
54              for i=2:nits
55                  %u=xx(i-1,1);
56                  theta=xx(i-1,1);
57                  x=xx(i-1,2);
58                  %% apply inverse map
59                  if x<1
60                      if theta<s
61                          xx(i,1)=theta/s;
62                          xx(i,2)=min((1/delta)*x,1);
63                      else
64                          xx(i,1)=(theta-s)/(1-s);
65                          xx(i,2)=delta*x;
66                      end
67                  else
68                      xx(i,2)=1;
69                  end
70              end
71              yy(ii)=min(abs(x),1);
72              if yy(ii)<1
73                  nb=nb+1;
74                  thetab(nb,1)=ytheta(ii);
75                  xb(nb,1)=yx(ii);
76              end
77          end
78          % dp(id) = the delta used
79          % yp(id) gives the proportion of the delta-nbhd in the basin
80          dp(id)=epsilon;
81          yp(id)=(nb)/(nii);
82
83          % get estimates for 95% CI using modified Wald method
84          temp=(nb+2)/(nii+4);
85          ypp(id)=temp;
86          ypu(id)=min(temp-1.96*sqrt((temp*(1-temp))/(nii+4)),1);
```

```
        ypl(id)=max(temp+1.96*sqrt((temp*(1-temp))/(nii+4)),0);
    end
    %% look at final approximation:
    % if it is zero or 1 then classify sigma
    if yp(np)==1
        sigma=Inf
    elseif yp(np)==0
        sigma=-Inf
    elseif yp(np)>0 & yp(np)<1
        %% yp increasing, so assume that yp->1 as delta->0
        % so that sigma_-=0; need to find sigma_+
        % yp2 is approximation for log(1-Sigma_delta)
        yp2=log(max(1-yp,1e-10));
        ldp=log(dp);
        figure(1);
        clf;
        [p,S]=polyfit(ldp,yp2,1)     % Degree 1 fit
        f=polyval(p,ldp);
        a=p(1);          %slope
        b=p(2);          %intercept
        % Plot the data and the fit.
        hdata=plot(ldp,yp2,'-m');
        hold on
        hbound=plot(ldp,log(1-ypu),'--m');
        plot(ldp,log(1-ypl),'--m');
        hold on
        hfit=plot(ldp,f,'b-');
        hold on
        % Add prediction intervals to the plot.
        [Y,DELTA] = polyval(p,ldp,S);
        hconf=plot(ldp,Y-DELTA,'b--');
        plot(ldp,Y+DELTA,'b--');
        approx_a=round(100*a)/100; % round for display
        %% label for x-axis and y-axis.
        xlabel('ln(\epsilon)');
        ylabel('ln(1-\Sigma_\epsilon)');
        legend([hdata,hbound,hfit,hconf],'yp','95% CI for yp','fit','
    95% CI for fit');
        title(['The slope for \delta= ',num2str(delta), ' is ',num2str(
    approx_a),'.']);
        sigma=a
    end
    sigval(idelta)=sigma
end
figure(2);
clf;
plot(deltaval,tanh(sigval));
xlabel('\delta');
ylabel('tanh(\sigma)');
```

C MATLAB codes for Chapter 5

Codes for Figure 5.2

```
%% plot for Figure 1 in Keller 2014
function attractor
ttrans=2000
tsteps=80000

u0=0.1
v0=0.765344
x0=0.00001;
%% if x0=0, it will give invariant set only since h(0)=0
%% if x0 negative, will give lower graph, symmetry

for i=1:ttrans
    [u1,v1,x1]=F(u0,v0,x0);
    u0=u1;
    v0=v1;
    x0=x1;
end

xx(1,1)=u0;
xx(1,2)=v0;
xx(1,3)=x0;
for i=1:tsteps
    [u1,v1,x1]=F(xx(i,1),xx(i,2),xx(i,3));
    xx(i+1,1)=u1;
    xx(i+1,2)=v1;
    xx(i+1,3)=x1;
end

% plot x vs. v
figure(1)
clf

% plot 2d
plot(xx(:,2),xx(:,3),'.','MarkerSize',3);
xlabel('v');
ylabel('x');
```

```
37
38 % plot 3d
39 figure(2)
40 clf
41 plot3(xx(:,1),xx(:,2),xx(:,3),'.','MarkerSize',3);
42 xlabel('u');
43 ylabel('v');
44 zlabel('x');
45
46 keyboard
47 return
48
49 function [u1,v1,x1]=F(u0,v0,x0)
50     beta=0.01
51     epsilon=0.01
52     s=0.45
53     r=2.5
54
55     if u0<s
56         u1=u0/s;
57         v1=v0*s;
58     else
59         u1=(u0-s)/(1-s);
60         v1=s+(1-s)*v0;
61     end
62     x1=r*(1+epsilon+cos(2*pi*v0))*atan(x0);
63 return
```

Codes for Figure 5.4

```
1 %% plot for basins for Keller's map
2 clear all;
3
4 %% parameters
5 epsilon=0.01
6 s=0.45
7 r=2.5
8
9 %% number of iterations for every points
10 nits=100;
11 xx=zeros(nits,3);
12
13 %% nv is for simulation and nx is for iterations
14 nv=500;
15 nx=500;
16 vmin=0;
17 vmax=1;
18 xmin=0;
```

```
xmax=8;

%% To set the size of vector
yy=zeros(nv,nx);
yv=zeros(nv,nx);
yx=zeros(nv,nx);

xx(1,1)=0.48932792356723;
for iv=1:nv
    xx(1,2)=(vmax-vmin)*(iv/nv)+vmin;
    for ix=1:nx
        xx(1,3)=(xmax-xmin)*(ix/nx)+xmin;
        yu(iv,ix)=xx(1,1);
        yv(iv,ix)=xx(1,2);
        yx(iv,ix)=xx(1,3);
        for i=2:nits
            u=xx(i-1,1);
            v=xx(i-1,2);
            x=xx(i-1,3);
            %% apply inverse map
            if v<s
                xx(i,1)=u*s;
                xx(i,2)=v/s;
                xa=x/(r*(1+epsilon+cos(2*pi*(v/s))));
                if xa<pi/2
                    xx(i,3)=tan(xa);
                else
                    xx(i,3)=Inf;
                end
            else
                xx(i,1)=s+(1-s)*u;
                xx(i,2)=(v-s)/(1-s);
                xa=x/(r*(1+epsilon+cos(2*pi*((v-s)/(1-s)))));
                if xa<pi/2
                    xx(i,3)=tan(xa);
                else
                    xx(i,3)=Inf;
                end
            end
        end
        yy(iv,ix)=min(abs(x),pi/2);
    end
end
%% create figure graphics objects
figure(1);
clf;

%% creates a pseudocolor plot with colors are determined by yy. The
   minimum and maximum of yy are assigned the first and last colors in
```

```
    the colormap. This is a two-dimensional plot.
pcolor(yv,yx,yy);
%% set color shading properties. Besides 'flat', can also use 'faceted'
    or 'interp'.
shading flat
%% label for x-axis and y-axis.
xlabel('v');
ylabel('x');

%% 'colormap' set the color for pcolor. 'copper' varies smoothly from
    black to bright copper, can also use other commands such as 'winter
    ', 'autumn', 'grey', etc.
%% if the last point gives value 0, then color black; if the value is
    1, then color orange
colormap copper;
%% to show color scale
%colorbar

%% stops execution of the file and gives control to the keyboard. To
    terminate the keyboard mode, type 'return' and then press Enter. To
     terminate the keyboard mode and exit the function, type 'dbquit'
    and then press Enter.
keyboard;
```

Codes for Figure 5.6

```
%% plot for basin using RNG
clear all;

%% parameters
epsilon=0.01
s=0.45
r=2.5

%% number of iterations for every points
nits=100;
xx=zeros(nits,3);

%% nii is number of points generated in [0,1]x[0,8]
nii=10000;
vmin=0;
vmax=1;
xmin=0;
xmax=8;

%% To set the size of vector
yy=zeros(nii,1);
yu=zeros(nii,1);
```

```
yv=zeros(nii,1);
yx=zeros(nii,1);
xb=zeros(1,1);
yb=zeros(1,1);
%% number of points in the basin of attraction in x=0
nb=0;

xx(1,1)=0.48932792356723;
for ii=1:nii
    xx(1,2)=(vmax-vmin)*rand+vmin;
        xx(1,3)=(xmax-xmin)*rand+xmin;
        yu(ii)=xx(1,1);
        yv(ii)=xx(1,2);
        yx(ii)=xx(1,3);
        for i=2:nits
            u=xx(i-1,1);
            v=xx(i-1,2);
            x=xx(i-1,3);
            %% apply inverse map
            if v<s
                xx(i,1)=u*s;
                xx(i,2)=v/s;
                xa=x/(r*(1+epsilon+cos(2*pi*(v/s))));
                if xa<pi/2
                    xx(i,3)=tan(xa);
                else
                    xx(i,3)=Inf;
                end
            else
                xx(i,1)=s+(1-s)*u;
                xx(i,2)=(v-s)/(1-s);
                xa=x/(r*(1+epsilon+cos(2*pi*((v-s)/(1-s)))));
                if xa<pi/2
                    xx(i,3)=tan(xa);
                else
                    xx(i,3)=Inf;
                end
            end
        end
        yy(ii)=min(abs(x),pi/2);
        if yy(ii)<pi/2
                nb=nb+1; % nb is number of points in basin x=0
                vb(nb,1)=yv(ii);
                xb(nb,1)=yx(ii);
            end
end
%% create figure graphics objects
figure(1);
clf;
```

```
72
73 hold on;
74 %% creates a pseudocolor plot with colors are determined by yy. The
       minimum and maximum of yy are assigned the first and last colors in
       the colormap. This is a two-dimensional plot.
75 plot(yv,yx,'.y'); %plot yellow points only (nii)
76 plot(vb,xb,'.b'); %plot blue points only (nb)
77
78 %% label for x-axis and y-axis.
79 xlabel('v');
80 ylabel('x');
81
82 %% stops execution of the file and gives control to the keyboard. To
       terminate the keyboard mode, type 'return' and then press Enter. To
       terminate the keyboard mode and exit the function, type 'dbquit'
       and then press Enter.
83 keyboard;
```

Codes for Figure 5.7

```
1 %% plot proportion of points in basin x=0 for various r
2 clear all;
3
4 %% parameters
5 epsilon=0.01
6 s=0.45
7
8 %% number of iterations for every points
9 nits=20;
10 xx=zeros(nits,3);
11
12 %% initial condition
13 % xx(1,1)=0.1;
14 % xx(1,2)=0.765344;
15 % xx(1,3)=0.00001;
16
17 %% number of parameter values to be used
18 nr=20;
19 rmin=0.2;
20 rmax=3.54;
21
22 pp=zeros(1,nr);
23 yp=zeros(1,nr);
24
25 %% nii is number of points generated in [0,1]x[0,8]
26 %nu=50;
27 nii=10000;
28 %umin=0;
```

```
%umax=1;
vmin=0;
vmax=1;
xmin=0;
xmax=8;

%% Scans over range of parameters
for ir=1:nr
    %% set value of parameter
    r=(rmax-rmin)*(ir/nr)+rmin

    %% To set the size of vector
    yy=zeros(nii);
    yu=zeros(nii);
    yv=zeros(nii);
    yx=zeros(nii);
    vb=zeros(1,1);
    xb=zeros(1,1);
    %% number of points in the basin of attraction in y=0
    nb=0;

    xx(1,1)=0.48932792356723;
    for ii=1:nii
        xx(1,2)=(vmax-vmin)*rand+vmin;
        xx(1,3)=(xmax-xmin)*rand+xmin;
        yu(ii)=xx(1,1);
        yv(ii)=xx(1,2);
        yx(ii)=xx(1,3);
        for i=2:nits
            u=xx(i-1,1);
            v=xx(i-1,2);
            x=xx(i-1,3);
            %% apply inverse map
            if v<s
                xx(i,1)=u*s;
                xx(i,2)=v/s;
                xa=x/(r*(1+epsilon+cos(2*pi*(v/s))));
                if xa<pi/2
                    xx(i,3)=tan(xa);
                else
                    xx(i,3)=Inf;
                end
            else
                xx(i,1)=s+(1-s)*u;
                xx(i,2)=(v-s)/(1-s);
                xa=x/(r*(1+epsilon+cos(2*pi*((v-s)/(1-s)))));
                if xa<pi/2
                    xx(i,3)=tan(xa);
                else
```

```
                    xx(i,3)=Inf;
                end
            end
        end
        yy(ii)=min(abs(x),pi/2);
        if yy(ii)<pi/2
            nb=nb+1;
            vb(nb,1)=yv(ii);
            xb(nb,1)=yx(ii);
        end
    end
    pp(ir)=r;
    % find proportion of image that is in basin of attraction x=0
    yp(ir)=(nb)/(nii);
end

%% create figure graphics objects
figure(1);
clf;

plot(pp,yp);
xlabel('r');
ylabel('\Sigma_\epsilon(v,0)');

%% stops execution of the file and gives control to the keyboard. To
    terminate the keyboard mode, type 'return' and then press Enter. To
     terminate the keyboard mode and exit the function, type 'dbquit'
    and then press Enter.
keyboard;
```

Codes for Figure 5.8

```
%% plot proportion of points in basin x=0 by varying epsilon
    neighbourhood
clear all;

%% parameters
epsilon=0.01
s=0.45
r=2.5

%% number of iterations for every points
nits=50;
xx=zeros(nits,3);
np=20;

nii=10000;
pp=zeros(1,np);
```

```
yp=zeros(1,np);

for id=1:np
    delta=10^(-id/5)
    %% define neighbourhood of y=0
    vmin=0.45-delta;
    vmax=0.45+delta;
    xmin=0;
    xmax=delta;

    %% number of points in the basin of attraction in y=0
    nb=0;

    %% To set the size of vector
    xb=zeros(1,1);
    yb=zeros(1,1);

    xx(1,1)=0.48932792356723;
    for ii=1:nii
        xx(1,2)=(vmax-vmin)*rand+vmin;
        xx(1,3)=(xmax-xmin)*rand+xmin;
        yu(ii)=xx(1,1);
        yv(ii)=xx(1,2);
        yx(ii)=xx(1,3);
        for i=2:nits
            u=xx(i-1,1);
            v=xx(i-1,2);
            x=xx(i-1,3);
            %% apply inverse map
            if v<s
                xx(i,1)=u*s;
                xx(i,2)=v/s;
                xa=x/(r*(1+epsilon+cos(2*pi*(v/s))));
                if xa<pi/2
                    xx(i,3)=tan(xa);
                else
                    xx(i,3)=Inf;
                end
            else
                xx(i,1)=s+(1-s)*u;
                xx(i,2)=(v-s)/(1-s);
                xa=x/(r*(1+epsilon+cos(2*pi*((v-s)/(1-s)))));
                if xa<pi/2
                    xx(i,3)=tan(xa);
                else
                    xx(i,3)=Inf;
                end
            end
        end
```

```
        yy(ii)=min(abs(x),pi/2);
        if yy(ii)<pi/2
            nb=nb+1;
            vb(nb,1)=yv(ii);
            xb(nb,1)=yx(ii);
        end
    end
    pp(id)=delta;
    yp(id)=nb/nii;
    ypp=(nb+2)/(nii+4);
    ypu(id)=min(ypp+1.96*(sqrt((ypp*(1-ypp))/nii)),1);
    ypl(id)=max(ypp-1.96*(sqrt((ypp*(1-ypp))/nii)),0);
end

%% create figure graphics objects
figure(1);
clf;

plot(pp,yp,pp,ypl,'--r',pp,ypu,'--r');
%% label for x-axis and y-axis.
xlabel('\epsilon');
ylabel('\Sigma_\epsilon');

%% stops execution of the file and gives control to the keyboard. To
    terminate the keyboard mode, type 'return' and then press Enter. To
     terminate the keyboard mode and exit the function, type 'dbquit'
    and then press Enter.
keyboard;
```

Codes for Figure 5.9(a)

```
%% plot for sigma_-
clear all;

%% parameters
epsilon=0.01
s=0.45
r=2.5

%% number of iterations for every points
nits=50;
xx=zeros(nits,3);
np=20;

nii=10000;
pp=zeros(1,np);
yp=zeros(1,np);

```

```
for id=1:np
    delta=10^(-id/5)
    %% define neighbourhood of x=0
    vmin=0.45-delta;
    vmax=0.45+delta;
    xmin=0;
    xmax=delta;

    %% number of points in the basin of attraction in x=0
    nb=0;
    xb=zeros(1,1);
    yb=zeros(1,1);

    xx(1,1)=0.48932792356723;
    for ii=1:nii
        xx(1,2)=(vmax-vmin)*rand+vmin;
        xx(1,3)=(xmax-xmin)*rand+xmin;
        yu(ii)=xx(1,1);
        yv(ii)=xx(1,2);
        yx(ii)=xx(1,3);
        for i=2:nits
            u=xx(i-1,1);
            v=xx(i-1,2);
            x=xx(i-1,3);
            %% apply inverse map
            if v<s
                xx(i,1)=u*s;
                xx(i,2)=v/s;
                xa=x/(r*(1+epsilon+cos(2*pi*(v/s))));
                if xa<pi/2
                    xx(i,3)=tan(xa);
                else
                    xx(i,3)=Inf;
                end
            else
                xx(i,1)=s+(1-s)*u;
                xx(i,2)=(v-s)/(1-s);
                xa=x/(r*(1+epsilon+cos(2*pi*((v-s)/(1-s)))));
                if xa<pi/2
                    xx(i,3)=tan(xa);
                else
                    xx(i,3)=Inf;
                end
            end
        end
        yy(ii)=min(abs(x),pi/2);
        if yy(ii)<pi/2
            nb=nb+1;
            vb(nb,1)=yv(ii);
```

```
            xb(nb,1)=yx(ii);
        end
    end
    pp(id)=log(delta);
    yp(id)=log(nb/nii);
    ypp=(nb+2)/(nii+4);
    ypu(id)=min(ypp+1.96*(sqrt((ypp*(1-ypp))/nii)),1);
    ypl(id)=max(ypp-1.96*(sqrt((ypp*(1-ypp))/nii)),0);
end

%% create figure graphics objects
figure(1);
clf;
plot(pp,yp,pp,log(ypl),'--r',pp,log(ypu),'--r');
%% label for x-axis and y-axis.
xlabel('log(\epsilon)');
ylabel('log(\Sigma_\epsilon)');

%% stops execution of the file and gives control to the keyboard. To
    terminate the keyboard mode, type 'return' and then press Enter. To
     terminate the keyboard mode and exit the function, type 'dbquit'
    and then press Enter.
keyboard;
```

Codes for Figure 5.9(b)

```
%% plot for sigma_+
clear all;

%% parameters
epsilon=0.01
s=0.45
r=2.5

%% number of iterations for every points
nits=50;
xx=zeros(nits,3);
np=20;

nii=10000;
pp=zeros(1,np);
yp=zeros(1,np);

for id=1:np
    delta=10^(-id/5)
    %% define neighbourhood of x=0
    vmin=0.45-delta;
    vmax=0.45+delta;
```

```
    xmin=0;
    xmax=delta;

    %% number of points in the basin of attraction in x=0
    nb=0;
    xb=zeros(1,1);
    yb=zeros(1,1);

    xx(1,1)=0.48932792356723;
    for ii=1:nii
        xx(1,2)=(vmax-vmin)*rand+vmin;
        xx(1,3)=(xmax-xmin)*rand+xmin;
        yu(ii)=xx(1,1);
        yv(ii)=xx(1,2);
        yx(ii)=xx(1,3);
        for i=2:nits
            u=xx(i-1,1);
            v=xx(i-1,2);
            x=xx(i-1,3);
            %% apply inverse map
            if v<s
                xx(i,1)=u*s;
                xx(i,2)=v/s;
                xa=x/(r*(1+epsilon+cos(2*pi*(v/s))));
                if xa<pi/2
                    xx(i,3)=tan(xa);
                else
                    xx(i,3)=Inf;
                end
            else
                xx(i,1)=s+(1-s)*u;
                xx(i,2)=(v-s)/(1-s);
                xa=x/(r*(1+epsilon+cos(2*pi*((v-s)/(1-s)))));
                if xa<pi/2
                    xx(i,3)=tan(xa);
                else
                    xx(i,3)=Inf;
                end
            end
        end
        yy(ii)=min(abs(x),pi/2);
        if yy(ii)<pi/2
            nb=nb+1;
            vb(nb,1)=yv(ii);
            xb(nb,1)=yx(ii);
        end
    end
    pp(id)=log(delta);
    yp(id)=log(1-nb/nii);
```

```
    ypp=(nb+2)/(nii+4);
    ypu(id)=min(ypp+1.96*(sqrt((ypp*(1-ypp))/nii)),1);
    ypl(id)=max(ypp-1.96*(sqrt((ypp*(1-ypp))/nii)),0);
end

%% create figure graphics objects
figure(1);
clf;
plot(pp,yp,pp,log(1-ypl),'--r',pp,log(1-ypu),'--r');
%% label for x-axis and y-axis.
xlabel('log(\epsilon)');
ylabel('log(1-\Sigma_\epsilon)');

%% stops execution of the file and gives control to the keyboard. To
   terminate the keyboard mode, type 'return' and then press Enter. To
    terminate the keyboard mode and exit the function, type 'dbquit'
   and then press Enter.
keyboard;
```

Codes for Figure 5.10

```
%% plot stability index vs parameter r
clear all;

%% parameters for Keller's map (arXiv)
epsilon=0.01
s=0.45

%% periodic point, before this we use v=0.45
vperiod = 0.7927

%% number of iterations for every points
nits=5000;

%% number of delta values used
np=20;

%% initial conditions
% xx(1,1)=0.1;
% xx(1,2)=0.765344;
% xx(1,3)=0.00001;

%% number and range of values for parameter scan in r
nr=100;
rmin=0.0;
rmax=5.0;

%% number of points sampled in delta-neighbourhood of attractor
```

```
nii=10000;

%% Scans over range of parameter r
for ir=1:nr
    %% set value of parameter
    r=(rmax-rmin)*(ir-1)/(nr-1)+rmin
    rval(ir)=r;

    xx=zeros(nits,3);
    pp=zeros(1,np);
    yp=zeros(1,np);

    %% scan through values of delta for fixed r
    for id=1:np
        delta=10^(-id/5)
        %% define neighbourhood of y=0
        vmin=vperiod-delta;
        vmax=vperiod+delta;
        xmin=0;
        xmax=delta;

        %% number of points in the basin of attraction in y=0
        nb=0;

        xx(1,1)=0.48932792356723;
        for ii=1:nii
            xx(1,2)=(vmax-vmin)*rand+vmin;
            xx(1,3)=(xmax-xmin)*rand+xmin;
            yu(ii)=xx(1,1);
            yv(ii)=xx(1,2);
            yx(ii)=xx(1,3);
            for i=2:nits
                u=xx(i-1,1);
                v=xx(i-1,2);
                x=xx(i-1,3);
                %% apply inverse map
                if v<s
                    xx(i,1)=u*s;
                    xx(i,2)=v/s;
                    xa=x/(r*(1+epsilon+cos(2*pi*(v/s))));
                    if xa<pi/2
                        xx(i,3)=tan(xa);
                    else
                        xx(i,3)=Inf;
                    end
                else
                    xx(i,1)=s+(1-s)*u;
                    xx(i,2)=(v-s)/(1-s);
                    xa=x/(r*(1+epsilon+cos(2*pi*((v-s)/(1-s)))));
```

```
                    if xa<pi/2
                        xx(i,3)=tan(xa);
                    else
                        xx(i,3)=Inf;
                    end
                end
            end
            yy(ii)=min(abs(x),pi/2);
            if yy(ii)<pi/2
                nb=nb+1;
                vb(nb,1)=yv(ii);
                xb(nb,1)=yx(ii);
            end
        end
        % dp(id) = the delta used
        % yp(id) gives the proportion of the delta-nbhd in the basin x
    =0
        dp(id)=delta;
        yp(id)=(nb)/(nii);

        % get estimates for 95% CI using modified Wald method
        temp=(nb+2)/(nii+4);
        ypp(id)=temp;
        ypu(id)=min(temp-1.96*sqrt((temp*(1-temp))/(nii+4)),1);
        ypl(id)=max(temp+1.96*sqrt((temp*(1-temp))/(nii+4)),0);
    end
    %% look at final approximation:
    % if it is zero or 1 then classify sigma
    if yp(np)==1
        sigma=Inf
    elseif yp(np)==0
        sigma=-Inf
    elseif yp(np)>0 & yp(np)<1
        %% yp increasing, so assume that yp->1 as delta->0
        % so that sigma_-=0; need to find sigma_+
        % yp2 is approximation for log(1-Sigma_delta)
        yp2=log(max(1-yp,1e-10));
        ldp=log(dp);
        figure(1);
        clf;
        [p,S]=polyfit(ldp,yp2,1)     % Degree 1 fit
        f=polyval(p,ldp);
        a=p(1);          %slope
        b=p(2);          %intercept
        % Plot the data and the fit.
        hdata=plot(ldp,yp2,'-m');
        hold on
        hbound=plot(ldp,log(1-ypu),'--m');
        plot(ldp,log(1-ypl),'--m');
```

```
125         hold on
126         hfit=plot(ldp,f,'b-');
127         hold on
128         % Add prediction intervals to the plot.
129         [Y,DELTA] = polyval(p,ldp,S);
130         hconf=plot(ldp,Y-DELTA,'b--');
131         plot(ldp,Y+DELTA,'b--');
132         approx_a=round(100*a)/100; % round for display
133         %% label for x-axis and y-axis.
134         xlabel('ln(\delta)');
135         ylabel('ln(1-\Sigma_\delta)');
136         legend([hdata,hbound,hfit,hconf],'yp','95% CI for yp','fit','
    95% CI for fit');
137         title(['The slope for r= ',num2str(r), ' is ',num2str(approx_a)
    ,'.']);
138         sigma=a
139     end
140     sigval(ir)=sigma
141 end
142 figure(2);
143 clf;
144 plot(rval,tanh(sigval));
145 xlabel('r');
146 ylabel('tanh(\sigma)');
```

D Maple codes for Chapter 6

Codes for Figure 6.2

Programme for periodic points

$> restart : with(plots) :$

$> stair := v- > ([v, v], [v, g(v)]);$

$> staircase := proc(v0, a, b, n)$
$local v, count, Curves, Staircase, Dots;$
$uses\ \ plots;$
$Curves := plot([v, g(v)], v = a..b, colour = [red, blue], discont = true);$
$v[0] := v0;$
$for\ \ count\ \ from\ \ 1\ \ to\ \ n-1\ \ do$
$v[count] := g(v[count-1])$
$end\ \ do;$
$Staircase := plot([seq(stair(v[j]), j = 0..n-1)], colour = black);$
$Dots := plot([[v[0], v[0]]]),$
$plot([[v[n-1], g(v[n-1])]]);$
$display([Curves, Staircase, Dots]);$
$end\ \ proc;$

Period 2 orbit 01

$> g := v- > piecewise(v < s, (v)/(s), v > s, (v-s)/((1-s))) :$
$s := 0.45 :$
$staircase(0.26910299, 0, 1, 3);$

Period 3 orbit 001

$> g := v- > piecewise(v < s, (v)/(s), v > s, (v-s)/((1-s))) :$
$s := 0.45 :$
$staircase(0.10255, 0, 1, 4);$

Period 4 orbit 0001

$> g := v- > piecewise(v < s, (v)/(s), v > s, (v-s)/((1-s))) :$
$s := 0.45 :$
$staircase(0.04317, 0, 1, 5);$

Period 6 orbit 001100

$> g := v- > piecewise(v < s, (v)/(s), v > s, (v-s)/((1-s))) :$
$s := 0.45 :$
$staircase(0.1430177987, 0, 1, 7);$

Codes for Figure 6.5

Plot for averages for periodic points over parameter ν.

$> restart(); with(combinat, cartprod); with(plots) :$

$> epsilon := 0.01; s := 45/(100);$

$> g := v- > r * (1 + epsilon + cos(2 * Pi * v))$

$> g(v)$

$> G := v- > log(g(v))$

$> G(v)$

$> f[0] := v- > v/(s)$

$> f[1] := v- > (v-s)/((1-s))$

$> N := 10; r := 2.5;$

$> Aveac := int(G(v), v = 0..1);$ %% find average for $G(v)$

$> CL := \{\};$

$> Ave := [\ ] : BigG := [\ ] :$
$for\ n\ from\ 1\ to\ N\ do;$
$T := cartprod([[0, 1]\$n]);$
$while\ not\ T[finished]\ do;$
$C := T[nextvalue]();$
$ff[1] := f[C[1]] :$
$for\ k\ from\ 2\ to\ n\ do :$
$ff[k] := f[C[k]]@ff[k-1] :$
$end\ do :$

$fff := fsolve(ff[n](v) = v, v) :$
$ffff := (G(fff) + \sum_{i=1}^{n-1} G((ff[i])(fff)))/(n) :$
$Ave := [op(Ave), evalf(ffff)\$n] :$
$for\ m\ from\ 1\ to\ n\ do :$
$BigG := [op(BigG), ff[m](fff)] :$
$end\ do :)$
$end\ do :)$
$end\ do :)$
$p3 := pointplot(BigG, Ave, axes = boxed, color = "Red", labels = [v, averageoflogg],$
$labeldirections = ["horizontal", "vertical"], title = "N = 10") :$
$p4 := plot([[0., Aveac], [1.0, Aveac]]) :$
$display([p3, p4]);$

E MATLAB codes for Chapter 7

Codes for Figure 7.2

```
%% plot for trajectories for a planar map with a riddled basin
clear all;

%% parameters for Fig 1 from Ashwin Buescu Stewart 1996
alpha=0.7
epsilon=0.5
nu=0.9

%% number of iterations for every points
nits=200;
xx=zeros(nits,2);

%% initial condition
xx(1,1)=0.4;
xx(1,2)=0.20001;

%% nx is for simulation and ny is for iterations
nx=1000;
ny=1000;
xmin=-1.5;
xmax=1.5;
ymin=-1.5;
ymax=1.5;

%% To set the size of vector
yy=zeros(nx,ny);
yx1=zeros(nx,ny);
yx2=zeros(nx,ny);

%% 3.0 is (xmax-xmin) and -1.5 is xmin. 2.2 is (ymax-ymin) and -1.1 is
   ymin. Therefore the range of axis is : [-1.5 1.5 -1.1 1.1]
for ix=1:nx
    xx(1,1)=(xmax-xmin)*(ix/nx)+xmin;
    for iy=1:ny
        xx(1,2)=(ymax-ymin)*(iy/ny)+ymin;
        yx1(ix,iy)=xx(1,1);
```

```
        yx2(ix,iy)=xx(1,2);
        for i=2:nits
            x1=xx(i-1,1);
            x2=xx(i-1,2);
            %% equation for f(x_1,x_2)
            xx(i,1)=2.5981*x1*(x1^2-1)+epsilon*x1*x2^2;
            xx(i,2)=nu*exp(-alpha*x1^2)*x2+x2^3;
        end
        %% yy gives the values between 0 and 1
        yy(ix,iy)=min(abs(x2),1.0);
    end
end

%% create figure graphics objects
figure(1);
clf;

%% creates a pseudocolor plot with colors are determined by yy. The minimum and maximum of yy are assigned the first and last colors in the colormap. This is a two-dimensional plot.
pcolor(yx1,yx2,yy);
%% set color shading properties. Besides 'flat', can also use 'faceted' or 'interp'.
shading flat
%% label for x-axis and y-axis.
xlabel('x_1');
ylabel('x_2');
%% 'colormap' set the color for pcolor. 'copper' varies smoothly from black to bright copper, can also use other commands such as 'winter', 'autumn', 'grey', etc.
%% if the last point gives value 0, then color black; if the value is 1, then color orange
colormap copper;
%% to show color scale
%colorbar

%% stops execution of the file and gives control to the keyboard. To terminate the keyboard mode, type 'return' and then press Enter. To terminate the keyboard mode and exit the function, type 'dbquit' and then press Enter.
keyboard;
```

Codes for Figure 7.3

```
%% plot random basin using random number generator (RNG)
clear all;

%% parameters for Fig 1(c) from Ashwin Buescu Stewart 1996
```

```
alpha=0.7
epsilon=0.5
nu=0.9

%% number of iterations for every points
nits=40;
xx=zeros(nits,2);

%% initial condition
% xx(1,1)=0.4;
% xx(1,2)=0.20001;

%% nii is number of points generated in [-1.5,1.5]x[-1.5,1.5]
nii=10000;
xmin=-1.5;
xmax=1.5;
ymin=-1.5;
ymax=1.5;

%% To set the size of vector
yy=zeros(nii,1);
yx1=zeros(nii,1);
yx2=zeros(nii,1);
xb=zeros(1,1);
yb=zeros(1,1);
%% number of points in the basin of attraction in y=0
nb=0;

%% 3.0 is (xmax-xmin) and -1.5 is xmin. 2.2 is (ymax-ymin) and -1.1 is
    ymin. Therefore the range of axis is : [-1.5 1.5 -1.1 1.1]
for ii=1:nii
        %% random number between xmin & xmax
        xx(1,1)=(xmax-xmin)*rand+xmin;
        %% random number between ymin & ymax
        xx(1,2)=(ymax-ymin)*rand+ymin;
        yx1(ii)=xx(1,1);
        yx2(ii)=xx(1,2);
             for i=2:nits
                 x1=xx(i-1,1);
                 x2=xx(i-1,2);
                 %% equation for f(x_1,x_2)
                 xx(i,1)=2.5981*x1*(x1^2-1)+epsilon*x1*x2^2;
                 xx(i,2)=nu*exp(-alpha*x1^2)*x2+x2^3;
             end
             %% yy gives the values between 0 and 1
             yy(ii)=min(abs(x2),1.0);
             if yy(ii)<1.0
                 nb=nb+1;
                 xb(nb,1)=yx1(ii);
```

```
                yb(nb,1)=yx2(ii);
            end
    end

%% create figure graphics objects
figure(1);
clf;

hold on;

%% creates a pseudocolor plot with colors are determined by yy. The
    minimum and maximum of yy are assigned the first and last colors in
     the colormap. This is a two-dimensional plot.
plot(yx1,yx2,'.y');
plot(xb,yb,'.b');

%% set color shading properties. Besides 'flat', can also use 'faceted'
     or 'interp'.
shading flat
%% label for x-axis and y-axis.
xlabel('x_1');
ylabel('x_2');

%% stops execution of the file and gives control to the keyboard. To
    terminate the keyboard mode, type 'return' and then press Enter. To
     terminate the keyboard mode and exit the function, type 'dbquit'
    and then press Enter.
keyboard;
```

Codes for Figure 7.4

```
%% plot for the proportion over nu
%% use random number generator
%% use nii instead of nx*ny (without grid)
clear all;

%% parameters for Fig 1 from Ashwin Buescu Stewart 1996
alpha=0.7
epsilon=0.5

%% number of iterations for every points
nits=20;
xx=zeros(nits,2);

%% initial condition
% xx(1,1)=0.4;
% xx(1,2)=0.20001;

```

```
%% number of parameter values to be used
np=20;
pmin=0.9;
pmax=1.8;

pp=zeros(1,np);
yp=zeros(1,np);

%% approximate the region in phase space using nii without gridpoints
nii=2500;
xmin=-1.5;
xmax=1.5;
ymin=-1.5;
ymax=1.5;

%% Scans over range of parameters
for ip=1:np
    %% set value of parameter
    nu=(pmax-pmin)*(ip/np)+pmin

    %% To set the size of vector
    yy=zeros(nii);
    yx1=zeros(nii);
    yx2=zeros(nii);

    %% Scans over range [xmin,max]x[ymin,ymax]
    for ii=1:nii
        %% random number between xmin & xmax
        xx(1,1)=(xmax-xmin)*(rand(1))+xmin;
        %% random number between ymin & ymax
        xx(1,2)=(ymax-ymin)*(rand(1))+ymin;
        yx1(ii)=xx(1,1);
        yx2(ii)=xx(1,2);
            for i=2:nits
                x1=xx(i-1,1);
                x2=xx(i-1,2);
                %% equation for f(x_1,x_2)
                xx(i,1)=2.5981*x1*(x1^2-1)+epsilon*x1*x2^2;
                xx(i,2)=nu*exp(-alpha*x1^2)*x2+x2^3;
            end
            %% yy gives the values between 0 and 1
            yy(ii)=min(abs(x2),1.0);
    end
    pp(ip)=nu;
    % find proportion of image that is in basin of attraction
    yp(ip)=1-sum(sum(yy==1.0))/(nii);

end
%% plot proportion in basin of attraction of y=0 vs parameter
```

```
plot(pp,yp,'b');
xlabel('\nu');
ylabel('\Sigma_\epsilon(A)');
legend('nits=20','nits=30','nits=60','nits=100','nits=400');
```

Codes for Figure 7.6

```
%% plot proportion Sigma over epsilon-neighbourhood
clear all;

%% parameters for Fig 1 from Ashwin Buescu Stewart 1996
alpha=0.7
epsilon=0.5
nu=0.9
np=20

%% number of iterations for every points
nits=300;
xx=zeros(nits,2);

%% nii is number of points generated in [-1.5,1.5]x[-1.5,1.5]
nii=10000;
pp=zeros(1,np);
yp=zeros(1,np);

for id=1:np
    delta=10^(-id/5)
    xmin=-1-delta;
    xmax=1+delta;
    ymin=-delta;
    ymax=delta;

%% To set the size of vector
xb=zeros(1,1);
yb=zeros(1,1);
%% number of points in the basin of attraction in y=0
nb=0;

%% 3.0 is (xmax-xmin) and -1.5 is xmin. 2.2 is (ymax-ymin) and -1.1 is
   ymin. Therefore the range of axis is : [-1.5 1.5 -1.1 1.1]
for ii=1:nii
        %% random number between xmin & xmax
        xx(1,1)=(xmax-xmin)*rand+xmin;
        %% random number between ymin & ymax
        xx(1,2)=(ymax-ymin)*rand+ymin;
        yx1(ii)=xx(1,1);
        yx2(ii)=xx(1,2);
            for i=2:nits
```

```
                    x1=xx(i-1,1);
                    x2=xx(i-1,2);
                    %% equation for f(x_1,x_2)
                     xx(i,1)=2.5981*x1*(x1^2-1)+epsilon*x1*x2^2;
                     xx(i,2)=nu*exp(-alpha*x1^2)*x2+x2^3;
                end
                %% yy gives the values between 0 and 1
                yy(ii)=min(abs(x2),1.0);
                if yy(ii)<1.0
                    nb=nb+1;
                    xb(nb,1)=yx1(ii);
                    yb(nb,1)=yx2(ii);
                end
    end
pp(id)=delta;
ymax=0.1;
yp(id)=sum(sum(yy<ymax))/(nii);
    % for modified Wald eqn
    ypp=(sum(sum(yy<ymax))+2)/(nii+4);
    ypu(id)=min(ypp+1.96*(sqrt((ypp*(1-ypp))/nii)),1);
    ypl(id)=max(ypp-1.96*(sqrt((ypp*(1-ypp))/nii)),0);
end

%% plot Sigma_epsilon vs epsilon with CI using modified wald equation
plot(pp,yp,pp,ypl,'--r',pp,ypu,'--r');

%% label for x-axis and y-axis.
xlabel('\epsilon');
ylabel('\Sigma_\epsilon(A)');
```

Codes for Figure 7.7

```
%% plot for sigma_-
clear all;

%% parameters for Fig 1 from Ashwin Buescu Stewart 1996
alpha=0.7
epsilon=0.5
nu=0.9
np=20

%% number of iterations for every points
nits=300;
xx=zeros(nits,2);

%% nii is number of points generated in [-1.5,1.5]x[-1.5,1.5]
nii=10000;
pp=zeros(1,np);
```

```
yp=zeros(1,np);

%% scan over delta
for id=1:np
    delta=10^(-id/5)
    xmin=-1-delta;
    xmax=1+delta;
    ymin=-delta;
    ymax=delta;

%% To set the size of vector
xb=zeros(1,1);
yb=zeros(1,1);

%% number of points in the basin of attraction in y=0
nb=0;

%% 3.0 is (xmax-xmin) and -1.5 is xmin. 2.2 is (ymax-ymin) and -1.1 is
   ymin. Therefore the range of axis is : [-1.5 1.5 -1.1 1.1]
for ii=1:nii
        %% random number between xmin & xmax
        xx(1,1)=(xmax-xmin)*rand+xmin;
        %% random number between ymin & ymax
        xx(1,2)=(ymax-ymin)*rand+ymin;
        yx1(ii)=xx(1,1);
        yx2(ii)=xx(1,2);
            for i=2:nits
                x1=xx(i-1,1);
                x2=xx(i-1,2);
                %% equation for f(x_1,x_2)
                xx(i,1)=2.5981*x1*(x1^2-1)+epsilon*x1*x2^2;
                xx(i,2)=nu*exp(-alpha*x1^2)*x2+x2^3;
            end
            %% yy gives the values between 0 and 1
            yy(ii)=min(abs(x2),1.0);
            if yy(ii)<1.0
                nb=nb+1;
                xb(nb,1)=yx1(ii);
                yb(nb,1)=yx2(ii);
            end
    end
pp(id)=log(delta);
temp(id)=nii-sum(sum(yy==1.0));
yp(id)=log((temp(id))/(nii));
ypp=(temp(id)+2)/(nii+4);
ypu(id)=min(ypp+1.96*(sqrt((ypp*(1-ypp))/nii)),1);
ypl(id)=max(ypp-1.96*(sqrt((ypp*(1-ypp))/nii)),0);
end

```

```
figure(1);

%% plot with CI for log(Sigma_delta) vs log(delta)
plot(pp,yp,pp,log(ypl),'--r',pp,log(ypu),'--r');

%% label for x-axis and y-axis.
xlabel('log(\epsilon)');
ylabel('log(\Sigma_\epsilon(A)');
```

Codes for Figure 7.8

```
%% plot for sigma_+
clear all;

%% parameters for Fig 1 from Ashwin Buescu Stewart 1996
alpha=0.7
epsilon=0.5
nu=1.48
np=20

%% number of iterations for every points
nits=300;
xx=zeros(nits,2);

%% nii is number of points generated in [-1.5,1.5]x[-1.5,1.5]
nii=10000;
pp=zeros(1,np);
yp=zeros(1,np);

for id=1:np
    delta=10^(-id/5)
    xmin=-1-delta;
    xmax=1+delta;
    ymin=-delta;
    ymax=delta;

%% To set the size of vector
xb=zeros(1,1);
yb=zeros(1,1);

%% number of points in the basin of attraction in y=0
nb=0;

%% 3.0 is (xmax-xmin) and -1.5 is xmin. 2.2 is (ymax-ymin) and -1.1 is
   ymin. Therefore the range of axis is : [-1.5 1.5 -1.1 1.1]
for ii=1:nii
        %% random number between xmin & xmax
        xx(1,1)=(xmax-xmin)*rand+xmin;
```

```
        %% random number between ymin & ymax
        xx(1,2)=(ymax-ymin)*rand+ymin;
        yx1(ii)=xx(1,1);
        yx2(ii)=xx(1,2);
            for i=2:nits
                x1=xx(i-1,1);
                x2=xx(i-1,2);
                %% equation for f(x_1,x_2)
                xx(i,1)=2.5981*x1*(x1^2-1)+epsilon*x1*x2^2;
                xx(i,2)=nu*exp(-alpha*x1^2)*x2+x2^3;
            end
            %% yy gives the values between 0 and 1
            yy(ii)=min(abs(x2),1.0);
            if yy(ii)<1.0
                nb=nb+1;
                xb(nb,1)=yx1(ii);
                yb(nb,1)=yx2(ii);
            end
    end
pp(id)=log(delta);
temp(id)=nii-sum(sum(yy==1.0));
yp(id)=log(1-(temp(id))/(nii));
ypp=(temp(id)+2)/(nii+4);
ypu(id)=min(ypp+1.96*(sqrt((ypp*(1-ypp))/nii)),1);
ypl(id)=max(ypp-1.96*(sqrt((ypp*(1-ypp))/nii)),0);
end

figure(1);

%% plot with CI for log(1-Sigma_delta) vs log(delta)
plot(pp,yp,pp,log(1-ypl),'--r',pp,log(1-ypu),'--r');

%% label for x-axis and y-axis.
xlabel('log(\epsilon)');
ylabel('log(1-\Sigma_\epsilon(A)');
```

Codes for Figure 7.9

```
%% Calculates stability index versus nu for attractor [-1,1]x{0}
clear all;

%% parameters for Fig 1 from Ashwin Buescu Stewart 1996
alpha=0.7
epsilon=0.5

%% number and range of values for parameter scan in nu
nn=41
numin=0
```

```
numax=1.6

%% number of iterations to test whether in basin of y=0 attractor
nits=10000;

%% number of delta values used
np=10

%% number of points sampled in delta-neighbourhood of attractor
nii=50000;

%% scan through values of nu
for in=1:nn
    nu=(numax-numin)*(in-1)/(nn-1)+numin
    nuval(in)=nu;

    xx=zeros(nits,2);
    pp=zeros(1,np);
    yp=zeros(1,np);

    %% scan through values of delta for fixed nu
    for id=1:np
        delta=10^(-id/5)
        %% define neighbourhood of y=0
        xmin=-1-delta;
        xmax=1+delta;
        ymin=-delta;
        ymax=delta;

        %% number of points in the basin of attraction in y=0
        nb=0;

        %% sample points in (rectangular) neighbourhood of attractor
        for ii=1:nii
            %% random number between xmin & xmax
            x=(xmax-xmin)*rand+xmin;
            %% random number between ymin & ymax
            y=(ymax-ymin)*rand+ymin;
            %% test if point is in basin of attraction of y=0
            for i=2:nits
                x1=x;
                y1=y;
                %% equation for f(x_1,x_2)
                x=2.5981*x1*(x1^2-1)+epsilon*x1*y1^2;
                y=nu*exp(-alpha*x1^2)*y1+y1^3;
            end
            %% yy(ii) gives the values between 0 and 1
            yy(ii)=min(y,1.0);
            %% if yy(ii)<1 then assume in basin of y=0
```

```
            if yy(ii)<1.0
                nb=nb+1;
            end
        end
        % dp(id) = the delta used
        % yp(id) gives the proportion of the delta-nbhd in the basin
        dp(id)=delta;
        yp(id)=(nb)/(nii);

        % get estimates for 95% CI using modified Wald method
        temp=(nb+2)/(nii+4);
        ypp(id)=temp;
        ypu(id)=min(temp-1.96*sqrt((temp*(1-temp))/(nii+4)),1);
        ypl(id)=max(temp+1.96*sqrt((temp*(1-temp))/(nii+4)),0);
    end
    %% look at final approximation:
    % if it is zero or 1 then classify sigma
    if yp(np)==1
        sigma=Inf
    elseif yp(np)==0
        sigma=-Inf
    elseif yp(np)>0 & yp(np)<1
        %% yp increasing, so assume that yp->1 as delta->0
        % so that sigma_-=0; need to find sigma_+
        % yp2 is approximation for log(1-Sigma_delta)
        yp2=log(max(1-yp,1e-10));
        ldp=log(dp);
        figure(1);
        clf;
        [p,S]=polyfit(ldp,yp2,1)     % Degree 1 fit
        f=polyval(p,ldp);
        a=p(1);          %slope
        b=p(2);          %intercept
        % Plot the data and the fit.
        hdata=plot(ldp,yp2,'-m');
        hold on
        hbound=plot(ldp,log(1-ypu),'--m');
        plot(ldp,log(1-ypl),'--m');
        hold on
        hfit=plot(ldp,f,'b-');
        hold on
        % Add prediction intervals to the plot.
        [Y,DELTA] = polyval(p,ldp,S);
        hconf=plot(ldp,Y-DELTA,'b--');
        plot(ldp,Y+DELTA,'b--');
        approx_a=round(100*a)/100; % round for display
        %% label for x-axis and y-axis.
        xlabel('ln(\delta)');
        ylabel('ln(1-\Sigma_\delta)');
```

```
109         legend([hdata,hbound,hfit,hconf],'yp','95% CI for yp','fit','
    95% CI for fit');
110         title(['The slope for \nu= ',num2str(nu), ' is ',num2str(
    approx_a),'.']);
111         sigma=a
112     end
113     sigval(in)=sigma
114 end
115 
116 figure(2);
117 clf;
118 plot(nuval,tanh(sigval));
119 
120 xlabel('\nu');
121 ylabel('tanh(\sigma)');
```

Bibliography

[1] J.C. Alexander, J.A. Yorke, Z. You, and I. Kan. Riddled basin. *International Journal of Bifurcation and Chaos*, 2:795–813, 1992.

[2] L. Alsedá and M. Misiurewicz. Skew product attractors and concavity. *Proceedings of the American Mathematical Society*, 143(2):703–716, 2014.

[3] P. Ashwin. Chaotic intermittency of patterns in symmetric systems. *In: Golubitsky, M., Luss, D. and Strogatz, S.H., Pattern Formation in Continuous and Coupled Systems: A Survey Volume, Springer-Verlag New York Inc.*, 1999.

[4] P. Ashwin. Minimal attractors and bifurcations of random dynamical systems. *Proceedings: Mathematical, Physical and Engineering Sciences*, 455(1987):2615–2634, 1999.

[5] P. Ashwin. Riddled basins and coupled dynamical systems. *Lecture Notes in Physics, In: Chazottes, J.-R. and Fernandez, B., Dynamics of Coupled Map Lattices and of Related Spatially Extended Systems, Springer-Verlag Berlin Heidelberg*, 671(1987):181–207, 2005.

[6] P. Ashwin, J. Buescu, and I. Stewart. Bubbling of attractors and synchronization of chaotic oscillators. *Physics Letters A*, 193:126–139, 1994.

[7] P. Ashwin, J. Buescu, and I. Stewart. From attractor to chaotic saddle: a tale of transverse instability. *Nonlinearity*, 9:703–737, 1996.

[8] P. Ashwin and J.R. Terry. On riddling and weak attractors. *Physica D*, 142:87–100, 2000.

[9] L. Barreira. *Thermodynamic formalism and applications to dimension theory.* Progress in Mathematics (volume 294), Birkhäuser, Basel, 2011.

[10] L. Barreira. *Ergodic theory, hyperbolic dynamics and dimension theory.* Springer-Verlag, Berlin, 2012.

[11] L. Barreira, Y. Pesin, and J. Schmeling. Dimension and product structure of hyperbolic measures. *Annals of Mathematics (2)*, 149(3):755–783, 1999.

[12] L. Barreira and C. Wolf. Pointwise dimension and ergodic decompositions. *Ergodic Theory and Dynamical Systems*, 26:653–671, 2006.

[13] S.K. Berberian. *Fundamental of real analysis*. Springer-Verlag, New York, 1999.

[14] G. Birkhoff. Higher-dimensional multifractal analysis. *Proceedings of the National Academy of Sciences of the United States of America*, 1931.

[15] A.B. Blaya and V.J. López. On the relations between positive lyapunov exponents, positive entropy, and sensitivity for interval maps. *Discrete and Continuous Dynamical Systems*, 32(2):433–466, 2012.

[16] D. Broomhead, D. Hadjiloucas, and M. Nicol. Random and deterministic pertubation of a class of skew-product systems. *Dynamics and Stability of Systems*, 14(2):115–128, 1999.

[17] J. Buescu. *Exotic attractors: from Liapunov stability to riddled basins*. Birkhäuser Verlag, Switzerland, 1997.

[18] S. Camargo, S.R. Lopes, and Viana R.L. Extreme fractal structures in chaotic mechanical systems: riddled basins of attraction. *Journal of Physics: Conference Series*, 246:1–15, 2010.

[19] K.M. Campbell. Observational noise in skew product systems. *Physica D*, 107:1–15, 1997.

[20] S.B.S.D Castro and A. Lohse. Stability in simple heteroclinic networks in $\mathbb{R}^4$. *Dynamical Systems*, 29(4):451–481, 2014.

[21] B. Cazelles. Dynamics with riddled basins of attraction in models of interacting population. *Chaos, Solitons and Fractals*, 12:301–311, 2001.

[22] R. Crandall and C. Pomerance. *Prime numbers: a computational perspective*. Springer Science+Business Media Inc., USA, 2nd edition, 2005.

[23] W. de Melo and S. van Strien. *One-dimensional dynamics*. Springer-Verlag, Berlin Heidelberg, 1993.

[24] J.P. Eckmann and D. Ruelle. Ergodic theory and of chaos and strange attractors. *Reviews of Modern Physics*, 57(3):617–656, 1985.

[25] K. Falconer. *Techniques in fractal geometry*. John Wiley & Sons Ltd., Sussex, England, 1997.

[26] K. Falconer. *Fractal geometry: mathematical foundations and applications*. John Wiley & Sons Ltd., Sussex, England, 2nd edition, 2003.

[27] J.D. Farmer, E. Ott, and J.A. Yorke. The dimension of chaotic attractors. *Physica D*, 7:153–180, 1983.

[28] O. Georgiou, C.P. Dettmann, and E.G. Altmann. Faster than expected escape for a class of fully chaotic maps. *Chaos: An Interdisciplinary Journal of Nonlinear Science*, 22(043115):1–10, 2012.

[29] P. Glendinning. *Stability, instability and chaos: an introduction to the theory of nonlinear differential equations*. Cambridge University Press, United Kingdom, 1994.

[30] P. Glendinning. Global attractors of pinched skew products. *Dynamical Systems: An International Journal*, 17(3):287–294, 2002.

[31] D. Hadjiloucas, M.J. Nicol, and C.P. Walkden. Regularity of invariant graphs over hyperbolic systems. *Ergodic Theory and Dynamical Systems*, 22:469–482, 2002.

[32] M. Hasler, Y. Maistrenko, and S. Popovych. Simple example of partial synchronization of chaotic systems. *Physical Review E*, 58:6843–6846, 1998.

[33] J.F. Heagy, T.L. Carroll, and L.M. Pecora. Experimental and numerical evidence for riddled basins in coupled chaotic systems. *Physical Review Letters*, 73:3528–3532, 1994.

[34] M.W. Hirsch, C.C. Pugh, and M. Shub. *Invariant manifolds (Lecture in Mathematics, 583)*. Springer, Berlin, 1977.

[35] W. Huang and P. Zhang. Pointwise dimension, entropy and lyapunov exponents for c^1 maps. *Transactions of the American Mathematical Society*, 364(12):6355–6370, 2012.

[36] B.R. Hunt, J.A. Kennedy, T.-Y. Li, and H.E. Nusse. Slyrb measures: natural invariant measures for chaotic systems. *Physica D*, 170:50–71, 2002.

[37] T.H. Jäger. On the structure of strange non-chaotic attractors in pinched skew products. *Ergodic Theory and Dynamical Systems*, 27:493–510, 2007.

[38] T.H. Jäger. *The creation of strange non-chaotic attractors in non-smooth saddle-node bifurcations*, volume 201. American Mathematical Society, USA, 2009.

[39] O. Jenkinson and M. Pollicott. *Entropy, exponents and invariant densities for hyperbolic systems: dependence and computations*. In: Brin, M., Hasselblatt, B.

and Pesin, Y. (Eds.), Modern Dynamical Systems and Applications, Cambridge University Press, Cambridge, 2004.

[40] T. Jordan, V. Naudot, and T. Young. Higher order birkhoff averages. *Dynamical Systems*, 24(3):299–313, 2009.

[41] J.L. Kaplan, J. Mallet-Parret, and J.A. Yorke. The lyapunov dimension of a nowhere differentiable attracting torus. *Ergodic Theory and Dynamical Systems*, 4:261–281, 1984.

[42] G. Keller. A note on strange nonchaotic attractors. *Fundamenta Mathematicae*, 151:139–148, 1996.

[43] G. Keller. *Equilibrium states in ergodic theory*. Cambridge University Press, Cambridge, 1998.

[44] G. Keller. Stability index for chaotically driven concave maps. *Journal of the London Mathematical Society*, pages 1–20, 2014.

[45] G. Keller, H.H. Jafri, and R. Ramaswamy. Nature of weak generalized synchronization in chaotically driven maps. *Physical Review E*, 042913:1–7, 2013.

[46] G. Keller and A. Otani. Bifurcation and hausdorff dimension in families of chaotically driven maps with multiplicative forcing. *Dynamical Systems: An International Journal*, 28(2):123–139, 2013.

[47] D. Knuth. Big omicron and big omega and big theta. *ACM SIGACT New*, 8(2):18–24, 1976.

[48] S.G. Krantz. *Handbook of complex variables*. Birkhäuser, Boston, 1999.

[49] Y.-C. Lai and T. Tél. *Transient chaos: complex dynamics on finite-time scales*. Springer, New York, 2011.

[50] F. Ledrappier and L.-S. Young. The metric entropy of diffeomorphisms: Part ii: relations between entropy, exponents and dimension. *Annals of Mathematics*, 122:540–574, 1985.

[51] J.M. Lee. *Introduction to topological manifolds*. Springer-Verlag, New York, 2000.

[52] A.S. Lohse. *Attraction properties and non-asymptotic stability of simple heteroclinic cyccles and networks in* $\mathbb{R}^4$. PhD thesis, Universität Hamburg, 2014.

[53] J. Marklof and C. Ulcigrai. Dynamical systems and ergodic theory. Lecture notes, 2014.

[54] J. Milnor. On the concept of attractor. *Communications in Mathematical Physics*, 99:177–195, 1985.

[55] H. Nakajima and Y. Ueda. Riddled basins of the optimal states in learning dynamical systems. *Physica D*, 99:35–44, 1996.

[56] L. Olsen. Multifractal analysis of divergence points of deformed measure theoretical birkhoff averages. *Journal de Mathématiques Pures et Appliquées*, 82:1591–1649, 2003.

[57] E. Ott, J.C. Alexander, I. Kan, and J.C. Sommerer. The transition to chaotic attractors with riddled basins. *Physica D*, 76:384–410, 1994.

[58] E. Ott, J.C. Sommerer, J.C. Alexander, I. Kan, and J.A. Yorke. Scaling behaviour of chaotic systems with riddled basins. *Physical Review Letters*, 71:4134–4137, 1993.

[59] O. Podvigina and P. Ashwin. On local attraction properties and a stability index for heteroclinic connections. *Nonlinearity*, 24:887–929, 2011.

[60] M. Pollicott and M. Yuri. *Dynamical systems and ergodic theory.* Cambridge University Press, Cambridge, 1998.

[61] J.C. Sommerer and E. Ott. A physical system with qualitatively uncertain dynamics. *Nature*, 365:138–140, 1993.

[62] J. Stark. Invariant graphs for forced systems. *Physica D*, 109:163–179, 1997.

[63] J. Stark. Regularity of invariant graphs for forced systems. *Ergodic Theory and Dynamical Systems*, 19:155–199, 1999.

[64] R. Sturman. *Strange nonchaotic attractors in quasiperiodically forced systems.* PhD thesis, University College London, 2000.

[65] P. Walters. *An introduction to ergodic theory.* Springer-Verlag, New York, 1982.

[66] R.L. Wheeden and A. Zygmund. *Measure and integral: An introduction to real analysis.* Marcel Dekker, Inc., New York, 1977.

[67] M. Woltering and M. Markus. Riddled basins of coupled elastic arches. *Physics Letters A*, 260:453–461, 1999.

[68] M. Woltering and M. Markus. Riddled basins in a model for the belousov–zhabotinsky reaction. *Chemical Physics Letters*, 321:473–478, 2000.

[69] H. Yamada and T. Fujisaka. Stability theory of synchronized motion in coupled-oscillator systems. *Progress of Theoretical Physics*, 72:885–894, 1984.

[70] L.-S. Young. Ergodic theory of attractors. *Proceedings of the International Congress of Mathematicicans, Zürich, Switzerland*, pages 1230–1237, 1995.

[71] L.S. Young. Dimension, entropy and lyapunov exponents. *Ergodic Theory and Dynamical Systems*, 2:109–124, 1982.

[72] S. Yousefi, Y. Maistrenko, and S. Popovych. Complex dynamics in a simple model of interdependent open economies. *Discrete Dynamics in Nature and Society*, 5:161–177, 2000.